

01 Oct 1984

## Design of automotive structural components using high strength sheet steels - structural behavior of beam webs subjected to web crippling and a combination of web crippling and bending

Chiravut Santaputra

Wei-Wen Yu

*Missouri University of Science and Technology, wwy4@mst.edu*

Follow this and additional works at: <https://scholarsmine.mst.edu/ccfss-library>

 Part of the [Structural Engineering Commons](#)

---

### Recommended Citation

Santaputra, Chiravut and Yu, Wei-Wen, "Design of automotive structural components using high strength sheet steels - structural behavior of beam webs subjected to web crippling and a combination of web crippling and bending" (1984). *CCFSS Library (1939 - present)*. 99.  
<https://scholarsmine.mst.edu/ccfss-library/99>

This Technical Report is brought to you for free and open access by Scholars' Mine. It has been accepted for inclusion in CCFSS Library (1939 - present) by an authorized administrator of Scholars' Mine. This work is protected by U. S. Copyright Law. Unauthorized use including reproduction for redistribution requires the permission of the copyright holder. For more information, please contact [scholarsmine@mst.edu](mailto:scholarsmine@mst.edu).

Civil Engineering Study 84-1  
Structural Series

Fifth Progress report

DESIGN OF AUTOMOTIVE STRUCTURAL COMPONENTS  
USING HIGH STRENGTH SHEET STEELS

STRUCTURAL BEHAVIOR OF BEAM WEBS SUBJECTED TO  
WEB CRIPPLING AND A COMBINATION OF WEB CRIPPLING AND BENDING

by

Chiravut Santaputra  
Research Assistant

Wei-Wen Yu  
Project Director

A Research Project Sponsored by American Iron and Steel Institute

October 1984

Department of Civil Engineering  
University of Missouri-Rolla  
Rolla, Missouri

## TABLE OF CONTENTS

	Page
LIST OF TABLES.....	iv
LIST OF FIGURES.....	vii
I. INTRODUCTION.....	1
II. CURRENT AISI DESIGN PROVISIONS.....	4
1. AISI 1981 Guide for Preliminary Design of Sheet Steel Automotive Structural Components.....	4
2. AISI 1980 Specification for the Design of Cold-Formed Steel Structural Members.....	6
III. EXPERIMENTAL STUDY.....	11
A. General.....	11
B. Test Specimens.....	12
C. Test Procedure.....	13
D. Results of Tests.....	14
IV. EVALUATION OF EXPERIMENTAL RESULTS.....	18
A. Hat Sections Subjected to Interior One-Flange Loading.....	19
B. Hat Sections Subjected to End One-Flange Loading.....	22
C. I-Sections Subjected to Interior One-Flange Loading.....	24
D. I-Sections Subjected to End One-Flange Loading.....	25
V. DEVELOPMENT OF NEW EQUATIONS.....	26
A. Single Webs Subjected to Interior One-Flange Loading Condition.....	30

	Page
B. Single Webs Subjected to End One-Flange Loading Condition.....	34
VI. PROPOSED FUTURE STUDY.....	36
VII. CONCLUSIONS.....	39
VIII. ACKNOWLEDGMENTS.....	41
IX. REFERENCES.....	42
APPENDIX A .- Loading Conditions for Web Crippling.....	107
APPENDIX B - Data from Previous UMR Study.....	110
APPENDIX C - Notation.....	123

## LIST OF TABLES

Table		Page
1	Material Properties and Thicknesses of Sheet Steels Used in the Experimental Study.....	45
2a	Nominal Dimensions of Hat Sections Designed for Experimental Study.....	45
2b	Nominal Dimensions of I-Sections Designed for Experimental Study.....	45
3a	Dimensions of Specimens for Hat Sections Used for Interior One-Flange Loading Condition.....	46
3b	Dimensions of Specimens for Hat Sections Used for End One-Flange Loading Condition.....	47
3c	Dimensions of Specimens for I-Sections Used for Interior One-Flange Loading Condition.....	48
3d	Dimensions of Specimens for I-Sections Used for End One-Flange Loading Condition.....	49
4a	Number of Web Crippling Tests on Hat Sections Subjected to Interior One-Flange Loading.....	50
4b	Number of Web Crippling Tests on Hat Sections Subjected to End One-Flange Loading.....	50
4c	Number of Web Crippling Tests on I-Sections Subjected to Interior One-Flange Loading.....	51
4d	Number of Web Crippling Tests on I-Sections Subjected to End One-Flange Loading.....	51
5	Parameters and Sectional Properties of Hat Sections for Interior One-Flange Loading Condition.....	52
6a	Comparisons of Tested and Predicted Failure Loads for Hat Sections for Interior One-Flange Loading Condition Based on the AISI 1981 Guide with Modified $f(F_y)$ .....	53
6b	Comparisons of Tested and Predicted Failure Loads for Hat Sections for Interior One-Flange Loading Condition Based on the AISI 1980 Specification with Modified $f(F_y)$ .....	54

Table		Page
7	Parameters and Sectional Properties of Hat Sections for End One-Flange Loading Condition.....	55
8	Comparisons of Tested and Predicted Failure Loads for Hat Sections for End One-Flange Loading Condition Based on the AISI 1981 Guide and 1980 Specification with Modified $f(F_y)$ .....	56
9	Parameters and Sectional Properties of I-Sections for Interior One-Flange Loading Condition.....	57
10	Comparisons of Tested and Predicted Failure Loads for I-Sections for Interior One-Flange Loading Condition Based on the AISI 1981 Guide and 1980 Specification.....	58
11	Parameters and Sectional properties of I-Sections for End One-Flange Loading Condition.....	59
12	Comparison of Tested and Predicted Failure Loads for Hat Sections for Interior One-Flange Loading Condition Based on Equations 29, 36 and 31.....	60
13	Comparison of Tested and Predicted Failure Loads for Hat Sections for Interior One-Flange Loading Condition Based on Equations 29, 37 and 31.....	61
14	Comparison of Tested and Predicted Failure Loads for Hat Sections for End One-Flange Loading Condition Based on Equations 40 and 41.....	62
15	Comparison of Tested and Predicted Failure Loads for Hat Sections for Interior One-Flange Loading Condition Based on Equations 29, 36 and 31.....	63
16	Comparison of Tested and Predicted Failure Loads for Hat Sections for Interior One-Flange Loading Condition Based on Equations 29, 37 and 31.....	65
17	Proposed Number of Hat Sections Used to Verify Equation (31).....	67
18	Proposed Number of Hat Sections Used to Verify Equation (29).....	67
19	Number of Web Crippling Tests on Hat Sections Subjected to Interior Two-Flange Loading.....	68

Table		Page
20	Number of Web Crippling Tests on Hat Sections Subjected to End Two-Flange Loading.....	68
21	Number of Web Crippling Tests on I-Sections Subjected to Interior Two-Flange Loading.....	69
22	Number of Web Crippling Tests on I-Sections Subjected to End Two-Flange Loading.....	69

## LIST OF FIGURES

Figure		Page
1	Tinius Olsen Universal Testing Machine.....	70
2	Hat Sections Used in the Experimental Study.....	71
3	I-Sections Used in the Experimental Study.....	71
4	Test Setup for Web Crippling.....	72
5	Photograph of Test Setup for Interior One-Flange Loading Condition of Hat Section.....	73
6	Photograph of Test Setup for Interior One-Flange Loading Condition of I-Sections.....	74
7	Photograph of Test Setup for End One-Flange Loading Condition of Hat Section.....	75
8	Photograph of Test Setup for End One-Flange Loading Condition of I-Section.....	76
9	Photograph Showing Wood Blocks Were Used at Both Ends of Hat Section Under Interior One-Flange Loading.....	77
10	Photograph Showing Wood Blocks Were Used at Both Ends of I-Section Under Interior One-Flange Loading.....	78
11	Photograph Showing Lateral and Vertical Deformation Measurements of Hat Section Used for Interior One-Flange Loading.....	79
12	Photograph Showing Lateral and Vertical Deformation Measurements of Hat Section Used for End One-Flange Loading.....	80
13	Photograph Showing Web Crippling Failure Caused by Overstressing.....	81
14	Laterally Deformed Web of a Hat Section Under Interior One-Flange Loading (Specimen No. 2-HI-21).....	82
15	Photograph Showing Web Crippling Failure caused by Web Buckling.....	83
16	Laterally Deformed Web of a Hat Section Under Interior One-Flange Loading (Specimen No. 3-HI-21).....	84



Figure	Page
17	Photograph Showing Typical Failure of I-Beam Subjected to Interior One-Flange Loading..... 85
18	Laterally Deformed Web of a Hat Section Under End One-Flange Loading (Specimen No. 1-HE-21)..... 86
19	Deformed Cross Section of a Hat Section Subjected to End One-Flange Loading..... 87
20	Photograph Showing Typical Failure of Hat Section Subjected to End One-Flange Loading..... 88
21	Sketch Showing Failure at Web-Flange Junction..... 89
22	Photograph Showing Failure of I-Beam Subjected End One-Flange Loading..... 90
23	Plot of Equations (13) and (14)..... 91
24	Effect of $F_y$ on the Ratio $P_{test}/P_{comp}$ for Interior One-Flange Loading Condition Based on the AISI 1981 Guide and 1980 Specification with Modified $f(F_y)$ ..... 92
25	Effect of $F_y$ on the Ratio $P_{test}/P_{comp}$ for End One-Flange Loading Condition Based on the AISI 1981 Guide and 1980 Specification with Modified $f(F_y)$ ..... 93
26	Plot of Applied Load vs. End Flange Tip Deflection of Hat Section Under End One-Flange Loading (Specimen No. 1-HE-21)..... 94
27	Effect of $F_y$ on the Ratio $P_{test}/P_{comp}$ for Interior One-Flange Loading of I-Section Based on..... 95
28	Function of $F_y$ for I-Sections Subjected to Interior One-Flange Loading..... 96
29	Simply Supported Plate Subjected to Uniformly Distributed Load..... 97

Figure	Page
30	Simply Supported Plate Subjected to Two Opposite Concentrated Load..... 98
31	Simply Supported Plate Subjected to Two Opposite Partially Distributed Load..... 99
32	Simply Supported Plate Subjected to Partial Edge Loading..... 100
33	Buckling Coefficient as the Function of N/h and L/h Ratios..... 101
34	Plot of Interaction Equations for Combined Bending and Web Crippling..... 102
35	Effect of $F_y$ on the Ratios $P_{test}/P_{comp}$ Using Equations (29), (36) and (31)..... 103
36	Effect of $F_y$ on the Ratios $P_{test}/P_{comp}$ Using Equations (40) and (41)..... 104
37	Test Setup to Verify Equation (31)..... 105
38	Test Setup to Verify Equation (29)..... 105
39	Test Setup for Interior Two-Flange Loading..... 106
40	Test Setup for End Two-Flange Loading..... 106

## I. INTRODUCTION

In recent years, high strength steels have been used in automotive structural components to achieve weight reduction while complying with Federal safety standards. The current design recommendations, the "Guide for Preliminary Design of Sheet Steel Automotive Structural Components"<sup>1</sup> was issued by American Iron and Steel Institute (AISI) in February 1981. It was recommended for application to materials with yield strength up to 80 ksi. These design expressions are based primarily on the 1968 Edition of the AISI "Specification for the Design of Cold-Formed Steel Structural Members"<sup>2</sup> which was written for the design of buildings.

The AISI Specification was revised in 1980.<sup>3</sup> Some of the design criteria were revised and others were added in keeping with technical developments and the results of continued research programs sponsored by the American Iron and Steel Institute. Furthermore, in view of the fact that many types of high strength steels with yield strengths from 80 to 190 ksi<sup>4-8</sup> are now used for automotive structural components, a comprehensive design guide is highly desirable.

Since early 1982, a research project entitled "Structural Design of Automotive Structural Components Using High Strength Sheet Steels" has been conducted at the University of Missouri-Rolla under the sponsorship of the American Iron and Steel Institute. The main purpose of this project has been to develop additional design criteria for the use of a broader range of high strength steels in automotive structures<sup>9,10</sup>.

The strength of beam webs is one area that has been studied as a part of this research project and was discussed previously in the Third Progress Report<sup>10</sup>, which was published in August 1983. Previous study was based on the tests conducted by Levy<sup>5</sup> and Vecchio<sup>6</sup> for the following design considerations<sup>4</sup>:

1. Moment resisting capacity
2. Bending capacity of webs
3. Shear capacity of webs
4. Combined bending and shear in webs
5. Web crippling
6. Combined bending and web crippling

Also included in the Third Progress Report was a proposal for an additional experimental study on web crippling of hat sections and I-beams with material yield strengths ranging from 55.8 to 141.2 ksi.

Since the issuance of the Third Progress Report, the possible development of design equations for web crippling under interior one-flange loading condition of single unreinforced webs has been continued. There have been some changes in the additional web crippling tests as proposed in the Third Progress Report. According to the recommendations of the AISI Task Force on Structural Research of the Transportation Department, the 80DF and the 80SK sheet steels have been omitted. This experimental program were completed in June 1984. After the evaluation of test data, new equations for the prediction of web crippling loads for single unreinforced webs under interior one-flange loading and end one-flange loading conditions were developed.

The purpose of this report is to summarize and discuss the research work that has been done on the structural behavior of beam webs

subjected to web crippling and the combination of web crippling and bending moment. This is the continuation of the study reported in the Third Progress Report. Section II is the review of design provisions for web crippling included in the 1981 Guide<sup>1</sup> and the 1980 Specification<sup>3</sup>. In Section III, the experimental study as proposed in the Third Progress Report is presented. Section IV contains an evaluation of the experimental results by using current AISI design procedures with some modification as proposed in the Third Progress Report. New equations for web crippling and combined bending and web crippling are developed and discussed in Section V. Several topics for future study are proposed in Section VI.

## II. CURRENT AISI DESIGN PROVISIONS

Included in this Section is a review of the AISI design provisions for web crippling and combined bending and web crippling as required by the 1981 Guide for Preliminary Design of Sheet Steel Automotive Structural Components and the 1980 Specification for the Design of Cold-Formed Steel Structural Members. It should be noted that all expressions presented in following sections are based on the ultimate strength approach. This review is limited only to the following two loading conditions:

1. Interior one-flange loading
2. End one-flange loading

The classification of loading conditions according to the current AISI provisions on web crippling is specified in Appendix A.

### II.1 AISI 1981 Guide for Preliminary Design of Sheet Steel Automotive Structural Components

According to Section 3.4.7 of the 1981 Guide, the ultimate strength for web crippling of unreinforced beam webs subjected to concentrated loads or reactions can be determined as follows:

(a) Beams having single webs and  $R/t$  up to 4:

1. For end reactions or for concentrated loads on outer ends of cantilevers:

$$P_c = t^2(2.13-0.28(R/t))(98+4.20(N/t)-0.022(N/t)(h/t) - 0.011(h/t))(1.33-0.33(F_y/33))(F_y/33) \quad (1)$$

2. For reactions of interior supports or for concentrated loads located on the span:

$$P_c = t^2(1.96-0.11(R/t))(305+2.30(N/t)-0.009(N/t)(h/t) - 0.50(h/t))(1.22-0.22(F_y/33))(F_y/33) \quad (2)$$

(b) I-beams or sections which provide a high degree of restraint against rotation of the web:

1. For end reactions or for concentrated loads on outer ends of cantilevers:

$$P_c = t^2 F_y (10.0 + 1.25 \sqrt{N/t}) \quad (3)$$

2. For reactions of interior supports or for concentrated loads located on the span:

$$P_c = t^2 F_y (15.0 + 3.25 \sqrt{N/t}) \quad (4)$$

In all of the above,  $P_c$  represents the load or reaction for one solid web sheet connecting top and bottom flanges.  $P_c$  shall be computed for each individual sheet and the results added to obtain the allowable load or reaction for the composite web.

For loads located close to ends of beams, provisions (a-2) and (b-2) apply, provided that for cantilevers the distance from the free end to the nearest edge of bearing, and for a load close to an end support the clear distance from edge of end bearing to nearest edge of load bearing is larger than  $1.5h$ . Otherwise provisions (a-1) and (b-1) apply.

In the above formulas,

$P_c$  = ultimate concentrated load or reaction, kips

$t$  = web thickness, in.

$N$  = actual length of bearing or "h", whichever is smaller, in.

$h$  = clear distance between flanges measured along the plane

of web, in.

$F_y$  = yield strength, ksi.

$R$  = inside bend radius, in.

As mentioned in Section I, the 1981 Guide is based primarily on the 1968 Edition of the AISI Specification. The interaction equation, stated in Addendum No. 2 of the 1968 Specification, which was excluded from the 1981 Guide, is reviewed as follows:

For failures caused by the combination of bending and web crippling the following interaction equation may be used to calculate the ultimate load<sup>4</sup>:

$$(P/P_c) + (M/M_u) \leq 1.3 \quad (5)$$

where  $P$  = concentrated load or reaction, kips

$P_c$  = ultimate web crippling load in the absence  
of bending moment, kips

$M$  = applied bending moment at or immediately  
adjacent to the point of application of the  
concentrated load or reaction, kip-in.

$M_u$  = ultimate bending moment if bending moment  
only exists, kip-in.

It should be noted that there is no design expression for the interaction of bending and web crippling for I-beams in the 1968 Specification.

## II.2 AISI 1980 Specification for the Design of Cold-Formed Steel Structural Members

### A. Web Crippling of Flexural Members



According to Section 3.5.1 of the 1980 Specification, the ultimate strength for web crippling of unreinforced beam webs subjected to concentrate loads or reactions with  $R/t$  up to 6,  $N/t$  up to 210 and  $N/h$  up to 3.5 can be determined as follows:

(a) Beams having single unreinforced webs:

1. For end reactions or for concentrated loads on outer ends of cantilevers when the distance from the edge of bearing to the end of the beam is less than  $1.5h$ :

1.1 Stiffened flanges:

$$P_c = 1.85t^2(F_y/33)(1.33-0.33(F_y/33))(1.15-0.15(R/t)) \\ (179-0.33(h/t))(1+0.01(N/t)) \quad (6)$$

1.2 Unstiffened flanges:

$$P_c = 1.85t^2(F_y/33)(1.33-0.33(F_y/33))(1.15-0.15(R/t)) \\ (117-0.15(h/t))(1+0.01(N/t)) \quad (7)$$

When  $N/t > 60$ , the factor  $(1+0.01(N/t))$  in Eq. (7) may be increased to  $(0.71+0.015(N/t))$ .

2. For reactions of interior supports or for concentrated loads when the distance from the edge of bearing to the end of the beam is equal to or larger than  $1.5h$ :

$$P_c = 1.85t^2(1.06-0.06(R/t))(291-0.40(h/t))(1+0.007(N/t)) \\ (1.22-0.22(F_y/33))(F_y/33) \quad (8)$$

When  $N/t > 60$ , the factor  $(1+0.007(N/t))$  in Eq. (8) may be increased to  $(0.75+0.011(N/t))$ .

- (b) I-beams made of two channels connected back to back or for similar sections which provide a high degree of restraint against rotation of the web, such as I-sections made by welding two angles to channels:

1. For end reactions or for concentrated loads on outer ends of cantilevers when the distance from the edge of bearing to the end of the beam is less than  $1.5h$ :

$$P_c = 2.0t^2 F_y (1+(h/t)/750)(5.0+0.63\sqrt{N/t}) \quad (9)$$

When  $h/t > 150$ , a constant value of 1.20 should be used for the factor  $(1+(h/t)/750)$  in Eq. (9)

2. For reactions of interior supports or for concentrated loads when the distance from the edge of bearing to the end of the beam is equal to or larger than  $1.5h$ :

$$P_c = 2.0t^2 F_y (1.49-0.53(F_y/33))(0.88+0.12(t/0.075)(7.5+1.63\sqrt{N/t})) \quad (10)$$

In Eq. (10), the factor  $(1.49-0.53(F_y/33))$  is not less than 0.6.

In all of the above,  $P_c$  represents the load or reaction for one solid web sheet connecting top and bottom flanges.  $P_c$  shall be computed for each individual sheet and the results added to obtain the allowable load or reaction for the composite web.

For cases that the clear distance between the closest opposite bearing plate is less than  $1.5h$  the provisions for interior two-flange loading or end two-flange loading should be applied. Since all test data used in this report do not belong to two-flange loading cases, the applicable design expressions included in the 1980 Specification are not reviewed here.

In the above formulas,

$P_c$  = ultimate concentrated load or reaction, kips

$t$  = web thickness, in.

$N$  = actual length of bearing, in.

$h$  = clear distance between flanges measured along the plane of web, in.

$F_y$  = yield strength, ksi.

$R$  = inside bend radius, in.

It should be noted that the factor of safety used for allowable web crippling load in the 1980 Specification is 1.85 for beams with single unreinforced webs. For I-beams, the factor of safety is 2.0.

#### B. Combined Bending and Web Crippling

Section 3.5.2 of the 1980 Specification provides design requirements for unreinforced flat webs of shapes subjected to a combination of bending and reaction or concentrated load for allowable stress design.<sup>3</sup> The following requirements should be used for ultimate strength approach:<sup>11</sup>

(a) Shapes having single webs:

$$1.07(P/P_c) + (M/M_u) \leq 1.42 \quad (11)$$

(b) I-beams made of two channels connected back to back or for similar sections which provide a high degree of restraint against rotation of the web, such as I-sections made by welding two angles to a channel:

$$0.82(P/P_c) + (M/M_u) \leq 1.32 \quad (12)$$

In the above formulas,

$P$  = concentrated load or reaction, kips

$P_c$  = ultimate web crippling load in the absence of bending moment, kips

$M$  = applied bending moment at or immediately

adjacent to the point of application of the  
concentrated load or reaction, kip-in.

$M_u$  = ultimate bending moment if bending moment  
only exists, kip-in.

### III. EXPERIMENTAL STUDY

#### A. General

As pointed out in the Third Progress Report, an additional experimental study was needed to confirm the validity of the proposed modification of the design formulas for web crippling under interior one-flange loading condition of single unreinforced webs and to improve the design criteria for other loading conditions. It was proposed that 72 hat sections and 60 I-beams fabricated from six different types of sheet steels (80DF, 80SK, 80DK, 80XF, 100XF and 140XF) be used in this experimental program. Based on the recommendation of the AISI Task Force on Structural Research of the Transportation Department, the 80DF and 80SK specimens were omitted.

The objective of this experimental study was to determine the ultimate web crippling loads for sections formed from high strength materials in order to extend the the range of material yield strengths beyond the present limitation of the AISI design criteria. In this phase of investigation, 48 hat sections and 36 I-beams were tested for the following two loading conditions:

1. Interior one-flange loading
2. End one-flange loading

All tests were performed in the 120,000 pound Tinius Olsen universal testing machine (Fig. 1) located in the Engineering Research Laboratory of the University of Missouri-Rolla. The materials used in this study include hot-rolled and cold-rolled sheet steels having yield strengths ranging from 58.3 to 141.2 ksi. The mechanical properties and

thicknesses of these four types of sheet steels which were studied in detail in Phase I of this research project<sup>9,12</sup> are given in Table 1.

#### B. Test Specimens

Hat sections, as shown in Fig. 2, were used for the study of single unreinforced webs while I-beams (Fig. 3) were used as sections that provide a high degree of restraint against rotation of the webs. Three different profiles for each kind of cross sections were designed for each type of material as shown in Tables 2a and 2b.

All specimens were formed by Wania Ornamental Wire and Iron Company, St. Louis, Missouri. Measured dimensions of these specimens are given for each type of tests in Tables 3a, 3b, 3c and 3d. The R values in these tables are the average of the two corner radii in the failure area. D1 is the average depth of the two webs. In Tables 3c and 3d, B1 is the average of the four flange widths. All measurements were performed at the sections of expected failure.

Initial imperfections due to forming were noted in most test specimens. Cracks at the corners of 140XF specimens, which have low ductility, were observed. These cracks were caused by the use of small inside radii (Tables 3a and 3b) as compared with the specified value of 0.25 in.. Cross sections of some of the I-beam specimens were not perfectly symmetric because they were fabricated from two unidentical channels. Specimens were selected in such a way that the best cross section was used at the location of expected failure.

In order to retest the specimens using 140XF sheet steels, additional nine hat sections were formed recently by the Research Laboratories of Inland Steel Company. These specimens will be tested to check the data obtained from the cracked sections mentioned above.

All I-beam specimens were fabricated from two channels connected back to back with the aid of self-tapping screws (14 x 3/4 Tek screws) at a distance of 1/2 in. from top and bottom flanges. The self tapping screws were spaced along the beam length at a constant distance of 2 in. from center to center. The screws were driven from alternate sides of webs during fabrication in order to minimize the initial deformations of webs.

All hat sections were braced by 1/8 x 3/4 in. rectangular bars at the 1/3 points of beams to maintain the shape of the cross section during the test.

#### C. Test Procedure

All specimens were tested as simply supported flexural members subjected to a concentrated load at mid span. During the testing, loads were applied at an increment of approximately 15% of the predicted ultimate load and maintained constant at each load level about 5 minutes. All specimens were loaded to failure. Vertical deflection at mid span was also recorded for all specimens at every loading steps by mean of dial gage.

The number of specimens and the testing arrangement for each case of loading conditions are as follows:

1. Interior One-Flange Loading:

A total of 24 hat sections and 18 I-beams (Tables 4a and 4c) were tested with two 4-in. bearing plates at both ends and a 2-in. bearing plate under a concentrated load applied at mid span. The clear distance between the opposite bearing plates were designed to be 1.5h. The testing arrangement are shown in Figs. 4a, 5 and 6.

To prevent the end failure from happening before the expected failure to develop, wood blocks were inserted at both ends of hat sections (Fig. 9) and I-beams (Fig. 10). Lateral deformations were measured for both webs at several points with 1/2 in. spacing along the center line of the mid span bearing plate at each load level (Fig. 11).

## 2. End One-Flange Loading:

As shown in Tables 4b and 4d, the same numbers of specimens as used for the previous loading case were tested. The test setup (Figs. 4b, 7 and 8) was the same as the interior one-flange loading case except that 2-in. bearing plates were used at both ends while a 4-in. bearing plate was under the concentrated load at mid span. The clear distance between the opposite bearing plates were also designed to be  $1.5h$ . In this case lateral deformations were measured along the center lines of the end bearing plates (Fig. 12).

Compression flanges of I-beams used in this loading case were braced against lateral movement to prevent twisting of the section. This lateral movement was not noted for the interior one-flange loading case because wood blocks were inserted at the ends to prevent the tension flange from tilting upward.

## D. Results of Tests

All lateral deformations, end flange tip deflections and vertical deflections at mid span were recorded at every loading step as discussed previously. The ultimate loads were recorded and appeared to be very consistent for identical specimens. Since the specimens were unstable



at the ultimate loads, all deflections and deformations measurements could not be obtained at this level.

The nature of failure was carefully inspected through out the testing and can be summarized as follows:

1. Interior one-flange loading condition:

- 1.1 Hat sections:

For 80DK and 80XF specimens the failures occurred just under the bearing plates with relatively small lateral deformations. For these specimens the loads increased smoothly up to the ultimate loads and maintained at that level for a long period of time. The bearing plates gradually penetrated into the flanges after failure occurred in the webs. It was believed that overstress underneath the bearing plates caused this type of failure. The typical failure and laterally deformed webs are shown in Figs. 13 and 14, respectively.

Buckling in the webs was observed in the 100XF and 140XF specimens. The loads increased smoothly up to the ultimate loads with relatively large lateral deformations and suddenly had a slight drop. The loads maintained at this level while the bearing plates penetrated into the flanges. Figure 15 shows this particular failure while the lateral deformations of the web were plotted in Fig. 16.

- 1.2 I-beams:

The behavior of all specimens in this group was the same as that of hat sections using 80DK and 80XF materials except that relatively small lateral deformations were observed through out the tests. This may be due to the fact that the bend radii have little or no effect on the ultimate web crippling loads of these I-beams which resulted in higher failure loads than that of hat sections using the same type of material.

For each type of material, there appeared to be only slight variation of the failure loads regardless of the variation in the depth for each profile. This indicates that the depth of the section has no effect on the ultimate web crippling loads for this group of specimens having  $h/t = 36.2$  to  $103.8$ . It was believed that the mode of failure is due to overstress under the bearing plate. This typical failure mode is shown in Fig. 17.

2. End one-flange loading condition:

2.1 Hat sections:

Under applied load all specimens sustained relatively large lateral deformations and flange tip deflections at both ends. A plot of lateral deformations at each load level and a sketch of a deformed cross section are shown in Figs. 18 and 19, respectively. Because of the small transverse flexural stiffness of the unstiffened flange of the hat section, the bearing edge of the web experienced large rotations.

As a result of the web rotations, relatively large flange tip deflection occurred. Figure 20 shows a typical mode of failure for this type of tests.

For 80DK, 80XF and 100XF specimens, the loads were increased up to the ultimate load and maintained at that level for some time before gradually dropping down. Sudden collapse of 140XF specimens was observed as the ultimate loads were reached.

## 2.2 I-beams:

Web crippling did not occur in these specimens. All failures were at the junction of the web and flange as can be seen from the sketch in Fig. 21. It can be seen that a considerable amount of cantilever action of flanges were induced due to bend radii and location of screws. Because the self tapping screws used in the fabrication of these I-sections were located 1/2 in. from flanges which is the minimum clearance of the electric drill used for driving the screws, these failure modes occurred before web crippling could be developed in the webs. It can be seen from Fig. 22 that under failure load the web still maintained the original shape.

#### IV. EVALUATION OF EXPERIMENTAL RESULTS

This Section presents the comparisons of the test results and the predicted failure loads. These predictions were determined on the basis of the AISI 1981 Guide and the 1980 Specification. The design provisions on web crippling and the combination of bending moment and web crippling were reviewed in Section II. Even though the design expressions included in these recommendations are intended for the use of materials having yield strength not greater than 80 ksi with proportional limit not less than 70% of the yield strength, these design equations have been used in this evaluation with some modification on the function of yield strength.

The relationships between the yield strength and the predicted ultimate web crippling load of single unreinforced webs under interior one-flange loading and end one-flange loading can be determined by Eqs. (13) and (14), respectively.

$$f_1(F_y) = (1.22 - .22(F_y/33))(F_y/33) \quad (13)$$

and 
$$f_2(F_y) = (1.33 - .33(F_y/33))(F_y/33) \quad (14)$$

As discussed in the Third Progress Report, the predicted failure load for a given section increases as the yield strength,  $F_y$ , increases up to a certain value, beyond which the ultimate web crippling load decreases as the yield strength increases. These functions of  $F_y$  are shown graphically in Fig. 23. It can be seen that the functions  $f_1(F_y)$  and  $f_2(F_y)$  reach the maximum values when  $F_y$  are 91.5 and 66.5 ksi, respectively. In this evaluation the values of 91.5 and 66.5 ksi are used in lieu of the actual yield strengths when they exceed these limits.

Based on the design considerations discussed in Section II, expected failure loads were predicted by using computer programs. The comparisons of test results and predicted failure loads are presented as follows:

A. Hat sections subjected to interior one-flange loading

In addition to web crippling and combined web crippling and bending moment, the test results were also checked against maximum moment capacity, shear, and combined bending moment and shear. These design considerations were reviewed in the Third Progress Report.

Tables 3a and 5 give the sectional properties and important parameters used for calculations in this case. The comparisons of tested failure loads and the predicted loads based on the 1981 Guide and 1980 Specification are presented in Tables 6a and 6b, respectively. The symbols used in these tables are defined as follows:

- 1)  $P_m$  is the ultimate load computed for the bending moment only, kips. It was calculated from the following equation:

$$P_m = 4M_u/L \quad (15)$$

where  $M_u$  is the computed ultimate bending moment if the bending moment only exists, kip-in., and  $L$  is the span length, in.. The bending moment was determined by using Eq. (16) as follows:

$$M_u = S_{eff} F_y \quad (16)$$

where  $S_{eff}$  is the effective section modulus of the cross

section and  $F_y$  is the material yield strength. This was determined by using the effective design width of the compression flange as reviewed in the Third Progress Report. Consideration was also given to the effect of shear lag and bending capacity of beam webs.

2)  $P_c$  is the computed ultimate web crippling load for the entire section in the absence of bending moment, kips. It was calculated by using Eqs. (2) and (8). These equations use the  $F_y$  function as given in Eq. (13). The maximum value of this  $F_y$  function is 1.69 at the value of  $F_y$  equals to 91.5 ksi. Hence, the value of  $F_y = 91.5$  was used for  $F_y$  in lieu of the actual yield strength when it is greater than 91.5 ksi.

3)  $P_{mc}$  is the ultimate load computed for the combined bending moment and web crippling, kips. It was determined by employing Eqs. (5) and (11). That is,

(i) Based on the 1981 Guide,

$$(P_{mc}/P_c) + ((P_{mc} L/4)/(P_m L/4)) = 1.3 \quad (17)$$

$$P_{mc} = 1.3(P_c P_m / (P_c + P_m)) \quad (18)$$

(ii) Based on the 1980 Specification,

$$1.07(P_{mc}/P_c) + ((P_{mc} L/4)/(P_m L/4)) = 1.42 \quad (19)$$

$$P_{mc} = 1.42(P_c P_m / (P_c + 1.07P_m)) \quad (20)$$

where  $P_c$ ,  $P_m$  and  $L$  are defined previously.

4)  $P_s$  and  $P_{ms}$  are the ultimate loads computed for shear in the webs and combined bending moment and shear in the webs, kips, respectively. These values were calculated

according to the procedure outlined in the Third Progress Report.

- 5)  $P_{\text{test}}$  is the tested failure load, kips.
- 6)  $P_{\text{test}}/P_{\text{comp}}$  is the ratio of the tested failure load to the predicted failure load for which  $P_{\text{comp}}$  is the smallest value of  $P_m$ ,  $P_c$ ,  $P_{mc}$ ,  $P_s$  and  $P_{ms}$  discussed above.

The governing modes of failure are also indicated in Tables 6a and 6b for all specimens. It should be noted that these modes of failure indicated in all tables are determined from the computed values.

It can be seen that both the 1981 Guide and the 1980 Specification can provide good estimates of the failure loads for 80DK and 80XF specimens which have the yield strengths up to 88.3 ksi. However, for the 100XF and 140XF specimens, underestimations were observed possibly due to the use of a constant yield strength of 91.5 ksi for all specimens. The relationships between the ratios  $P_{\text{test}}/P_{\text{comp}}$  and  $F_y$  are shown in Fig. 24.

For this group of data, it seems that the degree of underestimation increases as the yield strength increases beyond the limit of 80 ksi recommended by the present AISI Guide. This fact does not agree with the results of tests of M190 specimens conducted at Inland Steel Company<sup>4,5</sup>. For the Inland tests, the comparisons of the tested failure loads and the loads predicted by using the same method as reported herein can be observed from Table 7b of the Third Progress

Report for specimen Nos. 31 through 68. This comparison seems to indicate that the function of  $F_y$  is not the only factor that causes inaccuracy in the prediction of ultimate web crippling load for sections fabricated from sheet steels having yield strengths exceeding 80 ksi.

In order to improve the prediction, the format of the web crippling equation may be changed. This matter will be discussed later in Section V of this report.

B. Hat sections subjected to end one-flange loading

The 1980 Specification has two different equations to determine the ultimate web crippling loads for stiffened and unstiffened flanges of single unreinforced webs while the 1981 Guide has only one equation applying to both cases. Hat sections used in this experimental study were tested in such a way that the unstiffened flanges were in contact with the end bearing plates which should be considered as unstiffened flanges.

Cross sectional properties and parameters used in these calculations are given in Tables 3b and 7. The predicted failure loads were computed on the basis of the 1981 Guide and the 1980 Specification and are compared with the tested failure loads given in Table 8. The symbols used in this table are defined as follows:

- 1)  $P_{test}$  is the tested failure load per web, kips.
- 2)  $P_{cg}$  is the ultimate web crippling load per web calculated on the basis of the 1981 Guide (Eq. (1)), kips.



- 3)  $P_{cs}$  is the ultimate web crippling load per web calculated on the basis of the 1980 Specification (Eq. (7)), kips. The function of  $F_y$  for both  $P_{cg}$  and  $P_{cs}$  is given in Eq. (14). In this case the value of  $F_y = 66.5$  was used in lieu of the actual yield strength when it exceeds 66.5 ksi.
- 4)  $P_{test}/P_{cg}$  is the ratio of tested failure load to the predicted failure load based on the 1981 Guide.
- 5)  $P_{test}/P_{cs}$  is the ratio of tested failure load to the predicted failure load based on the 1980 Specification.

Table 8 shows the comparisons of tested and predicted web crippling loads for 24 hat sections tested in this program. The predicted web crippling loads for hat sections subjected to end one-flange loading are rather conservative partly because of the use of a constant  $F_y$  instead of the actual yield strength of sheet steels. The relationships between the ratio  $P_{test}/P_{comp}$  and  $F_y$  are shown in Fig. 25. Generally speaking, the 1981 Guide gives a somewhat better accuracy in predicting the failure load for this particular group of specimens.

As discussed in Section III, the flanges of all specimens bent upward at both ends and showed very large deformations. Figure 26 shows the typical relationship between the end reaction per web and end flange tip deformation. Also included in this plot are the deformations under the predicted ultimate load and the allowable web crippling load based on the 1980 Specification. It can be seen that, if the end flange tip deformation is considered as the design criteria, the web crippling equation of the 1980 Specification seems reasonable.

C. I-sections subjected to interior one-flange loading

Cross sectional properties of I-sections used for the interior one-flange loading tests are given in Table 3c and parameters used in the computations are given in Table 9. The comparisons of the predicted failure loads calculated on the basis of the 1981 Guide and the 1980 Specification and the tested failure loads are presented in Table 10. The symbols used in Table 10 are defined as follows:

- 1)  $P_{test}$  is the tested failure load per web, kips.
- 2)  $P_{cg}$  is the ultimate web crippling load per web calculated on the basis of the 1981 Guide (Eq. (4)), kips.
- 3)  $P_{cs}$  is the ultimate web crippling load per web calculated on the basis of the 1980 Specification (Eq. (10)), kips.
- 4)  $P_{test}/P_{cg}$  is the ratio of the tested failure load to the predicted failure load based on the 1981 Guide.
- 5)  $P_{test}/P_{cs}$  is the ratio of the tested failure load to the predicted failure load based on the 1980 Specification.

The relationship between the ratio  $P_{test}/P_{comp}$  and  $F_y$  is shown graphically in Fig. 27. It can be seen that the 1981 Guide can provide good estimates for all specimens. The accuracy of predictions based on the 1981 Guide are within 20%.

However, the predicted values based on the 1980 Specification are not quite as close. This discrepancy seems

to be, at least partially, because of the  $F_y$  function,  $F_y(1.49 - 0.5(F_y/33))$ . The value of this function must be  $\geq 0.6F_y$ . Figure 28 shows this function graphically both with and without the  $0.6F_y$  limitation. According to this group of test data, the limitation of this  $F_y$  function should be slightly smaller than  $0.6F_y$ .

D. I-sections subjected to end one-flange loading:

The cross sectional properties and important parameters for I-sections used for end one-flange loading tests are given in Tables 3d and 11, respectively.

As discussed in Section III, failure occurred by bending of the flanges about the screw locations and thus, the failure was not one of web crippling. Since the failure mode was not web crippling, a comparison of the predicted ultimate web crippling loads and the failure loads would be meaningless. By roughly checking, it appeared that the tested failure load occurred at about one half the capacity predicted by both the 1981 Guide and the 1980 Specification.

This subject should be considered in the future study.

## V. DEVELOPMENT OF NEW EQUATIONS

This Section includes the development of new equations for predicting the ultimate web crippling loads for single unreinforced webs and the comparisons with tested failure loads. These equations are derived for the interior one-flange loading condition and end one-flange loading condition. As discussed in Section IV, the AISI equations for predicting the ultimate web crippling loads are not suitable for single unreinforced webs using very high strength sheet steels. Even though some attempts have been made on the modification of the function of yield strength to accommodate this situation, comparisons of the tested and the predicted values indicate that further improvements of the function of  $F_y$  and the formulation of the design equation are desirable.

The research work has been concentrated on the possible improvement of the prediction of failure loads caused by web crippling. In order to obtain the desired general equations, the theoretical background information on the buckling of flat plates subjected to edge loading has been reviewed and summarized as follows:

### 1. Flat Plates Subjected to a Uniformly Distributed Load

The elastic critical buckling load for a simply supported flat plate subjected to a uniformly distributed load, as shown in Fig. 29a, can be determined by Eq. (21):<sup>13</sup>

$$P_{cr} = K \eta^2 D / h^2 \quad (21)$$

where  $P_{cr}$  = elastic critical buckling load (per unit

length of the plate)

$D$  = flexural rigidity of the plate,  $Et^2/12(1-\mu^2)$

$E$  = Young's modulus of elasticity

$\mu$  = Poisson's ratio

$t$  = thickness of the plate

$K$  = buckling coefficient depending on the aspect ratio,  $L/h$

$h$  = depth of the plate

$L$  = length of the plate

As shown in Fig. 29b, the buckling coefficient,  $k$ , approaches 1 for long plates.

## 2. Flat Plates Subjected to Two Equal and Opposite Concentrated Loads

The elastic critical buckling load for a simply supported rectangular plate subjected to two equal and opposite concentrated loads (Fig. 30a) can be determined by using Eq. (22):<sup>14,15</sup>

$$P_{cr} = K \pi^2 D/h \quad (22)$$

where  $P_{cr}$  is the elastic critical buckling load and  $K$ ,  $D$  and  $h$  are defined previously.

The relationship between the buckling coefficient,  $K$ , and the aspect ratio,  $L/h$ , is shown in Fig. 30b.

## 3. Flat Plates Subjected to Two Equal and Opposite Partial Loads

The critical load for a simply supported rectangular plate subjected to two opposite edge loading (Fig. 31a) can be computed from Eq. (23):<sup>16,17</sup>

$$P_{cr} = K\pi^2 D/h \quad (23)$$

where  $P_{cr}$  = elastic critical buckling load

$K$  = buckling coefficient depending on  $L/h$  and  $N/h$   
ratios  $D$  and  $h$  are defined previously.

Figure 31b shows the buckling coefficient,  $K$ , which is the function of the aspect ratio,  $L/h$ , and the parameter  $N/h$ .

#### 4. Flat Plates Subjected to Partial Load on One Edge

The elastic buckling load for a simply supported plate subjected to partial edge loading as shown in Fig. 32a can be determined from:<sup>18</sup>

$$P_{cr} = K\pi^2 D/L^2 \quad (24)$$

where  $P_{cr}$  = elastic critical buckling load

$K$  = buckling coefficient depending on  $N/L$   
 $h/L$  ratios

$N$  = bearing length of the applied load  $D$  and  $L$  are defined previously. The value of buckling coefficient,  $K$ , is shown in Fig. 32b.

According to Khan and Walker,<sup>16,17</sup> the buckling load of this type can also be determined from Eq. (23) with an appropriate buckling coefficient,  $K$ . Figure 33 gives the value of buckling coefficient,  $K$ , which is the function of nondimensional parameters  $N/h$  and  $L/h$ .

Equation (23) may be written as:

$$P_{cr} = K\pi^2 (Et^3/12(1-\mu^2))/h \quad (25)$$

By considering  $\pi$  and  $\mu$  as constants and noting that  $K$  is the function of  $L/h$  and  $N/h$ , Eq. (25) can be expressed in the form:

$$(P_{cr}/Et^2) = f(h/t, N/h, L/h) \quad (26)$$

It can be seen from Eq. (26) that all parameters are nondimensional which can be used in developing the empirical formulas.

The development of new equations reported herein are based on the available data from :

- 1) Previous UMR tests reported in Ref. 11
- 2) Recent UMR tests conducted by Lin<sup>19</sup>
- 3) New tests conducted in this phase of investigation

The data from Refs. 11 and 19 that were used in the derivation are presented in Appendix B. The ranges of parameters used in this study are:

<u>Parameter</u>	<u>Range</u>
Thickness of specimen, in.	0.047 - 0.082
Depth of section, in.	3.0 - 12.0
Yield strength, ksi	36.26 - 141.2
h/t	92.8 - 258.5
N/t	19.3 - 63.8
N/h	0.10 - 0.70
R/t	0.96 - 5.70

The data in Refs. 23 and 24 was not included in the derivation of equations. The data from Ref. 23 was not used since the exact span lengths and clear distances between bearing plates, which are important parameters in the derived equations, were not specified.

The test data reported in Ref. 24 is primarily for multi-web sections with slanted webs. Since the equations derived in this report apply only to vertical webs, the data in Ref. 24 was not applicable to the present study.

The nonlinear least square iteration technique has been used to develop the constants for these empirical formulas. The development of new equations are as follows:

A. Single Webs Subjected to Interior One-Flange Loading Condition

A total of 72 specimens (28 from Ref. 11, 20 from Ref. 19 and 24 new tests) were separated into two different types of web crippling failure. They are overstressing underneath the bearing plate and web buckling. The same approach has been used for the design of aluminum structures.<sup>20</sup>

Since the previous UMR study did not separate the failure modes into these two types, attempt has been made to categorize these data step by step as follows:

- 1) Select the UMR data with  $h/t$  values less than 150, which were believed to fail by overstressing.
- 2) Develop an equation to predict the failure load caused by overstressing.
- 3) Select the UMR data with  $h/t$  values greater than 200, which were believed to have the buckling type of failure.
- 4) Combine the data selected for web buckling with the data of 100XF and 140XF specimens, which were observed to fail by web buckling, and develop another equation.



- 5) Calculate the predicted failure loads for all specimens by using the equations obtained from steps 2 and 3 and use the smaller value of the two to govern the design.
- 6) Separate all UMR data into two types of failure based on the expected failure modes determined from step 5.
- 7) Reiterate steps 2, 4, 5 and 6 until there was no change in failure mode of each specimen.

For the type of failure caused by overstressing, the equation is determined from the basic nondimensional terms such as  $P/(t^2F_y)$ ,  $N/t$  and  $R/t$ . The European recommendations<sup>21</sup> indicate that the ratio  $h/t$  has little or no influence on this localized failure. The equation of this type was determined to be

$$(P_{cy}/(t^2F_y)) = f(N/t, R/t) \quad (27)$$

and the empirical equation was found to be

$$(P_{cy}/(t^2F_y)) = 13.15(1+.00711(N/t))(1-.064(R/t)) \quad (28)$$

$$\text{or } P_{cy} = 13.15t^2F_y(1+.00711(N/t))(1-.064(R/t)) \quad (29)$$

For the type of failure caused by buckling of webs, the equation was determined in the same manner as the buckling of plate subjected to partial edge loading. The important nondimensional parameters used in plate buckling as discussed previously are  $P/(t^2E)$ ,  $N/h$ ,  $h/t$  and  $L/h$ . In determining this equation the parameter  $L/h$  is replaced by  $e/h$ , where  $e$  is the clear distance between the closest opposite bearing plates. By using this "e" value, the newly developed equation may be applied to either symmetric or unsymmetric loading.

Furthermore, the modulus of elasticity for cold-formed steel structures is considered to be a constant value of 29,500 ksi.

The form of the web buckling equation may be written as

$$P_{cb} = t^2 f((N/h), (h/t), e/h) \quad (30)$$

This equation was derived as

$$P_{cb} = 818.7t^2(1+2.403(N/h))(1-.00172(h/t)) \\ (1-0.12(e/h)) \quad (31)$$

The above equation is applicable only for the following conditions:

$$(1+2.403(N/h)) \leq 1.96$$

$$(1-.00172(h/t)) \leq 0.81$$

and  $(1-0.120(e/h)) \geq 0.34$

An interaction equation for combined bending moment and web crippling was derived from 47 previous UMR tests (Appendix B). (The yield strength for these tests ranged from 33.5 to to 53.8 ksi.) Because two compressive stress components are applied to the web element under the bearing plate, stress ratios can be used in the derivation of the interaction equation as done in the aircraft industry<sup>22</sup>. The format of this equation can be expressed as

$$(f_b/F_{b_{wu}}) + A(f_c/F_y) \leq B \quad (32)$$

$$\text{or } (f_b/F_{b_{wu}})^C + (f_c/F_y)^D \leq 1.0 \quad (33)$$

where  $f_b$  = Actual compression stress at junction of

flange and web, ksi

$F_{b_{wu}}$  = Maximum compression stress in the flat web of

beam due to bending, ksi

$F_y$  = Yield stress, ksi

A,B,C,D = constants which may be determined from test data

The value of  $f_c$  is determined as follows:

First, compute the effective bearing width,  $N_e$ , as the width required to develop a uniform stress distribution equal to the yield stress such that the total load on this "effective width" is equal to the actual failure load,  $P_{cy}$ . In other words,

$$N_e = P_{cy}/F_y t \quad (34)$$

The equivalent uniform stress distribution,  $f_c$ , may then be expressed as

$$f_c = P_{mc}/N_e t \quad (35a)$$

or, substituting Eq. (34),

$$f_c = P_{mc}/(P_{cy}/F_y) \quad (35b)$$

in which  $P_{mc}$  is the ultimate load for combined bending moment and web crippling, kips, and  $P_{cy}$  can be determined from Eq. (29). These interaction formulas were determined to be

$$(f_b/F_{bwu}) + 1.055(f_c/F_y) \leq 1.38 \quad (36)$$

$$\text{or } (f_b/F_{bwu})^{2.33} + (f_c/F_y)^{1.53} \leq 1.0 \quad (37)$$

Equations (36) and (37) are plotted in Fig. 34.

For the convenience of performing calculations, the load ratio ( $P_{mc}/P_{cy}$ ) may be used in place of ( $f_c/F_y$ ) as:

$$(f_b/F_{bwu}) + 1.055(P_{mc}/P_{cy}) \leq 1.38 \quad (38)$$

$$\text{or } (f_b/F_{bwu})^{2.33} + (P_{mc}/P_{cy})^{1.53} \leq 1.0 \quad (39)$$

It should be noted that the predicted failure load  $P_{cy}$  (Eq. (29)) or  $P_{mc}$  (Eq. (38) or (39)) should be checked against  $P_{cb}$  determined by Eq. (31). The smaller value between these predicted loads will govern the design.

The failure loads predicted by employing these newly developed equations (Eqs. (29), (31), (38) and (39)) for the present UMR tests and Inland tests were compared with the tested failure loads and are presented in Tables 12, 13, 15 and 16. The symbols used in these tables are the same as that in Table 6 except that  $P_{cy}$ ,  $P_{mc}$  and  $P_{cb}$  are determined by Eqs. (29), (36 or 37) and (31), respectively. Figure 35 is a plot of the ratio  $P_{test}/P_{comp}$  vs.  $F_y$  for the specimens expected to fail by web crippling or the combination of web crippling and bending moment. It can be seen that these newly developed equations can give reasonable prediction of failure loads for specimens with any level of yield strengths. The predictions are within 20% of the actual failure loads.

#### B. Single Webs Subjected to End One-Flange Loading Condition

A total of 82 tests (38 from Ref. 11, 20 from Ref. 19 and 24 new tests) were used in the derivation of these equations. The technique used in this case is similar to that for the interior one-flange loading condition.

For the type of failure caused by overstressing the ultimate load may be predicted by

$$P_{cy} = 9.90t^2F_y(1+.0122(N/t))(1-.247(R/t)) \quad (40)$$

with  $(1-.247(R/t)) \leq 0.68$

For failure caused by web buckling the ultimate load is given as

$$P_{cb} = 1385t^2(1-.00348(h/t))(1-.298(e/h)) \quad (41)$$

In the above equation,  $(1-.00348(h/t)) \geq 0.68$  and  $(1-.298(e/h)) \geq 0.52$

It should be noted that the effect of  $N/h$  on web buckling had been considered in the derivation of Eq. (41) and was found to be negligible. The smaller value of  $P_{cy}$  and  $P_{cb}$  is considered to be the predicted web crippling load.

These new equations were used for determining the expected failure loads for 24 hat sections used in this experimental study. The comparisons of these predicted values and the tested failure loads are presented in Table 14 and are shown graphically in Fig. 36. In Table 14 the values of  $P_{cy}$  and  $P_{cb}$  were determined by Eqs. (40) and (41), respectively.  $P_{cu}$  is the governing web crippling load which is the smaller value of  $P_{cy}$  and  $P_{cb}$ , kips. The accuracy of prediction using these equations has been improved as illustrated by the mean value of 1.063 with a standard deviation of 0.063.

These newly developed equations are intended for application with any material strength and any clear distance between opposite bearing plates. Since Eqs. (31) and (41) are independent of  $F_y$ , these two equations are applicable to sections with any strength of material.

It should be noted that Eqs. (29) and (40) have not been verified by any test data using yield strengths exceeding 88.3 ksi. Furthermore, all the available data were obtained from the tests with symmetric loading condition only. In order to assure the generality of these equations, some future tests are needed as proposed in Section VI.

## VI. PROPOSED FUTURE STUDY

The development of new equations for predicting the ultimate web crippling load under interior one-flange loading condition for sections with single unreinforced webs was discussed in Section V. These equations are intended for the use of sections fabricated from different yield strengths and subjected to symmetric or unsymmetric loading. In order to ensure the validity of these equations for general application, additional future tests are needed as follows:

### 1) Unsymmetric Loading Tests to Verify Equation (31)

Web crippling caused by buckling in the web of single unreinforced web subjected to interior one-flange loading can be predicted by using Eq. (31). This equation was derived from the data obtained from the type of symmetric loading only. Testing of unsymmetric loading type is needed and should be performed in the same manner as the symmetric loading type except that the concentrated load will not be applied at midspan. Sections with high strength materials are used to ensure the buckling type failure. Span length should be kept relatively short to prevent bending failure.

The proposed specimens for this case are hat sections as shown in Fig. 2. These specimens will be cold-formed from 100XF and 140XF sheet steels. Three different profiles of cross sections as shown in Table 2a should be used. Two 4-in. bearing plates will be used at both ends, and a 2-in. bearing plate will be placed under the concentrated load. The number of specimens and the testing arrangement are shown in Table 17 and Fig. 37, respectively.

2) Tests of Sections With High Strength Materials to Verify Equation (29)

Equation (29) is used to predicted the web crippling caused by overstressing under the bearing plate of single unreinforced web subjected to interior one-flange loading. This equation has not been verified by any test data having yield strengths larger than 88.3 ksi.

The same profile of cross sections as proposed for the previous case will be used. The specimens will be cold-formed from 100XF and 140XF sheet steels. The testing arrangement (Fig. 38) is the same as the one used in this phase of study except that stiffeners will be attached to both webs to prevent the web buckling type of failure. The number of tests are shown in Table 18.

In order to prevent the webs from buckling, stiffeners should be attached to the webs. Since Eq. (29) is independent of  $h/t$  ratio, it is believed the addition of stiffeners will have no effect on the ultimate load caused by overstressing under the bearing plates.

As mentioned earlier, the 1981 Guide was based primarily on the 1968 edition of the AISI Specification. The provisions for web crippling under interior two-flange loading condition and end two-flange loading condition were added to the 1980 Specification. Furthermore, the present AISI design recommendations are applicable only to materials with low to moderate yield strengths. Additional data on web crippling of sections with high strength materials under these two

loading conditions are also needed to keep the Guide updated with the present Specification and to extend the limitation of yield strength.

The proposed specimens for the future study of these subjects are hat sections and I-beams (Figs. 2 and 3). These specimens will be cold-formed from 80DK, 80XF, 100XF and 140XF sheet steels which have been used in this phase of investigation. The cross sectional profiles are given in Tables 2a and 2b. The numbers of specimens and testing arrangement for these loading conditions are proposed as follows:

- 1) For the interior two-flange loading condition, 24 hat sections and 24 I-beams, as proposed in Tables 19 and 20, should be tested by using two 2-in. bearing plates above and below the beam specimens at mid length as shown in Fig. 39.
- 2) For the end two-flange loading condition, the same number of specimens (Tables 20 and 21) will also be used. As shown in Fig. 40, two 2-in. bearing plates will be placed above and below the beams at one end of the specimens. An elastic support will be placed under the other end to level the specimens during testing.

It should be noted that the sheet steels that are needed to form these specimens are not available. The proposed program for using these sheet steels is consistent with the present experimental study.



## VII. CONCLUSIONS

Various types of high strength sheet steels with yield strengths greater than 80 ksi are now available for engineers to reduce car weight for the purpose of achieving fuel economy and complying with Federal safety standards. In this phase of research work, 48 hat sections and 36 I-beams were tested as flexural members to determine their ultimate web crippling loads. These sections were fabricated from high strength sheet steels with yield strengths ranging from 58.2 to 141.2 ksi.

The results of tests have been evaluated according to the 1981 Guide<sup>1</sup> and the 1980 Specification<sup>3</sup> with some modification of the  $F_y$  function. It was found that the available design provisions for web crippling are capable of improving when they are used for hat sections cold-formed from very high strength materials.

Test data show that both the 1981 Guide and the 1980 Specification can provide reasonable predictions for web crippling loads for I-beams subjected to interior one-flange loading. However, for the end one-flange loading condition, it was unable to compare the test data with the design expressions because the specimens failed prematurely at the web-flange juncture under the loads much less than the expected web crippling loads.

Attempts have been made to develop new equations to determine the web crippling loads for single unreinforced webs. Two types of equations were developed for determining the ultimate loads dealing with the buckling type failure and overstressing failure. Interaction equations for the combination of bending moment and web crippling were also derived in terms of the stress ratio.

These newly developed equations have been used to compare the available test data. As indicated by the comparisons presented in various tables, the new equations can provide reasonable estimations of the web crippling strength.

More experimental investigation is needed for the future study in order to confirm the validity of the newly developed equations and to improve other design criteria. The required tests are proposed in this report.

## VIII. ACKNOWLEDGMENTS

The research work reported herein was conducted in the Department of Civil Engineering at the University of Missouri-Rolla under the sponsorship of the American Iron and Steel Institute.

The financial assistance granted by the Institute and the technical guidance provided by members of the AISI Task Force on Structural Design and Research of the Transportation Department and the AISI staff are gratefully acknowledged. These members are: Messrs. S. J. Errera, D. M. Bench, A. E. Cornford, Jim Davidson, Charles Haddad, Emil Hanburg, Al Houchens, L.J. Howell, A. L. Johnson, R. G. Lang, B. S. Levy, Kuang-Huei Lin, Hickmat Mahmood, Don Malen, D. J. Meuleman, M. S. Rashid, Joe Rice, W. J. Riffe, Brian Taylor, R. J. Traficanti, T. L. Treece, M. T. Vecchio and David Whittaker.

Also, special thanks are expressed to the Research Laboratory of Inland Steel Company for forming some of the specimens.

Appreciation is expressed to Messrs. K. Haas, J. Tucker, and R. Haselhorst, staff of the Department of Civil Engineering, for their support.

Thanks are due to Messr. M. B. Parks for his valuable assistance in preparing and testing the specimens and Mrs. Deanne Larson for the typing that she did in this report.

## IX. REFERENCES

1. American Iron and Steel Institute, "Guide for Preliminary Design of Sheet Steel Automotive Structural Components," 1981 Edition.
2. American Iron and Steel Institute, "Specification for the Design of Cold-Formed Steel Structural Members," 1968 Edition.
3. American Iron and Steel Institute, "Specification for the Design of Cold-Formed Steel Structural Members," 1980 Edition.
4. Errera, S.J., "Automotive Structural Design Using the AISI Guide," SAE Technical Paper Series 820021, February 22-26, 1982.
5. Levy, B.S., "Advances in Designing Ultra High Strength Steel Bumper Reinforcement Beams," SAE Technical Paper Series 830399.
6. Vecchio, M.T., "Design Analysis and Behavior of a Variety of As-Formed Mild and High Strength Sheet Materials in Large Deflection Bending," SAE Technical Paper Series 830398.
7. Levy, B.S., "Predicting Yield Strength and Tensile Strength After Forming for Automotive Integral Body Structural Rail Type Parts," SAE Technical Paper Series 840009.
8. Vecchio, M.T., "Forming Technology - A Design Parameter for the Eighties," Body Engineering Journal, Spring 1984.
9. Yu, W.W., Santaputra, C., and Parks, M.B., "Design of Automotive Structural Components Using High Strength Sheet Steels," First Progress Report, Civil Engineering Study 83-1, University of Missouri-Rolla, January 1983.

10. Santaputra, C., and Yu, W.W., "Design of Automotive Structural Components Using High Strength Sheet Steels: Strength of Beams," Third Progress Report, Civil Engineering Study 83-4, University of Missouri-Rolla, August 1983.
11. Hetrakul, N., and Yu, W.W., "Structural Behavior of Beam Webs Subjected to Web Crippling and a Combination of Web Crippling and Bending," Final Report, Civil Engineering Study 78-4, University of Missouri-Rolla, June 1978.
12. Parks, M.B., and Yu, W.W., "Design of Automotive Structural Components Using High Strength Sheet Steels: Mechanical Properties of Materials," Second Progress Report, Civil Engineering Study 83-3, University of Missouri-Rolla, August 1983.
13. Timoshenko, S. P., and Gere, G. M., "Theory of Elastic Stability," 2nd Edition, McGraw-Hill, New York, 1961.
14. Timoshenko, S. P., Zeitschrift fur Math. und Physik, Vol. 58, 1910.
15. Yamaki, N., "Buckling of a Rectangular Plate Under Locally Distributed Force Applied on the Two Opposite Edges," 1st and 2nd Report, The Institute of High Speed Mechanics, Tohoku University, Japan, Vol. 3, 1953.
16. Khan, M. Z., and Walker, A. C., "Buckling of Plates Subjected to Localised Edge Loading," The Structural Engineer, Vol. 50, No. 6, June 1972, pp. 225-232.
17. Walker, A. C., "Design and Analysis of Cold-Formed Sections," John Wiley and Sons, Inc., New York, 1975.
18. Zetlin, L., "Elastic Instability of Flat Plates Subjected to Partial Edge Loads," Proceedings, American Society of Civil Engineers, Vol. 81, September 1955.

19. Lin, S. H., "Structural Behavior of Cold-Formed Steel Beam Webs Subjected to Partial Edge Loading," Master Thesis, Civil Engineering Department, University of Missouri-Rolla, (in preparation).
20. Aluminum Association, "Specification for Aluminum Structures," 3rd Ed., April 1976.
21. StBK-N5., "Code for the Structural Use of Steel and Aluminum Sheeting," National Swedish Committee on Regulations for Steel Structures, Stockholm, 1978.
22. Peery, D.J., "Aircraft Structures," McGraw-Hill Book Company, New York, 1950.
23. Cornell University, 65th and 66th Progress Reports on Light Gage Steel Beams of Cold-Formed Steel, September 1952 and January 1953, respectively (unpublished).
24. Wing, Bradley A. and Schuster, R. M., "Web Crippling and the Interaction of Bending and Web Crippling of Unreinforced Multi-Web Cold Formed Steel Sections, Volumes 1 and 2, University of Waterloo, 1981.

TABLE 1  
Material Properties and Thicknesses of Sheet Steels  
Used in the Experimental Study<sup>9,12</sup>

Material Designation	$F_y$ (ksi)	$F_u$ (ksi)	t (in.)
80DK	58.2	87.6	0.048
80XF	88.3	98.7	0.082
100XF	113.1	113.1	0.062
140XF	141.2	141.2	0.047

TABLE 2a

Nominal Dimensions of Hat Sections Designed for Experimental Study

Profile No.	B1 (in.)	B2 (in.)	D1 (in.)	R (in.)
1	3.0	6.0	3.0	0.25
2	4.0	8.0	4.0	0.25
3	5.0	10.0	5.0	0.25

Note: See Fig. 2 for definitions of symbols.

TABLE 2b

Nominal Dimensions of I-Sections Designed for Experimental Study

Profile No.	B1 (in.)	D1 (in.)	R (in.)
1	3.0	3.0	0.25
2	4.0	4.0	0.25
3	5.0	5.0	0.25

Note: See Fig. 3 for definitions of symbols.

TABLE 3a  
 Dimensions of Specimens for Hat Sections Used for  
 Interior One-Flange Loading Condition

Specimen No.	Cross-Sectional Dimensions (in.)					Span Length (in.)
	t	B1	B2	D1	R	
1-HI-11	0.048	3.180	6.384	3.150	0.234	15.0
1-HI-12	0.048	3.250	6.374	3.140	0.234	15.0
1-HI-21	0.048	4.330	8.494	4.080	0.250	18.0
1-HI-22	0.048	4.330	8.454	4.070	0.273	18.0
1-HI-31	0.048	5.380	10.564	4.990	0.242	21.0
1-HI-32	0.048	5.400	10.544	5.000	0.250	21.0
2-HI-11	0.082	3.540	6.596	3.040	0.203	15.0
2-HI-12	0.082	3.560	6.576	3.070	0.227	15.0
2-HI-21	0.082	4.590	8.706	4.050	0.227	18.0
2-HI-22	0.082	4.550	8.666	4.060	0.227	18.0
2-HI-31	0.082	5.470	10.586	5.060	0.219	21.0
2-HI-32	0.082	5.490	10.626	5.070	0.219	21.0
3-HI-11	0.062	3.480	6.556	3.080	0.195	15.0
3-HI-12	0.062	3.490	6.506	3.090	0.164	15.0
3-HI-21	0.062	4.410	8.506	4.040	0.164	18.0
3-HI-22	0.062	4.370	8.526	4.050	0.156	18.0
3-HI-31	0.062	5.360	10.496	5.040	0.133	21.0
3-HI-32	0.062	5.340	10.496	5.010	0.172	21.0
4-HI-11	0.047	3.250	6.296	3.110	0.086	15.0
4-HI-12	0.047	3.210	6.216	3.130	0.070	15.0
4-HI-21	0.047	4.100	8.186	4.160	0.133	18.0
4-HI-22	0.047	4.090	8.196	4.190	0.125	18.0
4-HI-31	0.047	4.950	10.096	5.160	0.094	21.0
4-HI-32	0.047	5.010	10.116	5.160	0.102	21.0

See Fig. 2 for definitions of symbols.



TABLE 3b

Dimensions of Specimens for Hat Sections Used for  
End One-Flange Loading Condition

Specimen No.	Cross-Sectional Dimensions (in.)					Span Length (in.)
	t	B1	B2	D1	R	
1-HE-11	0.048	3.162	6.200	3.166	0.211	15.0
1-HE-12	0.048	3.185	6.178	3.166	0.203	15.0
1-HE-21	0.048	4.453	8.470	4.026	0.203	18.0
1-HE-22	0.048	4.330	8.454	4.046	0.211	18.0
1-HE-31	0.048	5.410	10.537	5.016	0.203	21.0
1-HE-32	0.048	5.390	10.313	5.006	0.211	21.0
2-HE-11	0.082	3.557	6.482	3.044	0.211	15.0
2-HE-12	0.082	3.593	6.420	3.054	0.203	15.0
2-HE-21	0.082	4.552	8.554	4.034	0.203	18.0
2-HE-22	0.082	4.596	8.656	4.034	0.203	18.0
2-HE-31	0.082	5.490	10.500	5.074	0.211	21.0
2-HE-32	0.082	5.558	10.626	5.054	0.203	21.0
3-HE-11	0.062	3.486	6.449	3.024	0.203	15.0
3-HE-12	0.062	3.517	6.612	3.034	0.180	15.0
3-HE-21	0.062	4.380	8.538	4.034	0.188	18.0
3-HE-22	0.062	4.397	8.510	4.014	0.188	18.0
3-HE-31	0.062	5.413	10.520	5.044	0.195	21.0
3-HE-32	0.062	5.380	10.482	5.044	0.211	21.0
4-HE-11	0.047	3.160	6.173	3.204	0.117	17.0
4-HE-12	0.047	3.275	6.366	3.084	0.156	17.0
4-HE-21	0.047	4.148	8.335	4.104	0.164	20.0
4-HE-22	0.047	4.224	8.347	4.084	0.180	20.0
4-HE-31	0.047	5.200	10.463	5.154	0.148	23.0
4-HE-32	0.047	5.052	10.130	5.144	0.117	23.0

See Fig. 2 for definitions of symbols.

TABLE 3c  
 Dimensions of Specimens for I-Sections Used for  
 Interior One-Flange Loading Condition

Specimen No.	Cross-Sectional Dimensions (in.)				Span Length (in.)
	t	B1	D1	R	
1-II-11	0.048	3.240	3.036	0.219	15.0
1-II-12	0.048	3.221	3.080	0.219	15.0
1-II-21	0.048	4.314	4.038	0.219	18.0
1-II-22	0.048	4.248	4.056	0.219	18.0
1-II-31	0.048	5.266	5.062	0.219	21.0
1-II-32	0.048	5.252	5.093	0.219	21.0
2-II-11	0.082	3.297	3.190	0.219	15.0
2-II-12	0.082	3.298	3.146	0.219	15.0
2-II-21	0.082	4.285	4.162	0.219	18.0
2-II-22	0.082	4.290	4.141	0.219	18.0
2-II-31	0.082	5.327	5.135	0.219	21.0
2-II-32	0.082	5.296	5.085	0.219	21.0
3-II-11	0.062	3.302	3.084	0.188	15.0
3-II-12	0.062	3.240	3.119	0.188	15.0
3-II-21	0.062	4.258	4.090	0.188	18.0
3-II-22	0.062	4.261	4.093	0.188	18.0
3-II-31	0.062	5.279	5.094	0.188	21.0
3-II-32	0.062	5.266	5.102	0.188	21.0

See Fig. 3 for definitions of symbols.

TABLE 3d  
 Dimensions of Specimens for I-Sections Used for  
 End One-Flange Loading Condition

Specimen No.	Cross-Sectional Dimensions (in.)				Span Length (in.)
	t	B1	D1	R	
1-IE-11	0.048	3.230	3.023	0.219	15.0
1-IE-12	0.048	3.227	3.071	0.219	15.0
1-IE-21	0.048	4.261	4.048	0.219	18.0
1-IE-22	0.048	4.266	4.022	0.219	18.0
1-IE-31	0.048	5.279	5.044	0.219	21.0
1-IE-32	0.048	5.237	5.080	0.219	21.0
2-IE-11	0.082	3.281	3.130	0.219	15.0
2-IE-12	0.082	3.283	3.152	0.219	15.0
2-IE-21	0.082	4.240	4.152	0.219	18.0
2-IE-22	0.082	4.304	4.128	0.219	18.0
2-IE-31	0.082	5.301	5.102	0.219	21.0
2-IE-32	0.082	5.347	5.098	0.219	21.0
3-IE-11	0.062	3.264	3.190	0.188	15.0
3-IE-12	0.062	3.267	3.102	0.188	15.0
3-IE-21	0.062	4.260	4.111	0.188	18.0
3-IE-22	0.062	4.355	4.072	0.188	18.0
3-IE-31	0.062	5.268	5.090	0.188	21.0
3-IE-32	0.062	5.249	5.093	0.188	21.0

See Fig. 3 for definitions of symbols.

TABLE 4a

Number of Web Crippling Tests on Hat Sections Subjected to  
Interior One-Flange Loading

Profile No.	Material Designation				Total
	80DK	80XF	100XF	140XF	
1	2	2	2	2	8
2	2	2	2	2	8
3	2	2	2	2	8
Total	6	6	6	6	24

Notes: See Fig. 4a for loading condition.  
Types of profiles are given in Table 2a.

TABLE 4b

Number of Web Crippling Tests on Hat Sections Subjected to  
End One-Flange Loading

Profile No.	Material Designation				Total
	80DK	80XF	100XF	140XF	
1	2	2	2	2	8
2	2	2	2	2	8
3	2	2	2	2	8
Total	6	6	6	6	24

Notes: See Fig. 4b for loading condition.  
Types of profiles are given in Table 2a.

TABLE 4c

Number of Web Crippling Tests on I-Sections Subjected to  
Interior One-Flange Loading

Profile No.	Material Designation				Total
	80DK	80XF	100XF	140XF	
1	2	2	2	-	6
2	2	2	2	-	6
3	2	2	2	-	6
Total	6	6	6	-	18

Notes: See Fig. 4a for loading condition.  
Types of profiles are given in Table 2b.

TABLE 4d

Number of Web Crippling Tests on I-Sections Subjected to  
End One-Flange Loading

Profile No.	Material Designation				Total
	80DK	80XF	100XF	140XF	
1	2	2	2	-	6
2	2	2	2	-	6
3	2	2	2	-	6
Total	6	6	6	-	18

Notes: See Fig. 4b for loading condition.  
Types of profiles are given in Table 2b.

TABLE 5

Parameters and Sectional Properties of Hat Sections  
for Interior One-Flange Loading Condition

Specimen No.	Material	t (in.)	F <sub>y</sub> (ksi.)	h/t	R/t	N/t	N/h
1-HI-11	80DK	0.048	58.2	63.6	4.883	41.7	0.655
1-HI-12	80DK	0.048	58.2	63.4	4.883	41.7	0.657
1-HI-21	80DK	0.048	58.2	83.0	5.208	41.7	0.502
1-HI-22	80DK	0.048	58.2	82.8	5.696	41.7	0.503
1-HI-31	80DK	0.048	58.2	102.0	5.046	41.7	0.409
1-HI-32	80DK	0.048	58.2	102.2	5.208	41.7	0.408
2-HI-11	80XF	0.082	88.3	35.1	2.477	24.4	0.695
2-HI-12	80XF	0.082	88.3	35.4	2.763	24.4	0.688
2-HI-21	80XF	0.082	88.3	47.4	2.763	24.4	0.515
2-HI-22	80XF	0.082	88.3	47.5	2.763	24.4	0.513
2-HI-31	80XF	0.082	88.3	59.7	2.668	24.4	0.408
2-HI-32	80XF	0.082	88.3	59.8	2.668	24.4	0.408
3-HI-11	100XF	0.062	113.1	47.7	3.150	32.3	0.677
3-HI-12	100XF	0.062	113.1	47.8	2.647	32.3	0.674
3-HI-21	100XF	0.062	113.1	63.2	2.647	32.3	0.511
3-HI-22	100XF	0.062	113.1	63.3	2.521	32.3	0.509
3-HI-31	100XF	0.062	113.1	79.3	2.142	32.3	0.407
3-HI-32	100XF	0.062	113.1	78.8	2.773	32.3	0.409
4-HI-11	140XF	0.047	141.2	64.2	1.828	42.6	0.663
4-HI-12	140XF	0.047	141.2	64.6	1.496	42.6	0.659
4-HI-21	140XF	0.047	141.2	86.5	2.826	42.6	0.492
4-HI-22	140XF	0.047	141.2	87.1	2.660	42.6	0.488
4-HI-31	140XF	0.047	141.2	107.8	1.996	42.6	0.395
4-HI-32	140XF	0.047	141.2	107.8	2.162	42.6	0.395

TABLE 6a

Comparisons of Tested and Predicted Failure Loads for Hat Sections  
for Interior One-Flange Loading Condition  
Based on the AISI 1981 Guide with Modified  $f(F_y)$

Specimen No.	$P_m$ (kips)	$P_c$ (kips)	$P_{mc}$ (kips)	$P_s$ (kips)	$P_{ms}$ (kips)	$P_{test}$ (kips)	Failure Mode*	$P_{test}/P_{comp}$
1-HI-11	7.273	3.312	2.958	7.699	5.366	2.850	MC	0.96
1-HI-12	7.232	3.313	2.954	7.699	5.351	2.800	MC	0.95
1-HI-21	9.324	3.069	3.002	7.699	5.987	2.930	MC	0.98
1-HI-22	9.316	2.950	2.913	7.699	5.985	2.930	MC	1.01
1-HI-31	11.146	2.952	2.952	6.418	5.585	2.900	C	0.98
1-HI-32	11.183	2.912	2.912	6.405	5.580	3.000	C	1.03
2-HI-11	19.856	12.865	10.149	24.031	15.791	10.800	MC	1.06
2-HI-12	20.151	12.612	10.084	24.282	15.994	10.730	MC	1.06
2-HI-21	26.493	12.289	10.913	27.675	19.514	11.480	MC	1.05
2-HI-22	26.561	12.286	10.920	27.675	19.538	11.400	MC	1.04
2-HI-31	32.454	12.032	11.411	27.675	21.315	12.530	MC	1.10
2-HI-32	32.572	12.029	11.420	27.675	21.346	12.750	MC	1.12
3-HI-11	16.991	7.156	6.546	17.906	12.566	8.580	MC	1.31
3-HI-12	16.920	7.401	6.693	17.906	12.538	8.600	MC	1.28
3-HI-21	21.948	7.138	7.002	17.284	13.718	8.580	MC	1.23
3-HI-22	22.029	7.195	7.051	17.240	13.714	8.530	MC	1.21
3-HI-31	24.812	7.093	7.093	13.768	12.039	8.650	C	1.22
3-HI-32	25.091	6.813	6.813	13.853	12.127	8.700	C	1.28
4-HI-11	13.904	4.548	4.455	9.776	8.066	5.440	MC	1.22
4-HI-12	13.941	4.639	4.525	9.712	8.036	5.200	MC	1.15
4-HI-21	11.805	4.019	3.898	7.252	6.179	5.450	MC	1.40
4-HI-22	11.745	4.057	3.920	7.199	6.138	5.480	MC	1.40
4-HI-31	9.334	3.999	3.640	5.820	4.939	5.400	MC	1.48
4-HI-32	9.342	3.957	3.614	5.820	4.940	5.260	MC	1.46
Mean Value								1.166
Standard Deviation								0.163

\* MC represents combined bending moment and web crippling  
C represents web crippling

TABLE 6b

Comparisons of Tested and Predicted Failure Loads for Hat Sections  
for Interior One-Flange Loading Condition  
Based on the AISI 1980 Specification with Modified  $f(F_y)$

Specimen No.	$P_m$ (kips)	$P_c$ (kips)	$P_{mc}$ (kips)	$P_s$ (kips)	$P_{ms}$ (kips)	$P_{test}$ (kips)	Failure Mode*	$P_{test}/P_{comp}$
1-HI-11	7.273	3.291	3.069	8.936	5.884	2.850	MC	0.93
1-HI-12	7.232	3.292	3.065	8.936	5.868	2.800	MC	0.91
1-HI-21	9.324	3.114	3.114	7.904	6.068	2.930	C	0.94
1-HI-22	9.316	2.993	2.993	7.924	6.077	2.930	C	0.98
1-HI-31	10.716	3.061	3.061	6.434	5.516	2.900	C	0.95
1-HI-32	10.746	3.021	3.021	6.421	5.512	3.000	C	0.99
2-HI-11	19.856	12.420	10.402	24.031	18.701	10.800	MC	1.04
2-HI-12	20.151	12.179	10.329	24.282	18.868	10.730	MC	1.04
2-HI-21	26.493	11.969	11.169	32.122	21.580	11.480	MC	1.03
2-HI-22	26.561	11.967	11.176	32.122	21.604	11.400	MC	1.02
2-HI-31	32.454	11.827	11.708	32.065	23.348	12.530	MC	1.07
2-HI-32	32.572	11.825	11.718	32.000	23.357	12.750	MC	1.09
3-HI-11	16.991	6.984	6.696	20.783	13.736	8.580	MC	1.28
3-HI-12	16.920	7.225	6.853	20.783	13.698	8.600	MC	1.25
3-HI-21	21.948	7.062	7.062	17.329	13.645	8.580	C	1.21
3-HI-22	22.029	7.119	7.119	17.284	13.639	8.530	C	1.20
3-HI-31	25.453	7.122	7.122	13.804	12.134	8.650	C	1.21
3-HI-32	25.473	6.838	6.838	13.888	12.194	8.700	C	1.27
4-HI-11	13.573	4.524	4.524	9.802	7.946	5.440	C	1.20
4-HI-12	13.582	4.616	4.616	9.737	7.913	5.200	C	1.13
4-HI-21	16.773	4.096	4.096	7.270	6.671	5.450	C	1.33
4-HI-22	16.884	4.138	4.138	7.217	6.636	5.480	C	1.32
4-HI-31	18.532	4.182	4.182	5.835	5.566	5.400	C	1.29
4-HI-32	18.546	4.138	4.138	5.835	5.566	5.260	C	1.27
Mean Value								1.123
Standard Deviation								0.139

\* MC represents combined bending moment and web crippling  
C represents web crippling



TABLE 7

Parameters and Sectional Properties of Hat Sections  
for End One-Flange Loading Condition

Specimen No.	Material	t (in.)	F <sub>y</sub> (ksi.)	h/t	R/t	N/t	N/h
1-HE-11	80DK	0.048	58.2	64.0	4.394	41.7	0.651
1-HE-12	80DK	0.048	58.2	64.0	4.231	41.7	0.651
1-HE-21	80DK	0.048	58.2	81.9	4.231	41.7	0.509
1-HE-22	80DK	0.048	58.2	82.3	4.394	41.7	0.506
1-HE-31	80DK	0.048	58.2	102.5	4.231	41.7	0.407
1-HE-32	80DK	0.048	58.2	102.3	4.394	41.7	0.407
2-HE-11	80XF	0.082	88.3	35.1	2.572	24.4	0.694
2-HE-12	80XF	0.082	88.3	35.2	2.477	24.4	0.692
2-HE-21	80XF	0.082	88.3	47.2	2.477	24.4	0.517
2-HE-22	80XF	0.082	88.3	47.2	2.477	24.4	0.517
2-HE-31	80XF	0.082	88.3	59.9	2.572	24.4	0.407
2-HE-32	80XF	0.082	88.3	59.6	2.477	24.4	0.409
3-HE-11	100XF	0.062	113.1	46.8	3.276	32.3	0.690
3-HE-12	100XF	0.062	113.1	46.9	2.898	32.3	0.687
3-HE-21	100XF	0.062	113.1	63.1	3.024	32.3	0.512
3-HE-22	100XF	0.062	113.1	62.7	3.024	32.3	0.514
3-HE-31	100XF	0.062	113.1	79.4	3.150	32.3	0.407
3-HE-32	100XF	0.062	113.1	79.4	3.402	32.3	0.407
4-HE-11	140XF	0.047	141.2	66.2	2.494	42.6	0.643
4-HE-12	140XF	0.047	141.2	63.6	3.326	42.6	0.669
4-HE-21	140XF	0.047	141.2	85.3	3.491	42.6	0.499
4-HE-22	140XF	0.047	141.2	84.9	3.823	42.6	0.501
4-HE-31	140XF	0.047	141.2	107.7	3.157	42.6	0.395
4-HE-32	140XF	0.047	141.2	107.4	2.494	42.6	0.396

TABLE 8

Comparisons of Tested and Predicted Failure Loads for Hat Sections  
for End One-Flange Loading Condition  
Based on the AISI 1981 Guide and 1980 Specification with Modified  $f(F_y)$

Specimen No.	$P_{test}$ (kips)	$P_{cg}$ (kips)	$P_{cs}$ (kips)	$P_{test}/P_{cg}$	$P_{test}/P_{cs}$
1-HE-11	0.719	0.600	0.428	1.20	1.68
1-HE-12	0.700	0.619	0.441	1.13	1.59
1-HE-21	0.694	0.571	0.430	1.22	1.61
1-HE-22	0.688	0.553	0.417	1.24	1.65
1-HE-31	0.669	0.515	0.417	1.30	1.60
1-HE-32	0.643	0.500	0.405	1.28	1.59
2-HE-11	2.919	2.308	1.770	1.26	1.65
2-HE-12	2.981	2.350	1.803	1.27	1.65
2-HE-21	2.994	2.265	1.774	1.32	1.69
2-HE-22	3.125	2.265	1.774	1.38	1.76
2-HE-31	2.713	2.135	1.711	1.27	1.58
2-HE-32	2.825	2.177	1.744	1.30	1.62
3-HE-11	2.050	1.254	0.913	1.63	2.25
3-HE-12	2.106	1.361	0.991	1.55	2.12
3-HE-21	2.006	1.248	0.944	1.61	2.13
3-HE-22	2.075	1.249	0.944	1.66	2.20
3-HE-31	1.894	1.138	0.897	1.66	2.11
3-HE-32	1.869	1.075	0.847	1.74	2.21
4-HE-11	1.313	0.909	0.648	1.44	2.02
4-HE-12	1.300	0.772	0.546	1.68	2.38
4-HE-21	1.219	0.672	0.509	1.81	2.39
4-HE-22	1.125	0.620	0.469	1.82	2.40
4-HE-31	1.088	0.647	0.532	1.68	2.04
4-HE-32	1.063	0.743	0.611	1.43	1.74
Mean Value				1.453	1.903
Standard Deviation				0.216	0.301

TABLE 9

Parameters and Sectional Properties of I-Sections  
for Interior One-Flange Loading Condition

Specimen No.	Material	t (in.)	F <sub>y</sub> (ksi.)	h/t	R/t	N/t	N/h
1-II-11	80DK	0.048	58.2	61.3	4.562	41.7	0.674
1-II-12	80DK	0.048	58.2	62.2	4.562	41.7	0.670
1-II-21	80DK	0.048	58.2	82.1	4.562	41.7	0.507
1-II-22	80DK	0.048	58.2	82.5	4.562	41.7	0.505
1-II-31	80DK	0.048	58.2	103.5	4.562	41.7	0.403
1-II-32	80DK	0.048	58.2	104.1	4.562	41.7	0.400
2-II-11	80XF	0.082	88.3	36.9	2.671	24.4	0.661
2-II-12	80XF	0.082	88.3	36.4	2.671	24.4	0.671
2-II-21	80XF	0.082	88.3	48.8	2.671	24.4	0.500
2-II-22	80XF	0.082	88.3	48.5	2.671	24.4	0.503
2-II-31	80XF	0.082	88.3	60.6	2.671	24.4	0.402
2-II-32	80XF	0.082	88.3	60.0	2.671	24.4	0.406
3-II-11	100XF	0.062	113.1	47.7	3.032	32.3	0.676
3-II-12	100XF	0.062	113.1	48.3	3.032	32.3	0.668
3-II-21	100XF	0.062	113.1	64.0	3.032	32.3	0.504
3-II-22	100XF	0.062	113.1	64.0	3.032	32.3	0.504
3-II-31	100XF	0.062	113.1	80.2	3.032	32.3	0.402
3-II-32	100XF	0.062	113.1	80.3	3.032	32.3	0.402

TABLE 10

Comparisons of Tested and Predicted Failure Loads for I-Sections  
for Interior One-Flange Loading Condition  
Based on the AISI 1981 Guide and 1980 Specification

Specimen No.	$P_{test}$ (kips)	$P_{cg}$ (kips)	$P_{cs}$ (kips)	$P_{test}/P_{cg}$	$P_{test}/P_{cs}$
1-II-11	2.450	2.423	2.775	1.01	0.88
1-II-12	2.400	2.423	2.775	0.99	0.86
1-II-21	2.625	2.423	2.775	1.08	0.95
1-II-22	2.450	2.423	2.775	1.01	0.88
1-II-31	2.325	2.423	2.775	0.96	0.84
1-II-32	2.350	2.423	2.775	0.97	0.85
2-II-11	8.750	9.603	11.203	0.91	0.78
2-II-12	8.775	9.603	11.203	0.91	0.78
2-II-21	9.300	9.603	11.203	0.97	0.83
2-II-22	9.463	9.603	11.203	0.99	0.84
2-II-31	9.175	9.603	11.203	0.96	0.82
2-II-32	9.500	9.603	11.203	0.99	0.85
3-II-11	6.175	7.434	8.561	0.83	0.72
3-II-12	6.325	7.434	8.561	0.85	0.74
3-II-21	6.825	7.434	8.561	0.92	0.80
3-II-22	6.563	7.434	8.561	0.88	0.77
3-II-31	5.912	7.434	8.561	0.80	0.69
3-II-32	6.250	7.434	8.561	0.84	0.73
Mean Value				0.937	0.812
Standard Deviation				0.075	0.066

TABLE 11

Parameters and Sectional Properties of I-Sections  
for End One-Flange Loading Condition

Specimen No.	Material	t (in.)	F <sub>y</sub> (ksi.)	h/t	R/t	N/t	N/h
1-IE-11	80DK	0.048	58.2	61.0	4.562	41.7	0.683
1-IE-12	80DK	0.048	58.2	62.0	4.562	41.7	0.672
1-IE-21	80DK	0.048	58.2	82.3	4.562	41.7	0.506
1-IE-22	80DK	0.048	58.2	81.8	4.562	41.7	0.509
1-IE-31	80DK	0.048	58.2	103.1	4.562	41.7	0.404
1-IE-32	80DK	0.048	58.2	103.8	4.562	41.7	0.401
2-IE-11	80XF	0.082	88.3	36.2	2.671	24.4	0.674
2-IE-12	80XF	0.082	88.3	36.4	2.671	24.4	0.669
2-IE-21	80XF	0.082	88.3	48.6	2.671	24.4	0.502
2-IE-22	80XF	0.082	88.3	48.3	2.671	24.4	0.505
2-IE-31	80XF	0.082	88.3	60.2	2.671	24.4	0.405
2-IE-32	80XF	0.082	88.3	60.2	2.671	24.4	0.405
3-IE-11	100XF	0.062	113.1	49.5	3.032	32.3	0.652
3-IE-12	100XF	0.062	113.1	48.0	3.032	32.3	0.672
3-IE-21	100XF	0.062	113.1	64.3	3.032	32.3	0.502
3-IE-22	100XF	0.062	113.1	63.7	3.032	32.3	0.507
3-IE-31	100XF	0.062	113.1	80.1	3.032	32.3	0.403
3-IE-32	100XF	0.062	113.1	80.1	3.032	32.3	0.402

TABLE 12

Comparisons of Tested and Predicted Failure Loads for Hat Sections  
for Interior One-Flange Loading Condition  
Based on Equations 29, 36 and 31

Specimen No.	$P_m$ (kips)	$P_{cy}$ (kips)	$P_{mc}$ (kips)	$P_{cb}$ (kips)	$P_{ms}$ (kips)	$P_{test}$ (kips)	Failure Mode*	$P_{test}/P_{comp}$
1-HI-11	7.273	3.143	2.925	4.938	5.884	2.850	MC	0.97
1-HI-12	7.232	3.143	2.923	4.935	5.868	2.800	MC	0.96
1-HI-21	9.324	3.048	3.039	4.915	6.068	2.930	MC	0.96
1-HI-22	9.316	2.905	2.905	4.912	6.077	2.930	C	1.01
1-HI-31	10.716	3.095	3.095	4.896	5.516	2.900	C	0.94
1-HI-32	10.746	3.048	3.048	4.898	5.512	3.000	C	0.98
2-HI-11	19.856	15.418	11.823	14.220	18.701	10.800	MC	0.91
2-HI-12	20.151	15.082	11.740	14.254	18.868	10.730	MC	0.91
2-HI-21	26.493	15.082	12.924	14.263	21.580	11.480	MC	0.89
2-HI-22	26.561	15.082	12.931	14.271	21.604	11.400	MC	0.88
2-HI-31	32.454	15.194	13.818	14.289	23.348	12.530	MC	0.91
2-HI-32	32.572	15.194	13.843	14.295	23.357	12.750	MC	0.92
3-HI-11	16.991	11.223	9.117	8.180	13.736	8.580	B	1.05
3-HI-12	16.920	11.675	9.328	8.186	13.698	8.600	B	1.05
3-HI-21	21.948	11.675	10.133	8.168	13.645	8.580	B	1.05
3-HI-22	22.029	11.789	10.204	8.173	13.639	8.530	B	1.04
3-HI-31	25.453	12.130	10.875	8.176	12.134	8.650	B	1.06
3-HI-32	25.473	11.562	10.516	8.165	12.194	8.700	B	1.07
4-HI-11	13.573	9.435	7.401	4.722	7.946	5.440	B	1.15
4-HI-12	13.582	9.662	7.513	4.728	7.913	5.200	B	1.10
4-HI-21	16.773	8.753	7.617	4.733	6.671	5.450	B	1.15
4-HI-22	16.884	8.866	7.709	4.740	6.636	5.480	B	1.16
4-HI-31	18.532	9.320	8.210	4.699	5.566	5.400	B	1.15
4-HI-32	18.546	9.207	8.153	4.699	5.566	5.260	B	1.12
Mean Value								1.016
Standard Deviation								0.092

\* MC represents combined bending moment and web crippling  
C represents web crippling caused by overstressing  
B represents web crippling caused by buckling

TABLE 13

Comparisons of Tested and Predicted Failure Loads for Hat Sections  
for Interior One-Flange Loading Condition  
Based on Equations 29, 37 and 31

Specimen No.	$P_m$ (kips)	$P_{cy}$ (kips)	$P_{mc}$ (kips)	$P_{cb}$ (kips)	$P_{ms}$ (kips)	$P_{test}$ (kips)	Failure Mode*	$P_{test}/P_{comp}$
1-HI-11	7.273	3.143	2.902	4.938	5.884	2.850	MC	0.98
1-HI-12	7.232	3.143	2.900	4.935	5.868	2.800	MC	0.97
1-HI-21	9.324	3.048	2.927	4.915	6.068	2.930	MC	1.00
1-HI-22	9.316	2.905	2.802	4.912	6.077	2.930	MC	1.05
1-HI-31	10.716	3.095	2.982	4.896	5.516	2.900	MC	0.97
1-HI-32	10.746	3.048	2.958	4.898	5.512	3.000	MC	1.01
2-HI-11	19.856	15.418	12.291	14.220	18.701	10.800	MC	0.88
2-HI-12	20.151	15.082	12.189	14.254	18.868	10.730	MC	0.88
2-HI-21	26.493	15.082	13.195	14.263	21.580	11.480	MC	0.87
2-HI-22	26.561	15.082	13.207	14.271	21.604	11.400	MC	0.86
2-HI-31	32.454	15.194	13.846	14.289	23.348	12.530	MC	0.90
2-HI-32	32.572	15.194	13.855	14.295	23.357	12.750	MC	0.92
3-HI-11	16.991	11.223	9.416	8.180	13.736	8.580	B	1.05
3-HI-12	16.920	11.675	9.656	8.186	13.698	8.600	B	1.05
3-HI-21	21.948	11.675	10.311	8.168	13.645	8.580	B	1.05
3-HI-22	22.029	11.789	10.397	8.173	13.639	8.530	B	1.04
3-HI-31	25.453	12.130	10.951	8.176	12.134	8.650	B	1.06
3-HI-32	25.473	11.562	10.539	8.165	12.194	8.700	B	1.07
4-HI-11	13.573	9.435	7.684	4.722	7.946	5.440	B	1.15
4-HI-12	13.582	9.662	7.802	4.728	7.913	5.200	B	1.10
4-HI-21	16.773	8.753	7.751	4.733	6.671	5.450	B	1.15
4-HI-22	16.884	8.866	7.839	4.740	6.636	5.480	B	1.16
4-HI-31	18.532	9.320	8.323	4.699	5.566	5.400	B	1.15
4-HI-32	18.546	9.207	8.243	4.699	5.566	5.260	B	1.12
Mean Value								1.018
Standard Deviation								0.096

\* MC represents combined bending moment and web crippling  
B represents web crippling caused by buckling

TABLE 14

Comparisons of Tested and Predicted Failure Loads for Hat Sections  
for End One-Flange Loading Condition  
Based on Equation 40 and 41

Specimen No.	$P_{test}$ (kips)	$P_{cy}$ (kips)	$P_{cb}$ (kips)	$P_{cu}$ (kips)	$P_{test}/P_{cu}$
1-HE-11	0.719	0.642	1.397	0.642	1.12
1-HE-12	0.700	0.642	1.397	0.642	1.09
1-HE-21	0.694	0.642	1.243	0.642	1.08
1-HE-22	0.683	0.642	1.246	0.642	1.07
1-HE-31	0.669	0.642	1.120	0.642	1.04
1-HE-32	0.643	0.642	1.129	0.642	1.00
2-HE-11	2.919	2.781	4.368	2.781	1.05
2-HE-12	2.981	2.960	4.379	2.960	1.01
2-HE-21	2.994	2.960	4.187	2.960	1.01
2-HE-22	3.125	2.960	4.187	2.960	1.06
2-HE-31	2.713	2.781	4.016	2.781	0.98
2-HE-32	2.825	2.960	4.007	2.960	0.95
3-HE-11	2.050	1.923	2.396	1.923	1.07
3-HE-12	2.106	1.923	2.401	1.923	1.09
3-HE-21	2.006	1.923	2.255	1.923	1.04
3-HE-22	2.075	1.923	2.248	1.923	1.08
3-HE-31	1.894	1.923	2.103	1.923	0.98
3-HE-32	1.869	1.923	2.103	1.923	0.97
4-HE-11	1.313	1.801	1.127	1.127	1.17
4-HE-12	1.300	1.504	1.140	1.140	1.14
4-HE-21	1.219	1.504	1.032	1.032	1.18
4-HE-22	1.125	1.504	1.031	1.031	1.09
4-HE-31	1.088	1.504	0.955	0.955	1.14
4-HE-32	1.063	1.801	0.954	0.954	1.11
Mean Value					1.063
Standard Deviation					0.063



TABLE 15

Comparisons of Tested and Predicted Failure Loads for Hat Sections  
for Interior One-Flange Loading Condition  
Based on Equations 29, 36 and 31

Specimen No.	$P_m$ (kips)	$P_{cy}$ (kips)	$P_{mc}$ (kips)	$P_{cb}$ (kips)	$P_{ms}$ (kips)	$P_{test}$ (kips)	Failure Mode*	$P_{test}/P_{comp}$
1	0.251	0.941	0.251	1.388	0.196	0.216	MS	1.10
2	0.415	0.941	0.402	1.388	0.473	0.414	MC	1.03
3	0.707	0.941	0.554	1.562	0.765	0.618	MC	1.12
4	1.026	0.941	0.667	2.078	1.055	0.762	MC	1.14
5	1.384	0.941	0.755	2.418	1.333	0.900	MC	1.19
6	2.080	0.941	0.864	2.654	1.739	0.975	MC	1.13
7	0.350	1.817	0.350	2.047	0.268	0.306	MS	1.14
8	0.621	1.817	0.621	2.047	0.652	0.594	M	0.96
9	1.000	1.817	0.886	2.281	1.110	0.876	MC	0.99
10	1.461	1.817	1.100	3.049	1.547	1.090	MC	0.99
11	1.973	1.817	1.286	3.556	1.988	1.320	MC	1.03
12	3.085	1.817	1.530	4.132	2.712	1.610	MC	1.05
13	0.414	2.164	0.414	2.047	0.318	0.384	MS	1.21
14	0.667	2.164	0.667	2.047	0.770	0.726	M	1.09
15	1.160	2.164	1.047	2.281	1.273	1.100	MC	1.05
16	1.690	2.164	1.301	3.049	1.762	1.380	MC	1.06
17	2.282	2.164	1.511	3.556	2.243	1.610	MC	1.07
18	3.490	2.164	1.790	4.132	2.975	1.960	MC	1.09
19	0.462	2.584	0.462	2.047	0.377	0.498	MS	1.32
20	0.796	2.584	0.796	2.047	0.912	0.905	M	1.14
21	1.349	2.584	1.228	2.281	1.460	1.360	MC	1.11
22	1.960	2.584	1.528	3.049	2.008	1.640	MC	1.07
23	2.648	2.584	1.770	3.556	2.522	1.930	MC	1.09
24	3.947	2.584	2.093	4.132	3.244	2.340	MC	1.12
25	0.754	5.301	0.754	2.976	0.582	0.678	MS	1.16
26	1.218	5.301	1.218	2.976	1.417	1.260	M	1.03
27	2.118	5.301	2.100	3.277	2.332	1.840	MC	0.88
28	3.089	5.301	2.676	4.409	3.223	2.370	MC	0.89
29	4.178	5.301	3.171	5.154	4.090	2.740	MC	0.86
30	6.373	5.301	3.856	6.072	5.377	3.190	MC	0.83
31	0.786	5.371	0.786	1.160	0.851	0.705	M	0.90
32	1.090	10.526	1.090	2.095	1.257	1.185	M	1.09
33	0.816	5.371	0.816	1.160	0.893	0.698	M	0.86
34	1.183	10.526	1.183	2.095	1.380	1.178	M	1.00
35	0.825	5.371	0.825	1.160	0.903	0.690	M	0.84
36	1.206	10.526	1.206	2.095	1.408	1.140	M	0.95
37	0.772	3.720	0.772	1.160	0.838	0.705	M	0.91
38	0.903	7.366	0.903	1.975	1.043	1.134	M	1.26
39	1.557	3.720	1.482	1.160	1.516	1.071	B	0.92
40	2.037	7.366	2.037	1.975	2.142	1.890	B	0.96

TABLE 15 (Cont'd)

Comparisons of Tested and Predicted Failure Loads for Hat Sections  
for Interior One-Flange Loading Condition  
Based on Equations 29, 36 and 31

Specimen No.	$P_m$ (kips)	$P_{cy}$ (kips)	$P_{mc}$ (kips)	$P_{cb}$ (kips)	$P_{ms}$ (kips)	$P_{test}$ (kips)	Failure Mode*	$P_{test}/P_{comp}$
41	2.271	3.720	1.896	1.311	2.061	1.470	B	1.12
42	3.262	7.366	3.054	2.203	3.127	2.592	B	1.18
43	2.771	5.371	2.463	1.740	2.259	1.655	B	0.95
44	4.364	10.526	4.170	3.121	3.968	2.898	B	0.93
45	2.480	4.854	2.211	1.700	2.071	1.584	B	0.93
46	4.311	10.432	4.120	3.156	3.940	2.979	B	0.94
47	2.902	5.371	2.538	1.740	2.328	1.718	B	0.99
48	4.750	10.526	4.421	3.121	4.251	3.142	B	1.01
49	2.723	4.854	2.349	1.700	2.206	1.635	B	0.96
50	4.726	10.432	4.392	3.156	4.249	3.069	B	0.97
51	2.956	3.720	2.208	1.740	2.356	1.746	B	1.00
52	4.611	7.953	3.930	3.121	4.151	3.012	B	0.97
53	2.976	4.854	2.483	1.700	2.335	1.599	B	0.94
54	5.157	10.432	4.654	3.156	4.554	3.168	B	1.00
55	2.921	5.371	2.550	1.740	2.338	1.805	B	1.04
56	4.808	10.526	4.455	3.121	4.293	3.048	B	0.98
57	2.774	5.213	2.440	1.700	2.233	1.536	B	0.90
58	4.442	9.848	4.132	2.944	3.958	3.243	B	1.10
59	3.557	3.720	2.433	2.002	2.395	2.091	B	1.04
60	5.513	7.366	4.229	3.432	4.385	3.522	B	1.03
61	4.060	5.371	3.101	2.153	2.078	2.302	B	1.11
62	7.622	10.526	5.935	4.242	4.664	4.135	B	0.97
63	4.194	5.371	3.156	2.153	2.096	2.470	MS	1.18
64	8.101	10.526	6.135	4.242	4.768	4.405	B	1.04
65	4.210	5.371	3.163	2.153	2.098	2.475	MS	1.18
66	8.164	10.526	6.166	4.242	4.780	4.628	B	1.09
67	4.293	3.720	2.657	2.153	2.108	2.607	MS	1.24
68	7.535	7.366	4.978	3.970	4.386	4.562	B	1.15
Mean Value								1.038
Standard Deviation								0.107

\* MC represents combined bending moment and web crippling  
M represents bending moment  
B represents web crippling caused by buckling  
MS represents combined bending moment and shear

TABLE 16

Comparisons of Tested and Predicted Failure Loads for Hat Sections  
for Interior One-Flange Loading Condition  
Based on Equations 29, 37 and 31

Specimen No.	$P_m$ (kips)	$P_{cy}$ (kips)	$P_{mc}$ (kips)	$P_{cb}$ (kips)	$P_{ms}$ (kips)	$P_{test}$ (kips)	Failure Mode*	$P_{test}/P_{comp}$
1	0.251	0.941	0.251	1.388	0.196	0.216	MS	1.10
2	0.415	0.941	0.381	1.388	0.473	0.414	MC	1.09
3	0.707	0.941	0.561	1.562	0.765	0.618	MC	1.10
4	1.026	0.941	0.691	2.078	1.055	0.762	MC	1.10
5	1.384	0.941	0.780	2.418	1.333	0.900	MC	1.15
6	2.080	0.941	0.863	2.654	1.739	0.975	MC	1.13
7	0.350	1.817	0.350	2.047	0.268	0.306	MS	1.14
8	0.621	1.817	0.621	2.047	0.652	0.594	M	0.96
9	1.000	1.817	0.874	2.281	1.110	0.876	MC	1.00
10	1.461	1.817	1.126	3.049	1.547	1.090	MC	0.97
11	1.973	1.817	1.326	3.556	1.988	1.320	MC	1.00
12	3.085	1.817	1.568	4.132	2.712	1.610	MC	1.03
13	0.414	2.164	0.414	2.047	0.318	0.384	MS	1.21
14	0.667	2.164	0.648	2.047	0.770	0.726	MC	1.12
15	1.160	2.164	1.020	2.281	1.273	1.100	MC	1.08
16	1.690	2.164	1.323	3.049	1.762	1.380	MC	1.04
17	2.282	2.164	1.565	3.556	2.243	1.610	MC	1.03
18	3.490	2.164	1.839	4.132	2.975	1.960	MC	1.07
19	0.462	2.584	0.462	2.047	0.377	0.498	MS	1.32
20	0.796	2.584	0.774	2.047	0.912	0.905	MC	1.17
21	1.349	2.584	1.192	2.281	1.460	1.360	MC	1.14
22	1.960	2.584	1.551	3.049	2.008	1.640	MC	1.06
23	2.648	2.584	1.831	3.556	2.522	1.930	MC	1.05
24	3.947	2.584	2.159	4.132	3.244	2.340	MC	1.08
25	0.754	5.301	0.754	2.976	0.582	0.678	MS	1.16
26	1.218	5.301	1.218	2.976	1.417	1.260	M	1.03
27	2.118	5.301	1.972	3.277	2.332	1.840	MC	0.93
28	3.089	5.301	2.646	4.409	3.223	2.370	MC	0.90
29	4.178	5.301	3.243	5.154	4.090	2.740	MC	0.84
30	6.373	5.301	4.017	6.072	5.377	3.190	MC	0.79
31	0.786	5.371	0.786	1.160	0.851	0.705	M	0.90
32	1.090	10.526	1.090	2.095	1.257	1.185	M	1.09
33	0.816	5.371	0.816	1.160	0.893	0.698	M	0.86
34	1.183	10.526	1.183	2.095	1.380	1.178	M	1.00
35	0.825	5.371	0.825	1.160	0.903	0.690	M	0.84
36	1.206	10.526	1.206	2.095	1.408	1.140	M	0.95
37	0.772	3.720	0.772	1.160	0.838	0.705	M	0.91
38	0.903	7.366	0.903	1.975	1.043	1.134	M	1.26
39	1.557	3.720	1.394	1.160	1.516	1.071	B	0.92
40	2.037	7.366	1.989	1.975	2.142	1.890	B	0.96

TABLE 16 (Cont'd)

Comparisons of Tested and Predicted Failure Loads for Hat Sections  
for Interior One-Flange Loading Condition  
Based on Equations 29, 37 and 31

Specimen No.	$P_m$ (kips)	$P_{cy}$ (kips)	$P_{mc}$ (kips)	$P_{cb}$ (kips)	$P_{ms}$ (kips)	$P_{test}$ (kips)	Failure Mode*	$P_{test}/P_{comp}$
41	2.271	3.720	1.880	1.311	2.061	1.470	B	1.12
42	3.262	7.366	2.893	2.203	3.127	2.592	B	1.18
43	2.771	5.371	2.387	1.740	2.259	1.655	B	0.95
44	4.364	10.526	3.914	3.121	3.968	2.898	B	0.93
45	2.480	4.854	2.141	1.700	2.071	1.584	B	0.93
46	4.311	10.432	3.868	3.156	3.940	2.979	B	0.94
47	2.902	5.371	2.474	1.740	2.328	1.718	B	0.99
48	4.750	10.526	4.198	3.121	4.251	3.142	B	1.01
49	2.723	4.854	2.302	1.700	2.206	1.635	B	0.96
50	4.726	10.432	4.176	3.156	4.249	3.069	B	0.97
51	2.956	3.720	2.253	1.740	2.356	1.746	B	1.00
52	4.611	7.953	3.867	3.121	4.151	3.012	B	0.97
53	2.976	4.854	2.461	1.700	2.335	1.599	B	0.94
54	5.157	10.432	4.482	3.156	4.554	3.168	B	1.00
55	2.921	5.371	2.488	1.740	2.338	1.805	B	1.04
56	4.808	10.526	4.241	3.121	4.293	3.048	B	0.98
57	2.774	5.213	2.374	1.700	2.233	1.536	B	0.90
58	4.442	9.848	3.928	2.944	3.958	3.243	B	1.10
59	3.557	3.720	2.516	2.002	2.395	2.091	B	1.04
60	5.513	7.366	4.293	3.432	4.385	3.522	B	1.03
61	4.060	5.371	3.149	2.153	2.078	2.302	MS	1.11
62	7.622	10.526	5.998	4.242	4.664	4.135	B	0.97
63	4.194	5.371	3.217	2.153	2.096	2.470	MS	1.18
64	8.101	10.526	6.246	4.242	4.768	4.405	B	1.04
65	4.210	5.371	3.226	2.153	2.098	2.475	MS	1.18
66	8.164	10.526	6.277	4.242	4.780	4.628	B	1.09
67	4.293	3.720	2.767	2.153	2.108	2.607	MS	1.24
68	7.535	7.366	5.165	3.970	4.386	4.562	B	1.15
Mean Value								1.036
Standard Deviation								0.107

\* MC represents combined bending moment and web crippling  
M represents bending moment  
B represents web crippling caused by buckling  
MS represents combined bending moment and shear

TABLE 17

Proposed Number of Hat Sections Used to Verify Equation (31)

Arrangement	Profile No.	Material		Total
		100XF	140XF	
A	1	2	2	4
A	2	2	2	4
A	3	2	2	4
B	1	2	2	4
B	2	2	2	4
B	3	2	2	4
C	1	2	2	4
C	2	2	2	4
C	3	2	2	4
Total		18	18	36

Notes: Types of profile are given in Table 2a.

See Fig. 37 for testing arrangement.

Arrangement A:  $e_1/h = 1.25$  and  $e_2/h = 1.75$ Arrangement B:  $e_1/h = 1.00$  and  $e_2/h = 2.00$ Arrangement C:  $e_1/h = 0.75$  and  $e_2/h = 2.25$ 

TABLE 18

Proposed Number of Hat Sections Used to Verify Equation (29)

Profile No.	Material		Total
	100XF	140XF	
1	2	2	4
2	2	2	4
3	2	2	4
Total	6	6	12

Notes: Types of profile are given in Table 2a.

See Fig. 38 for testing arrangement

TABLE 19

Number of Web Crippling Tests on Hat Sections Subjected to  
Interior Two-Flange Loading

Profile No.	Material Designation				Total
	80DK	80XF	100XF	140XF	
1	2	2	2	2	8
2	2	2	2	2	8
3	2	2	2	2	8
Total	6	6	6	6	24

Notes: See Fig. 39 for loading condition.  
Types of profiles are given in Table 2a.

TABLE 20

Number of Web Crippling Tests on Hat Sections Subjected to  
End Two-Flange Loading

Profile No.	Material Designation				Total
	80DK	80XF	100XF	140XF	
1	2	2	2	2	8
2	2	2	2	2	8
3	2	2	2	2	8
Total	6	6	6	6	24

Notes: See Fig. 40 for loading condition.  
Types of profiles are given in Table 2a.

TABLE 21

Number of Web Crippling Tests on I-Sections Subjected to  
Interior Two-Flange Loading

Profile No.	Material Designation				Total
	80DK	80XF	100XF	140XF	
1	2	2	2	2	8
2	2	2	2	2	8
3	2	2	2	2	8
Total	6	6	6	6	24

Notes: See Fig. 39 for loading condition.  
Types of profiles are given in Table 2b.

TABLE 22

Number of Web Crippling Tests on I-Sections Subjected to  
End Two-Flange Loading

Profile No.	Material Designation				Total
	80DK	80XF	100XF	140XF	
1	2	2	2	2	8
2	2	2	2	2	8
3	2	2	2	2	8
Total	6	6	6	6	24

Notes: See Fig. 40 for loading condition.  
Types of profiles are given in Table 2b.

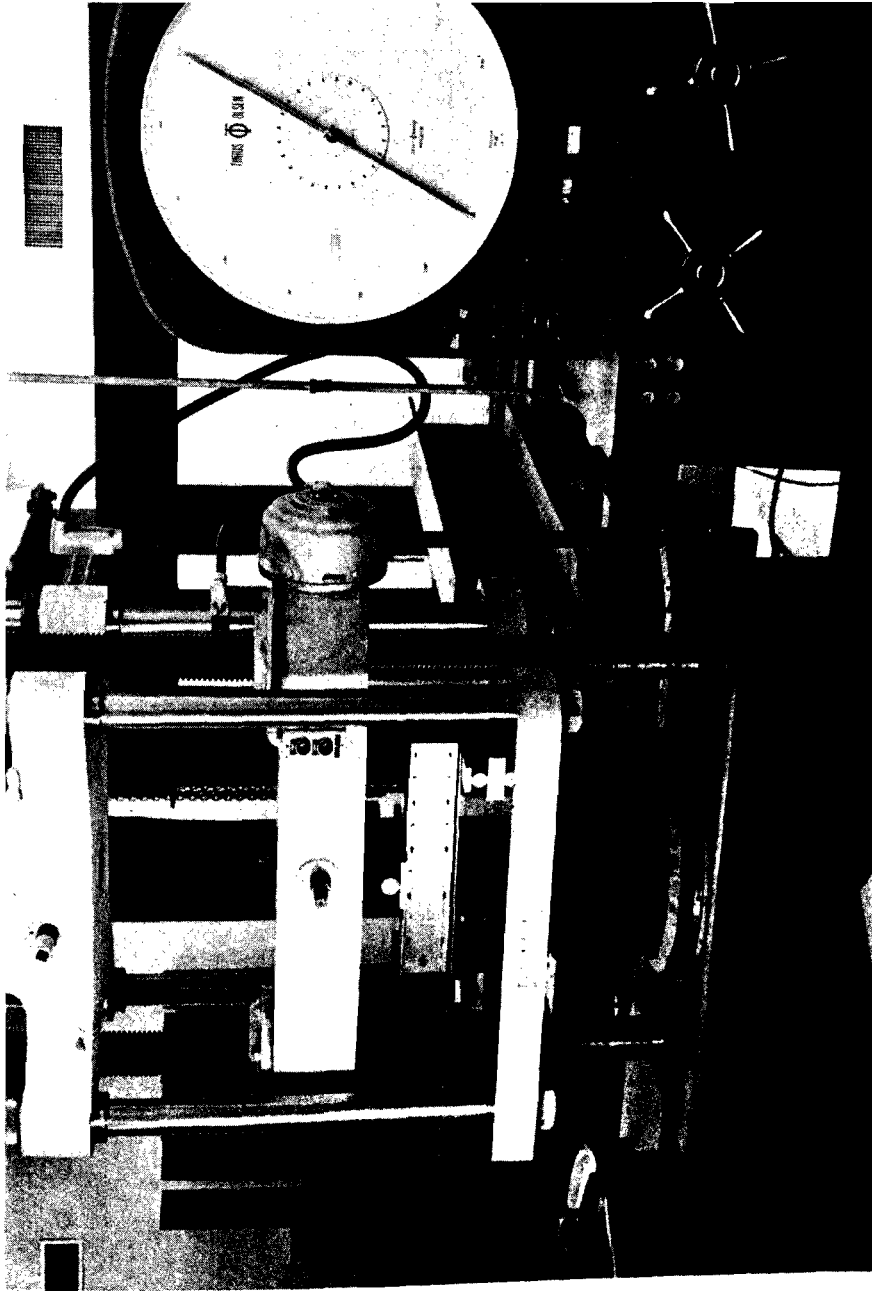


Fig. 1. Tinius Olsen Universal Testing Machine



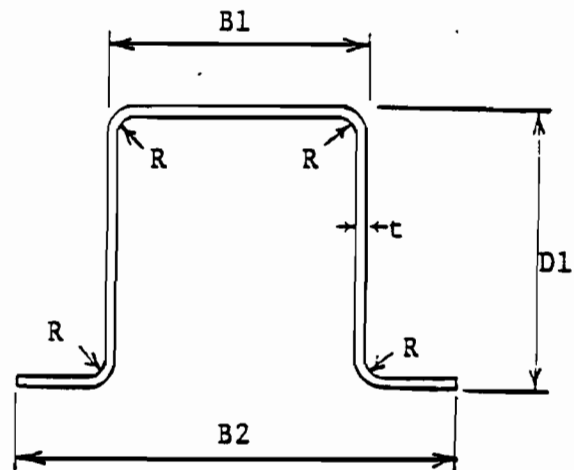


Fig. 2. Hat Sections Used in the Experimental Study

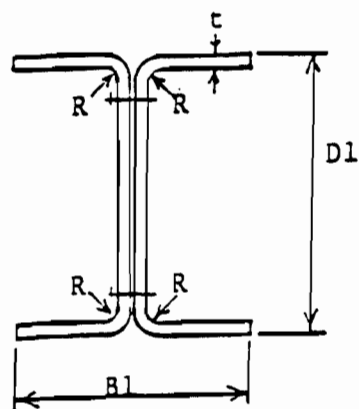
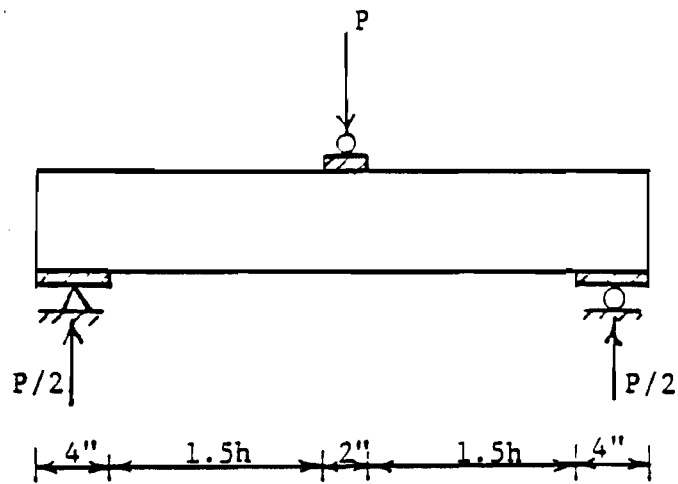
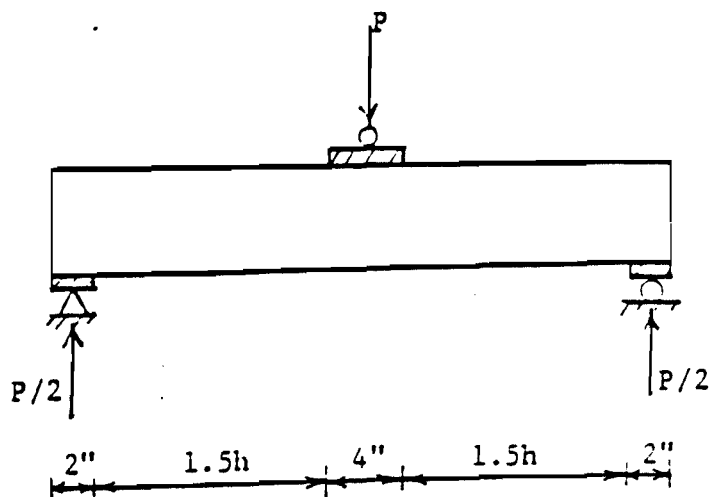


Fig. 3. I-Sections Used in the Experimental Study



(a) Interior One-Flange Loading



(b) End One-Flange Loading

Fig. 4. Test Setup for Web Crippling



Fig. 5. Photograph of Test Setup for Interior One-Flange  
Loading Condition of Hat Sections

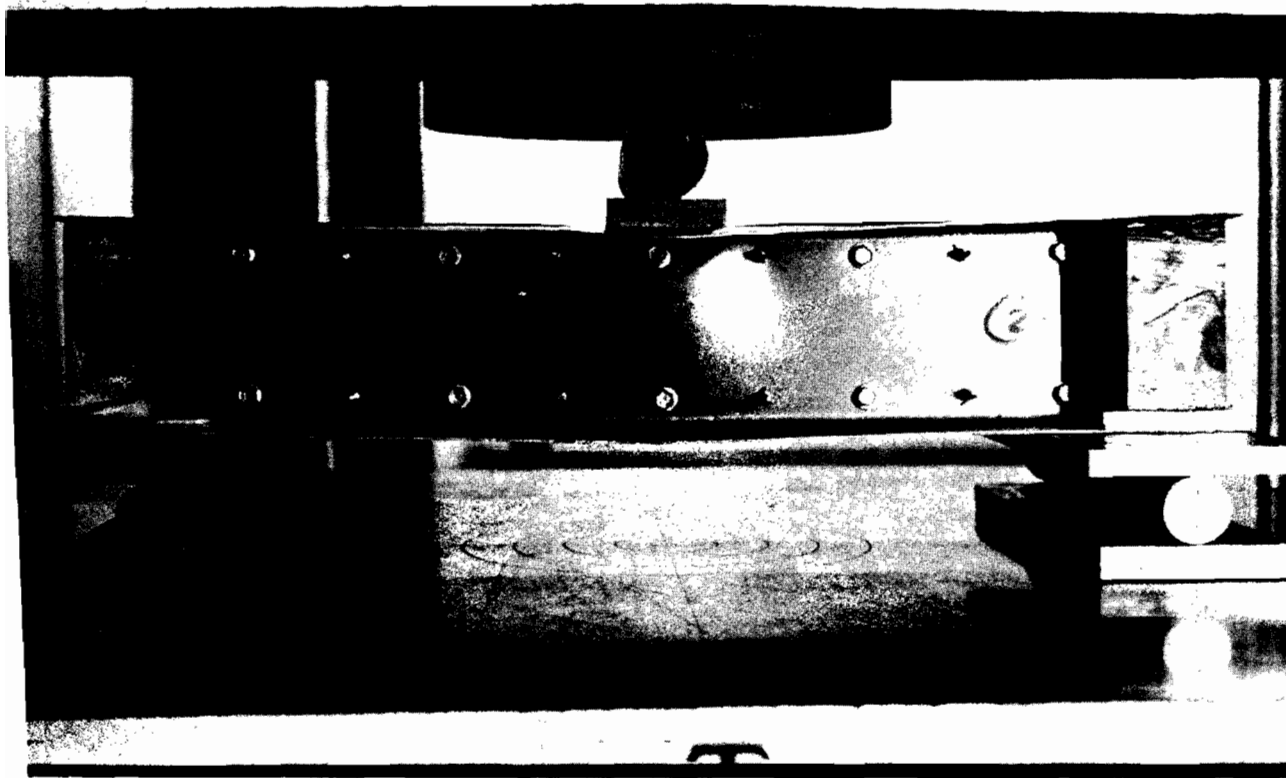


Fig. 6. Photograph of Test Setup for Interior One-Flange  
Loading Condition of I-beams

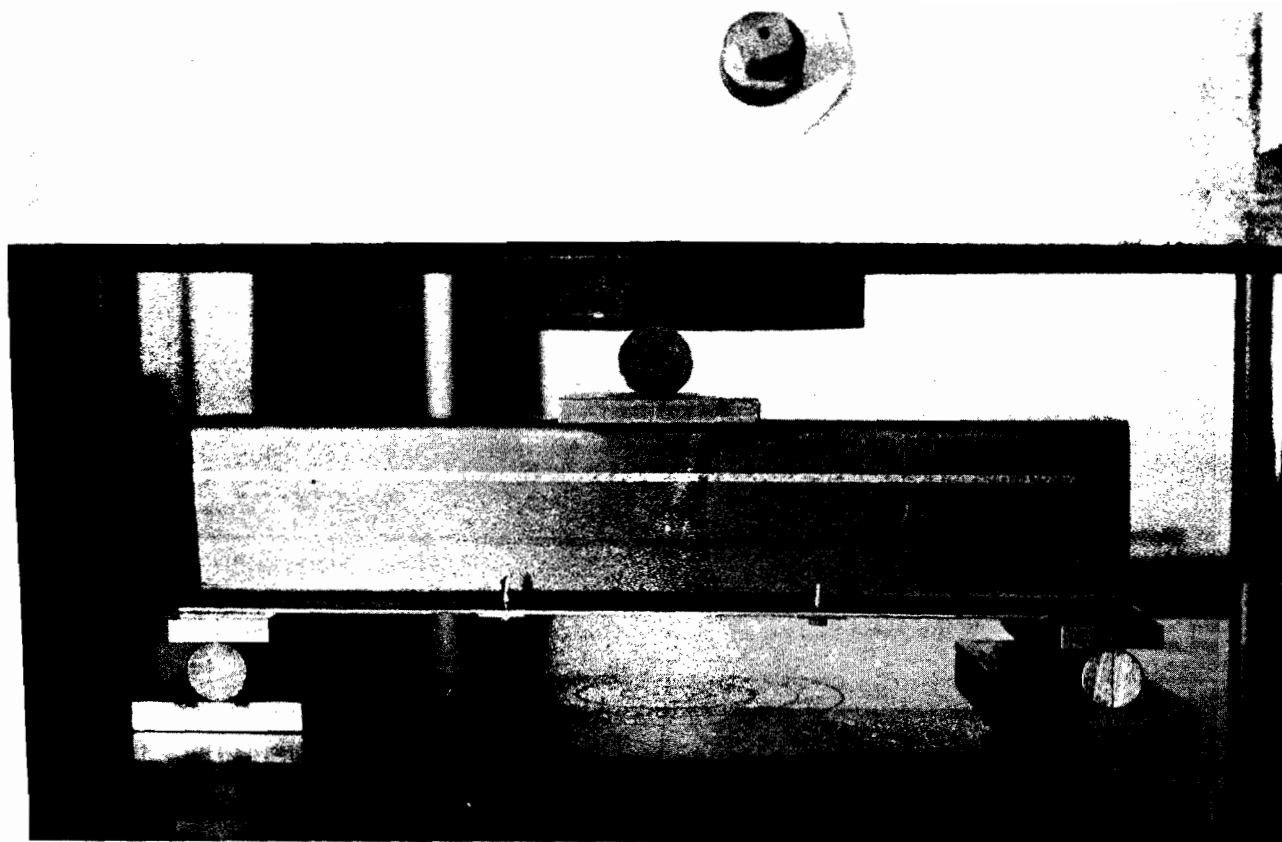


Fig. 7. Photograph of Test Setup for End One-Flange  
Loading Condition of Hat Sections

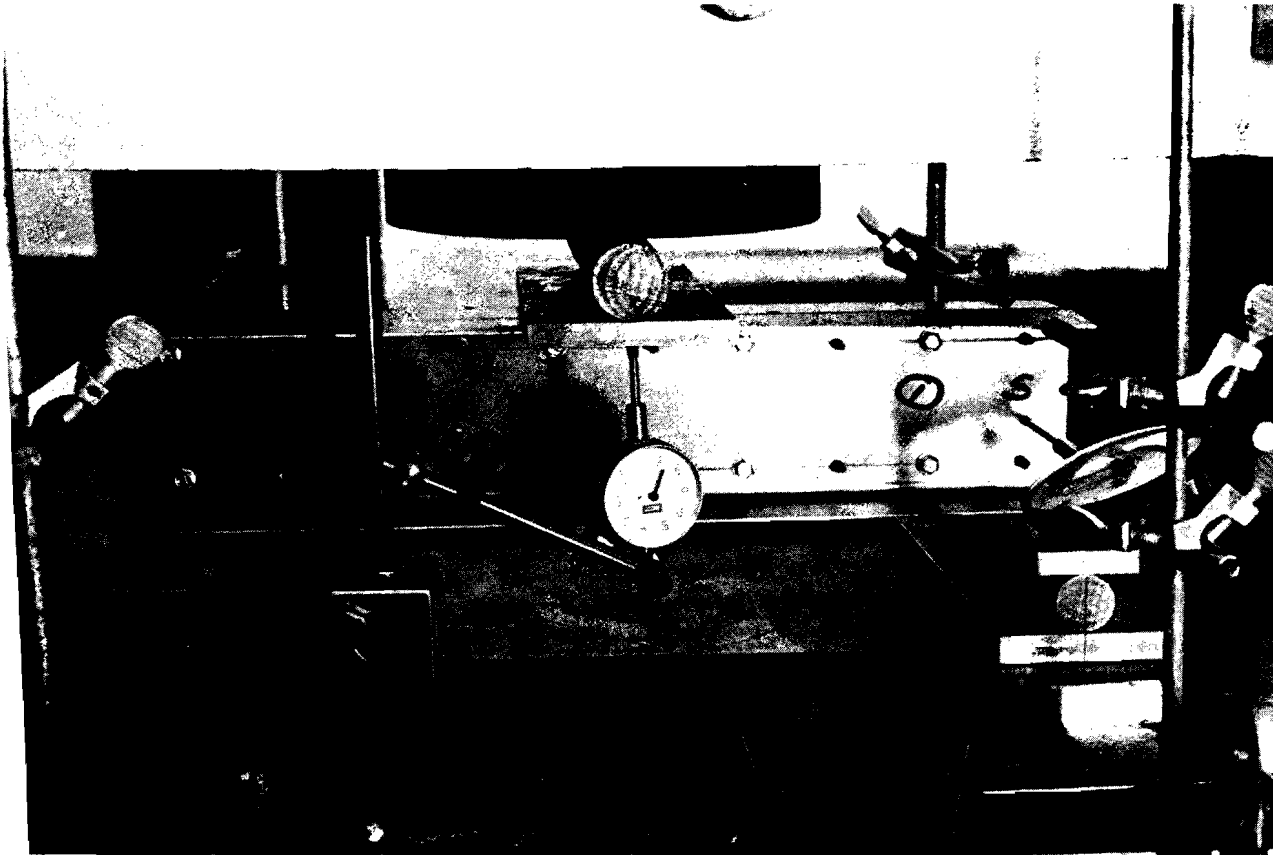


Fig. 8. Photograph of Test Setup for End One-Flange Loading Condition of I-beams

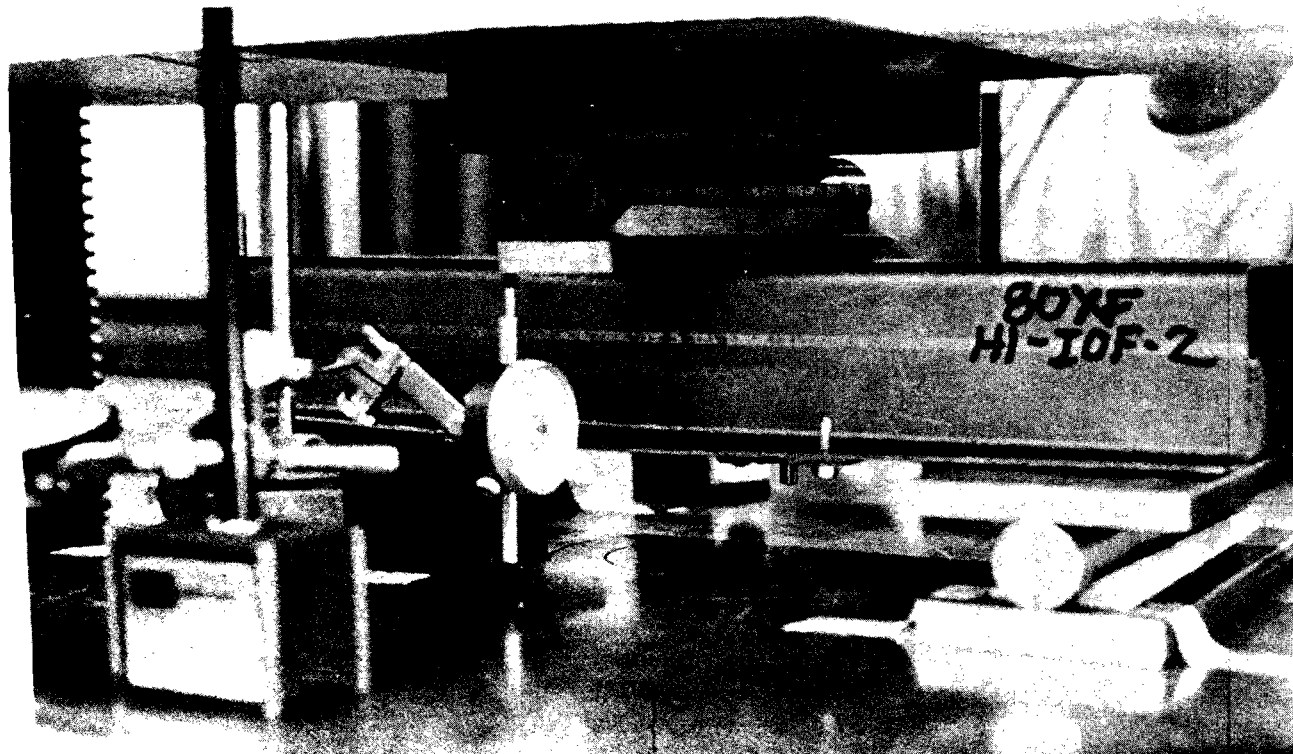


Fig. 9. Photograph Showing Wood Blocks Were Used at Both Ends of the Hat Section Under Interior One-Flange Loading

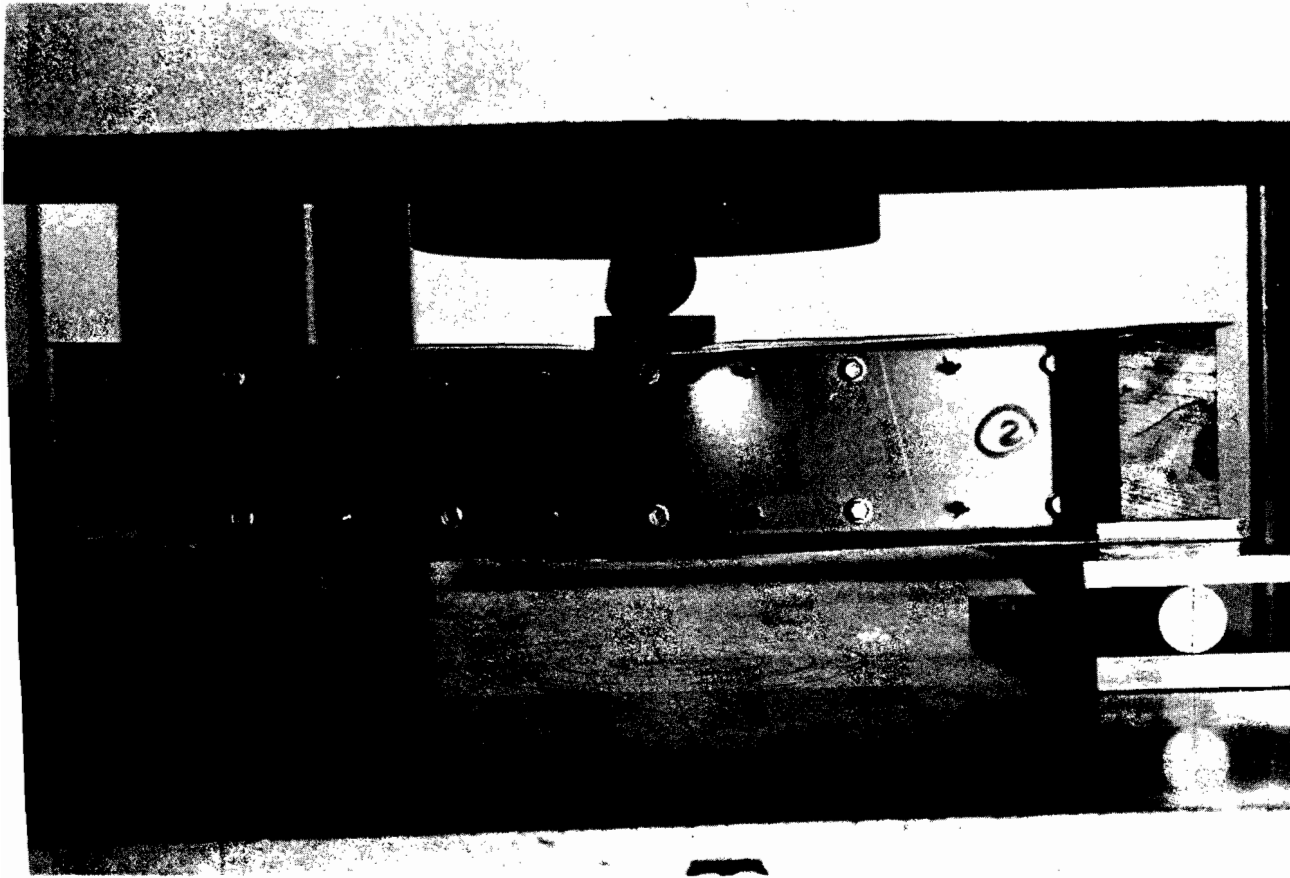


Fig. 10. Photograph Showing Wood Blocks Were Used at Both Ends of the I-beam Under Interior One-Flange Loading



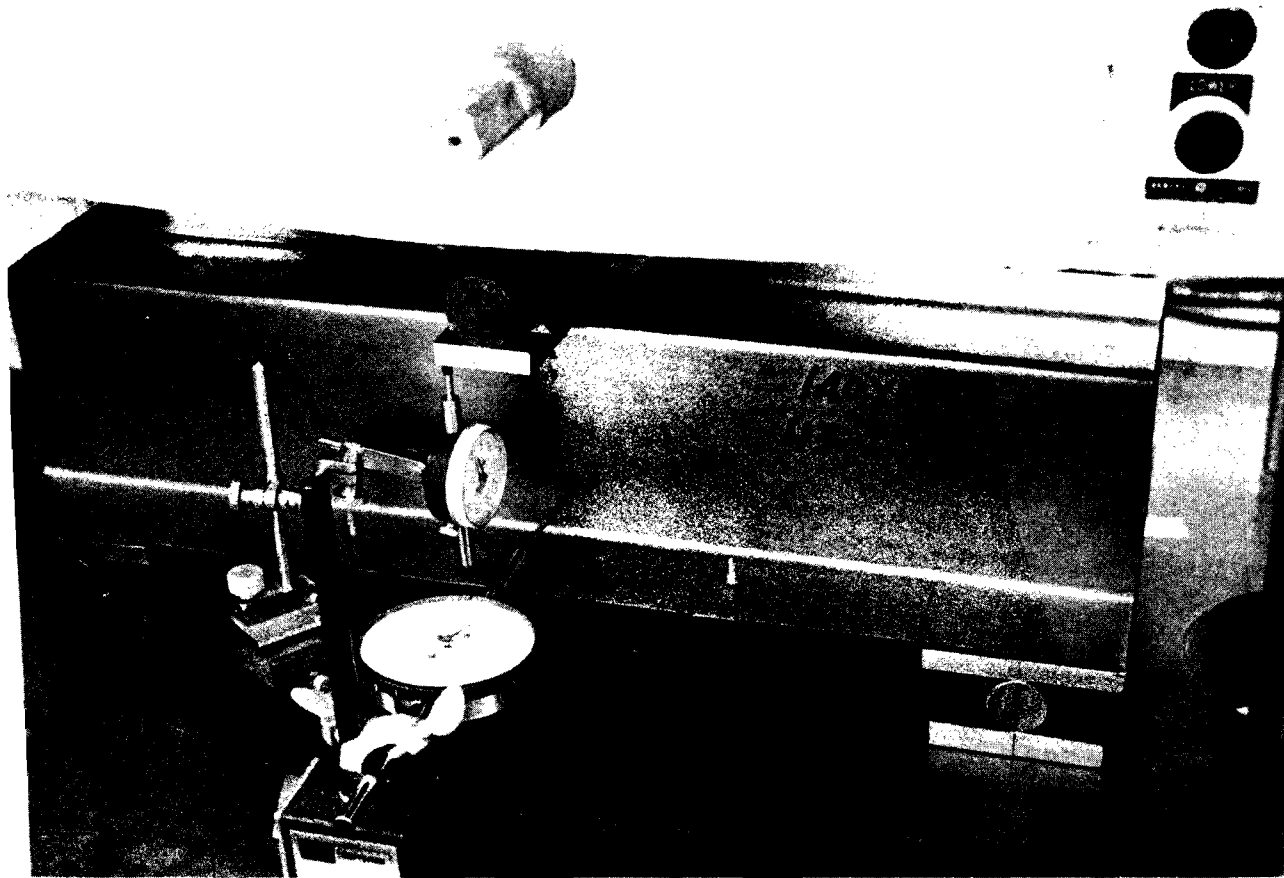


Fig. 11. Photograph Showing Lateral and Vertical Deformations of Hat Sections Used for Interior One-Flange Loading

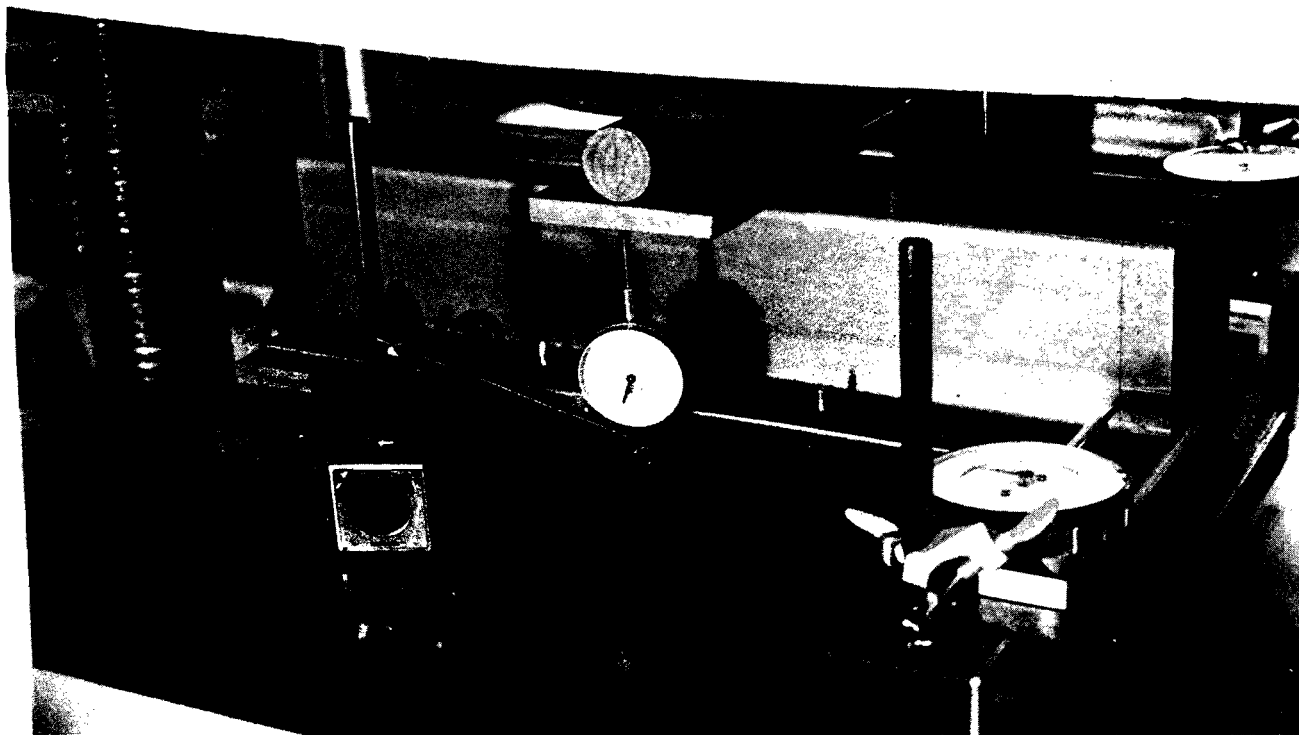


Fig. 12. Photograph Showing Lateral and Vertical Deformations of Hat Sections Used for End One-Flange Loading

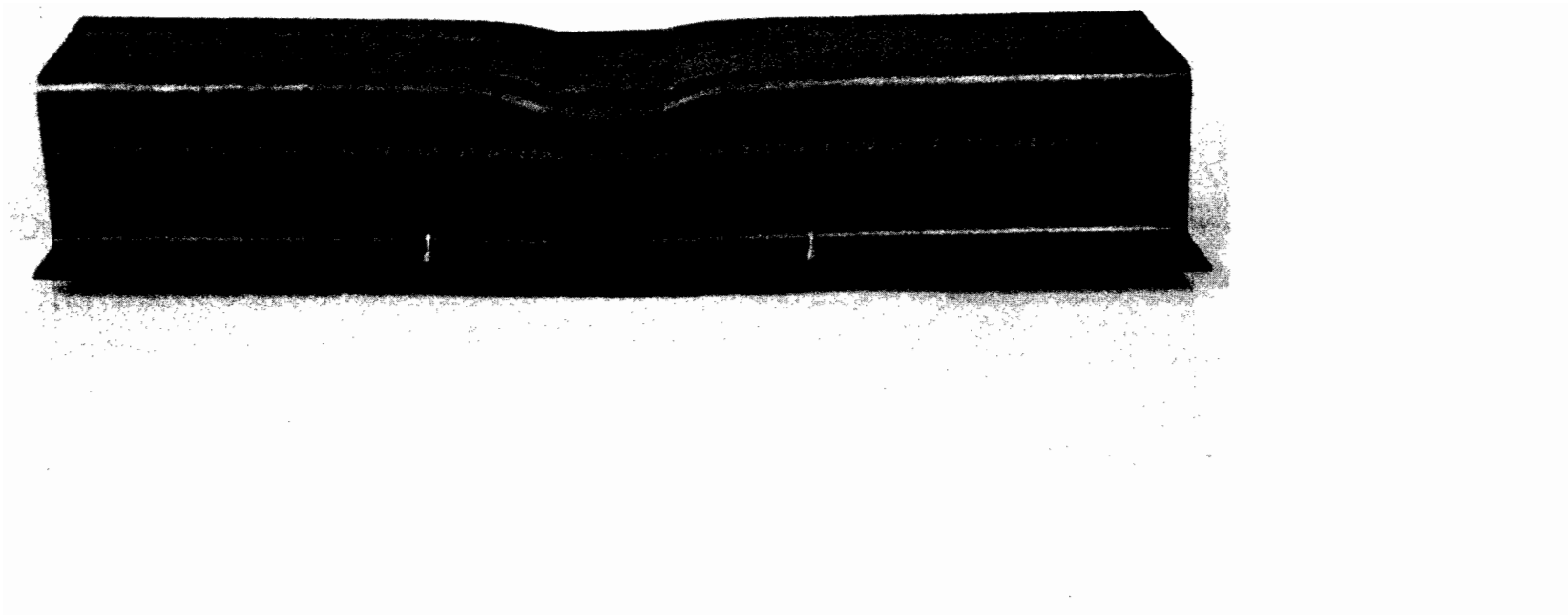


Fig. 13. Photograph Showing Web Crippling Failure Caused by Overstressing

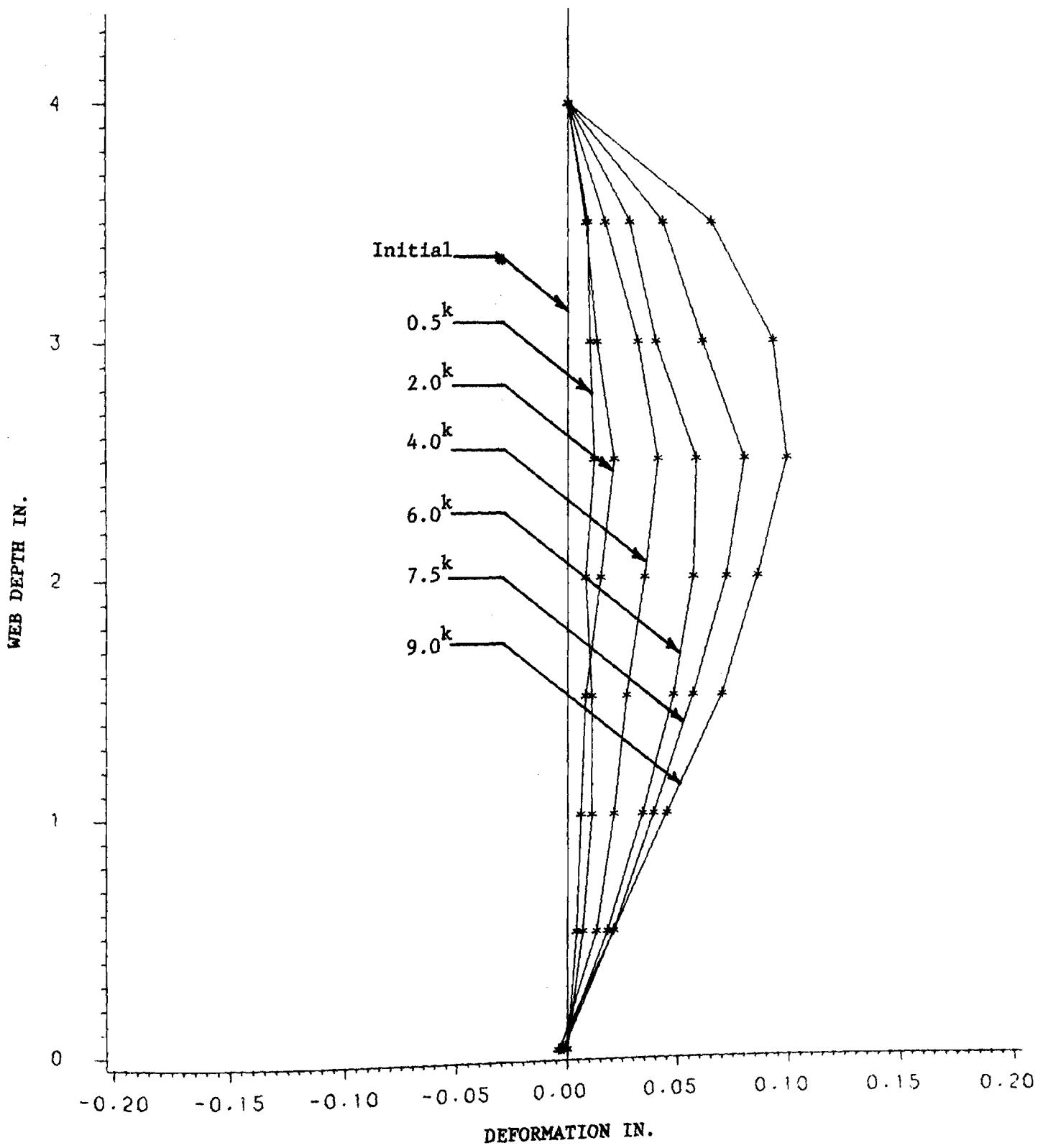


Fig. 14. Laterally Deformed Web of a Hat Section Under Interior One-Flange Loading (Specimen No. 2-HI-21)

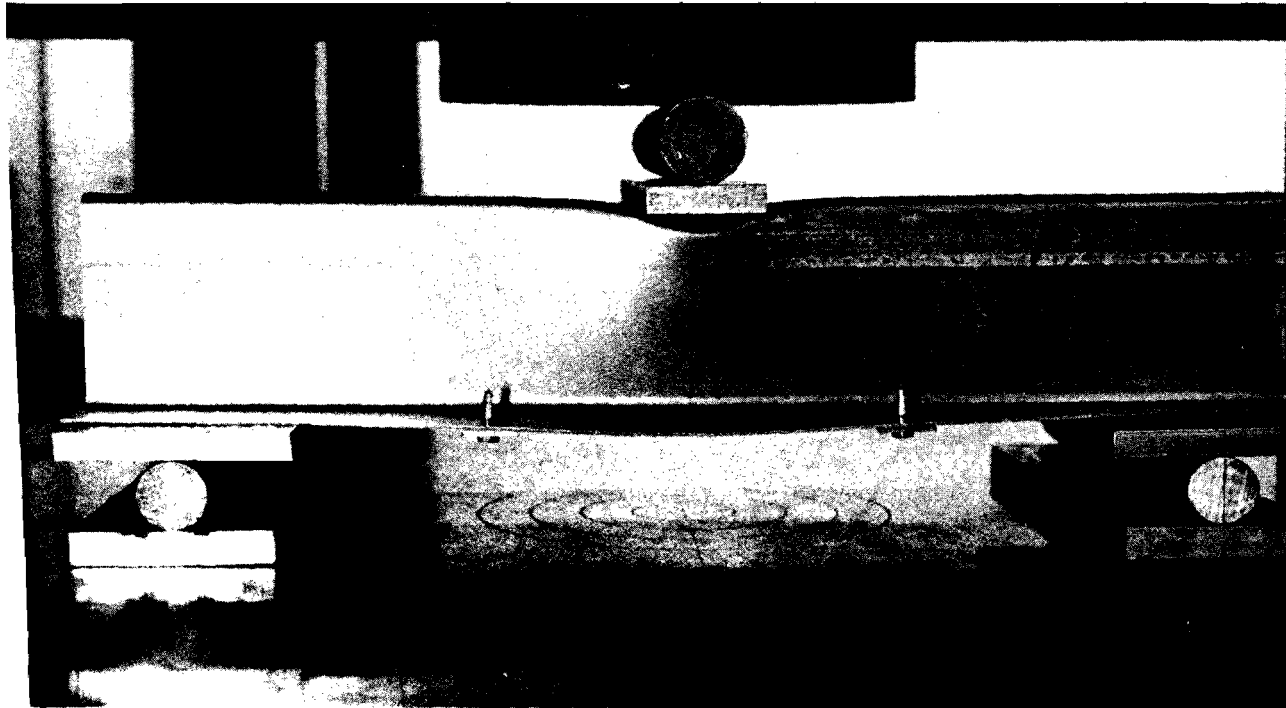


Fig. 15. Photograph Showing Web Crippling Failure Caused by Web Buckling

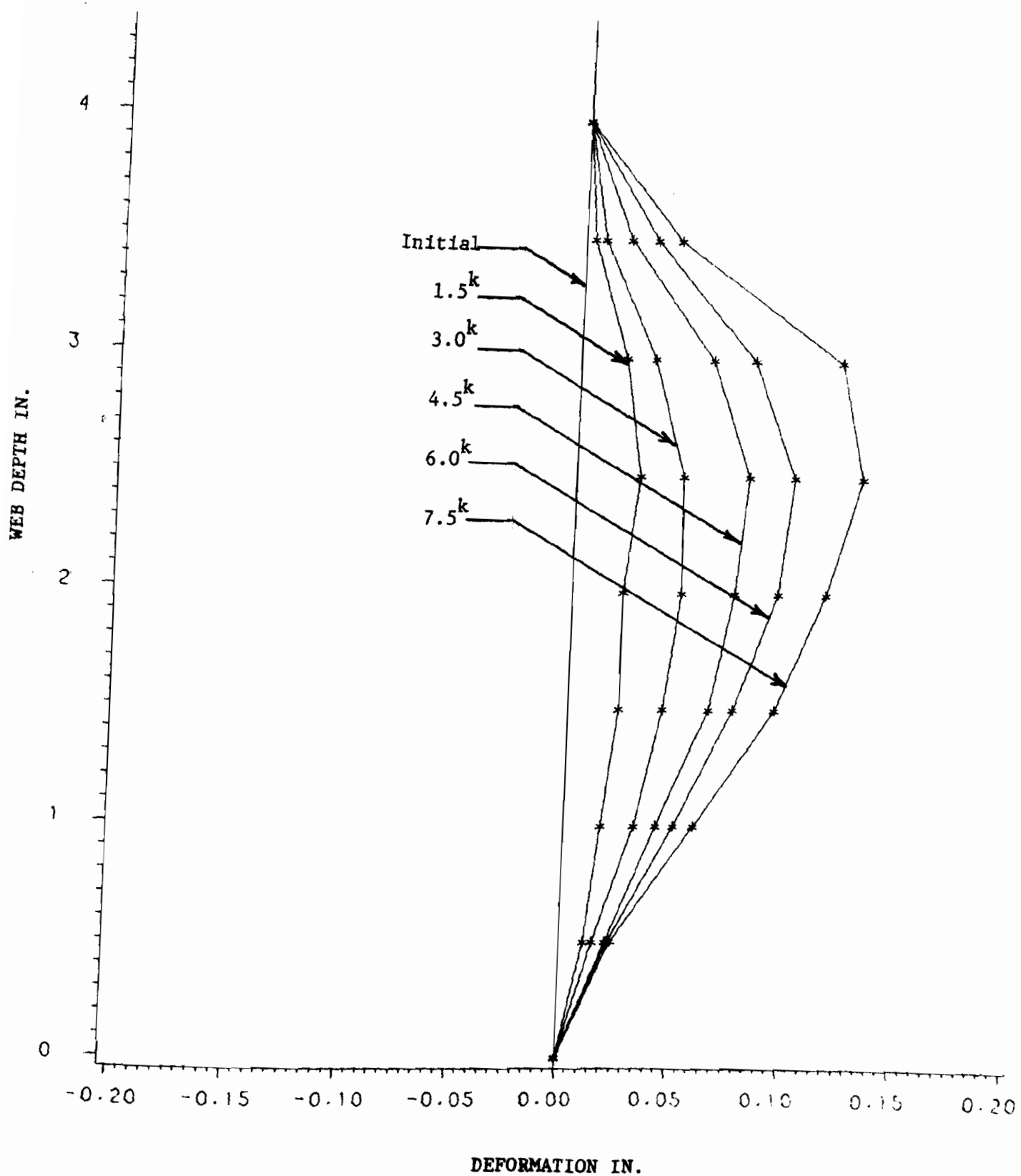


Fig. 16. Laterally Deformed Web of a Hat Section Under Interior One-Flange Loading (Specimen No. 3-HI-21)

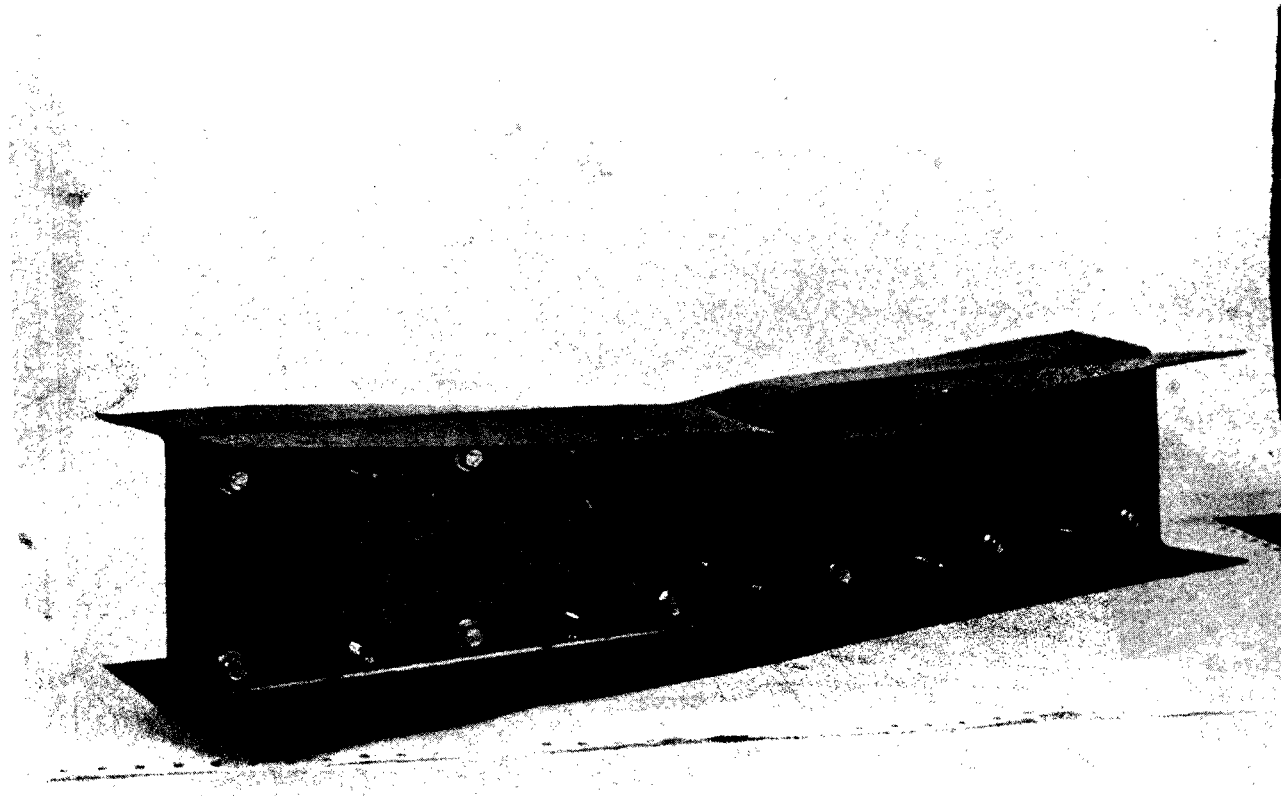


Fig. 17. Photograph Showing Typical Failure of I-beams  
Subjected to Interior One-Flange Loading

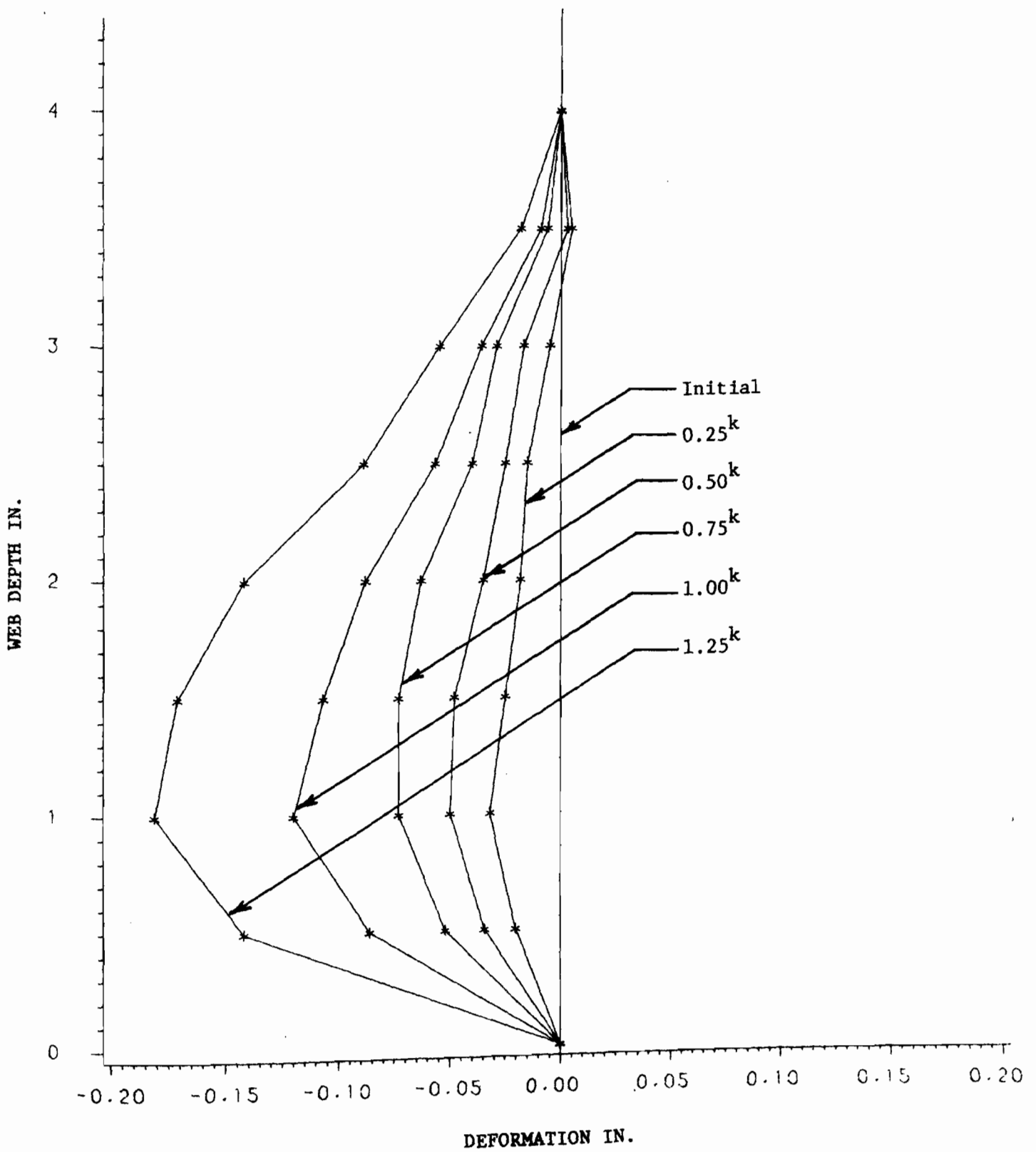


Fig. 18. Laterally Deformed Web of a Hat Section Under End One-Flange Loading (Specimen No. 1-HE-21)



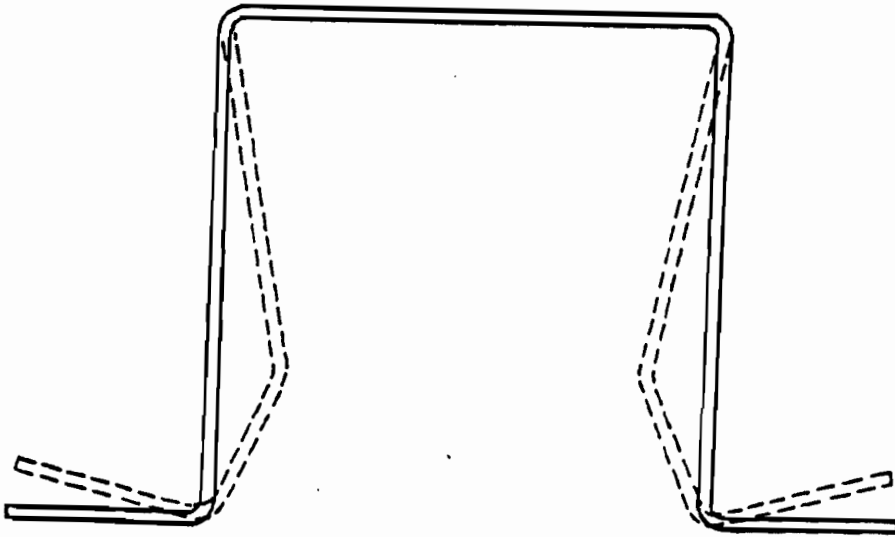


Fig. 19. Deformed Cross Section of a Hat Section  
Subjected to End One-Flange Loading

---

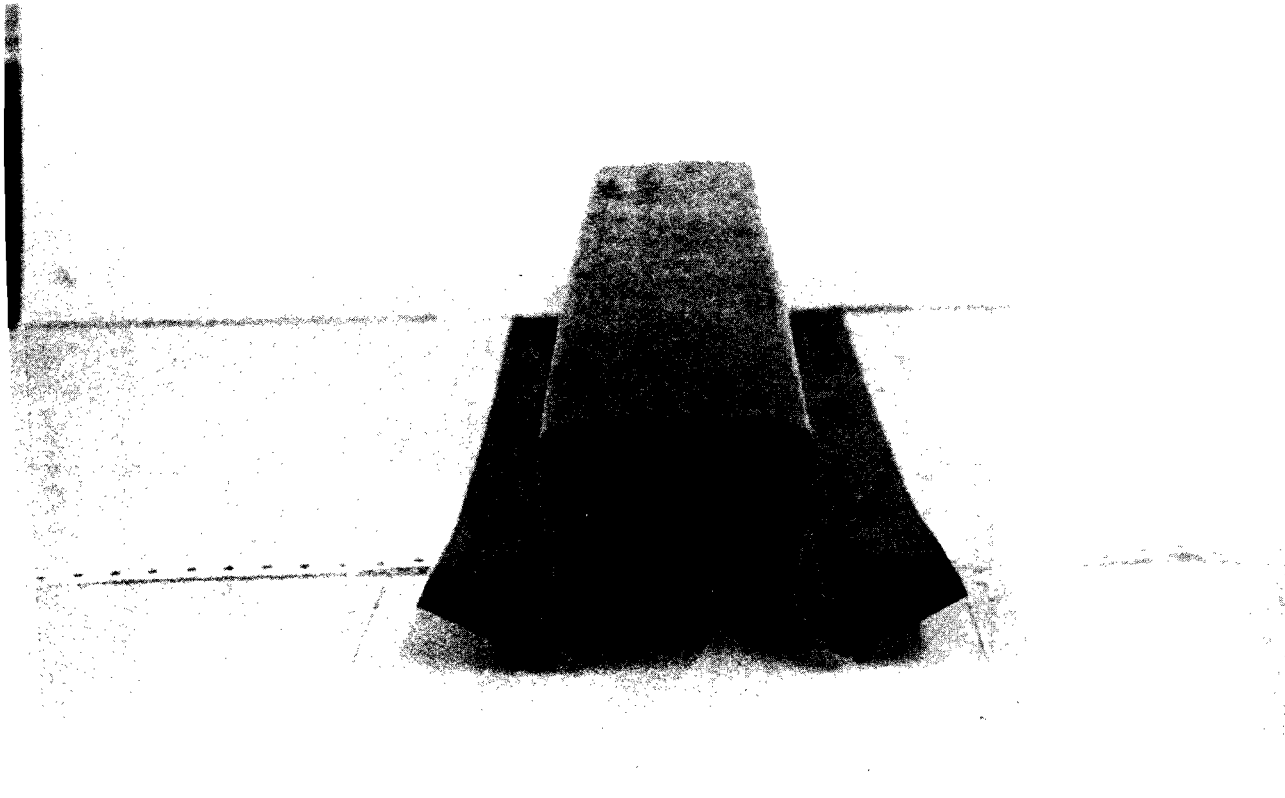


Fig. 20. Photograph Showing Typical Failure of Hat Section  
Subjected to End One-Flange Loading

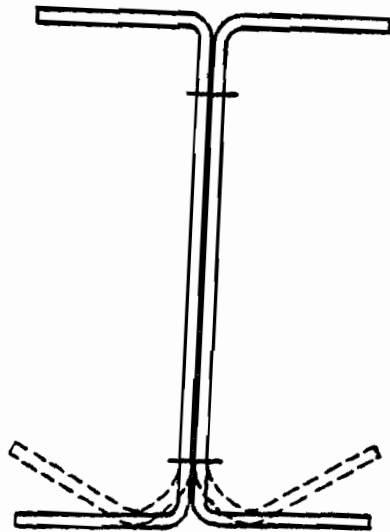


Fig. 21. Sketch Showing Failure at Web-Flange  
Junction

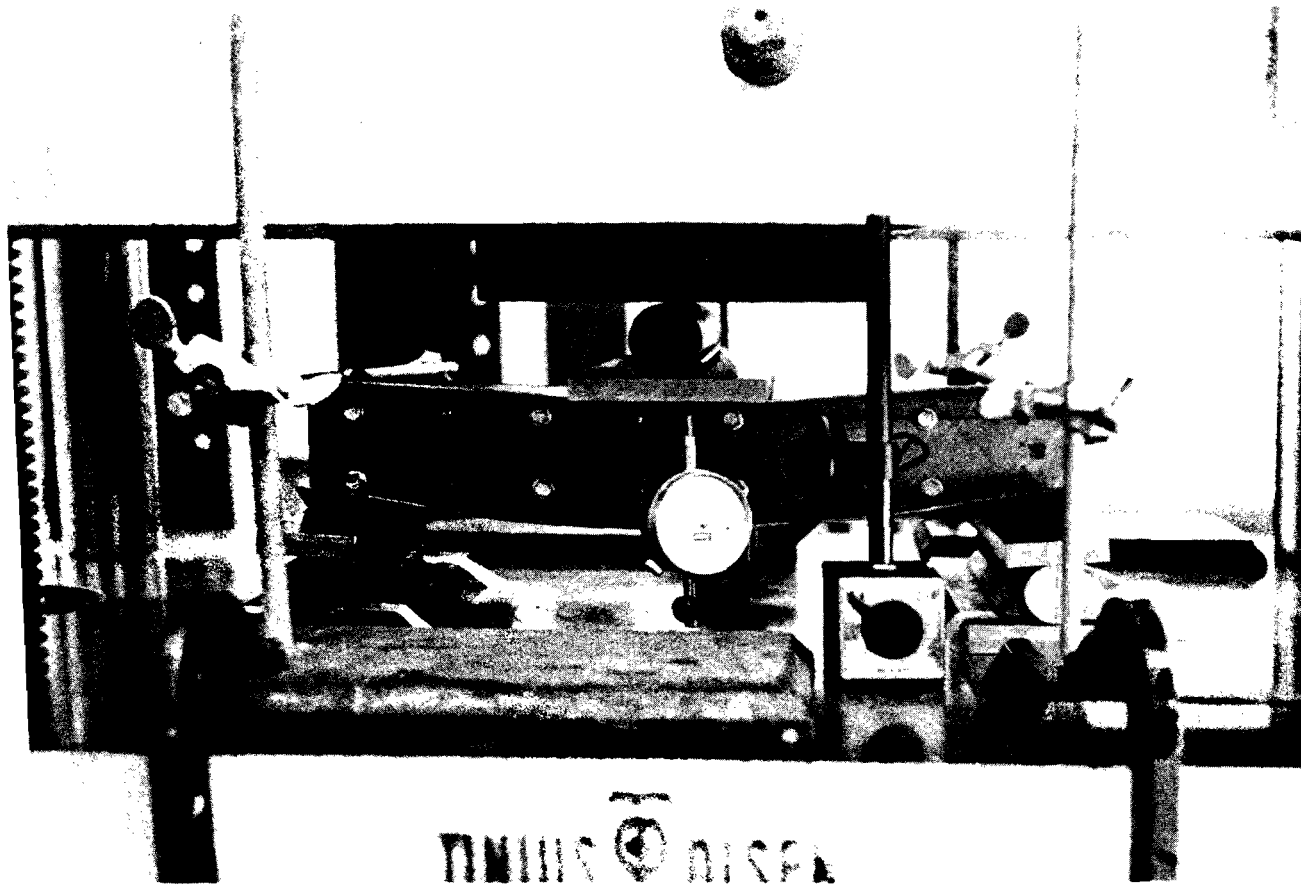


Fig. 22. Photograph Showing I-beams Subjected to End One-Flange Loading at Failure

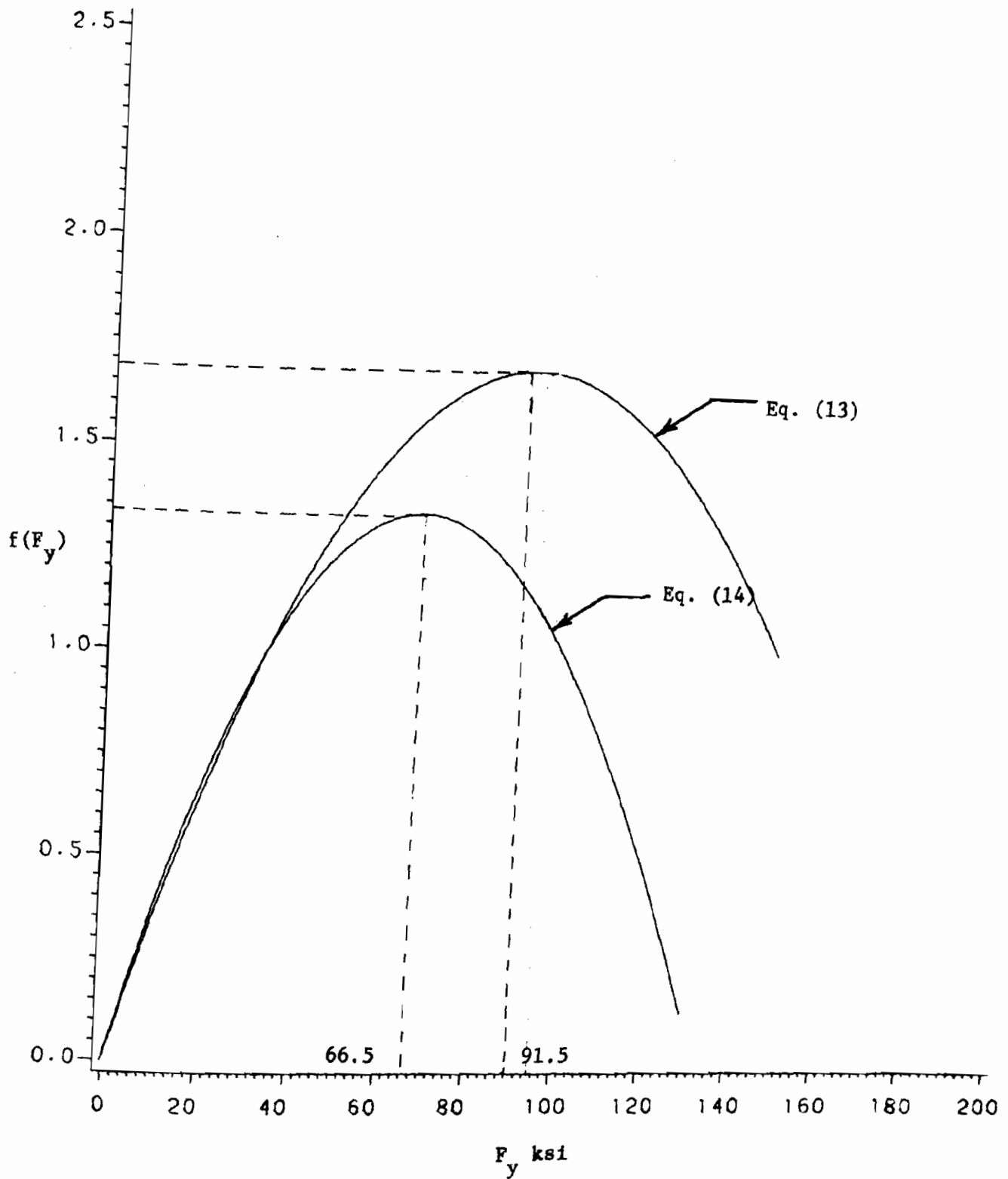


Fig. 23. Plot of Equations (13) and (14)

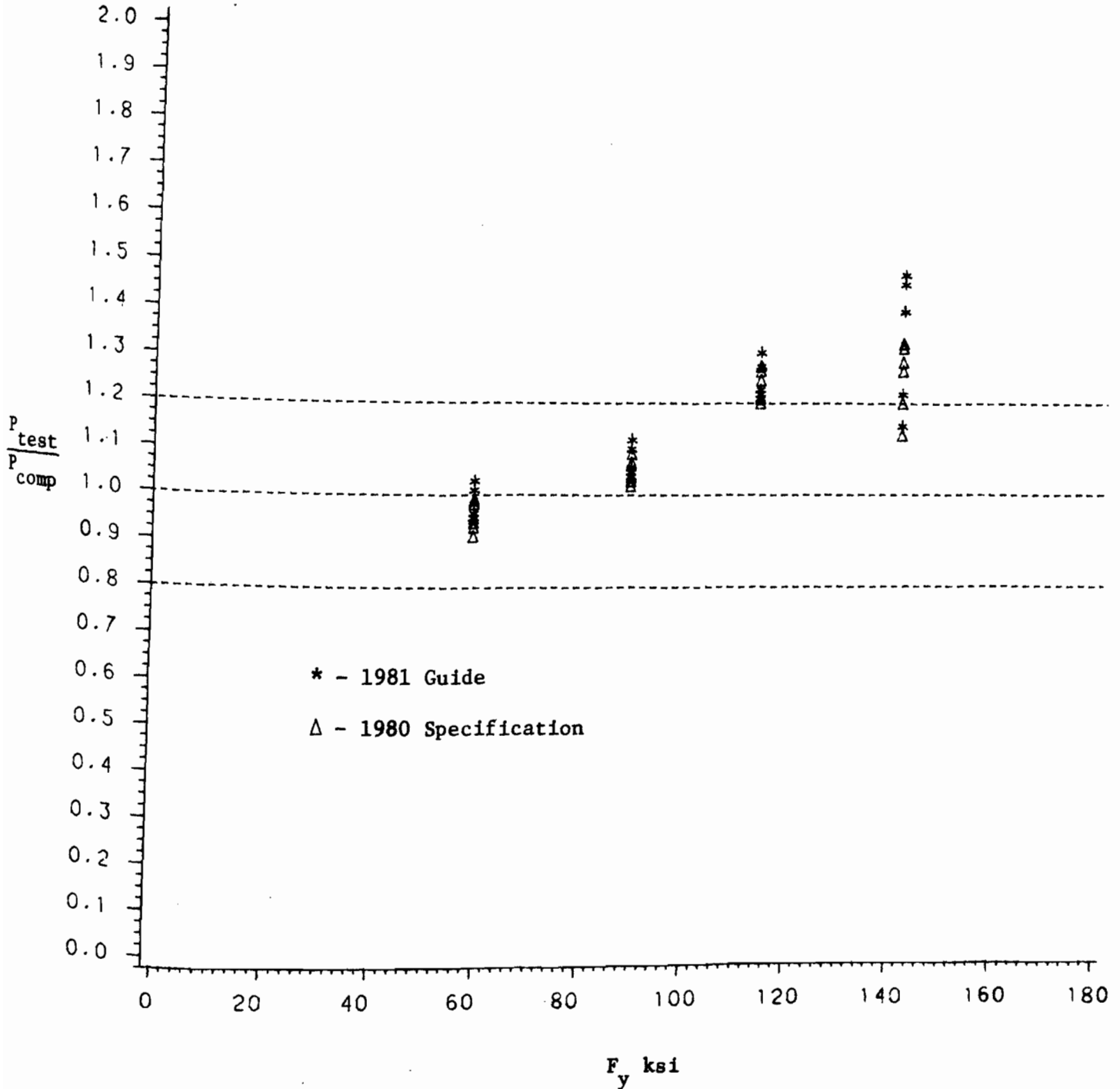


Fig. 24. Effect of  $F_y$  on the Ratio  $\frac{P_{test}}{P_{comp}}$  for Hat Sections Subjected to Interior One-Flange Loading Condition Based on the AISI 1981 Guide and 1980 Specification with Modified  $f(F_y)$

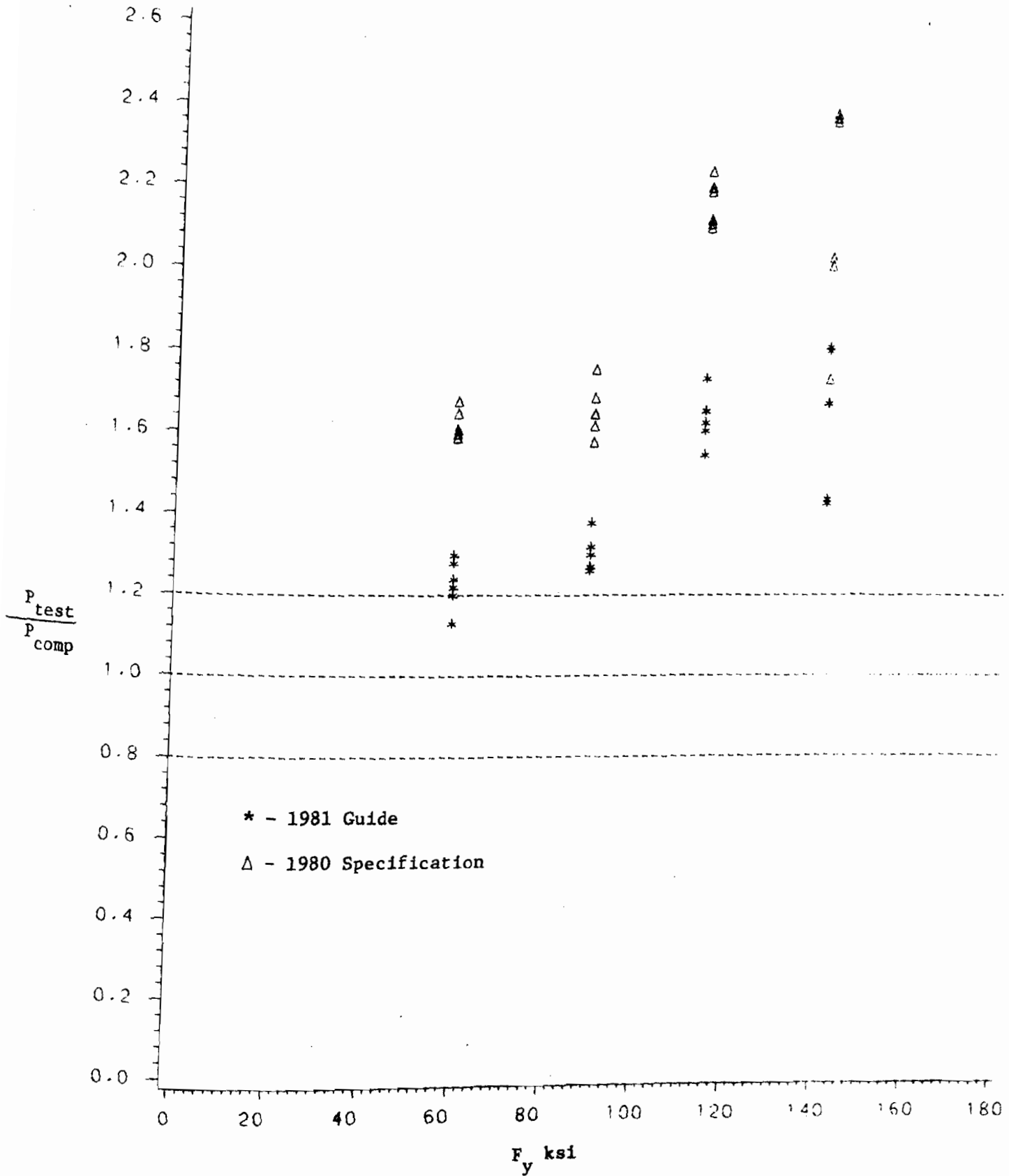


Fig. 25. Effect of  $F_y$  on the Ratio  $P_{test}/P_{comp}$  for Hat Sections  
 Subjected to End One-Flange Loading Condition  
 Based on the AISI 1981 Guide and 1980 Specification  
 with Modified  $f(F_y)$

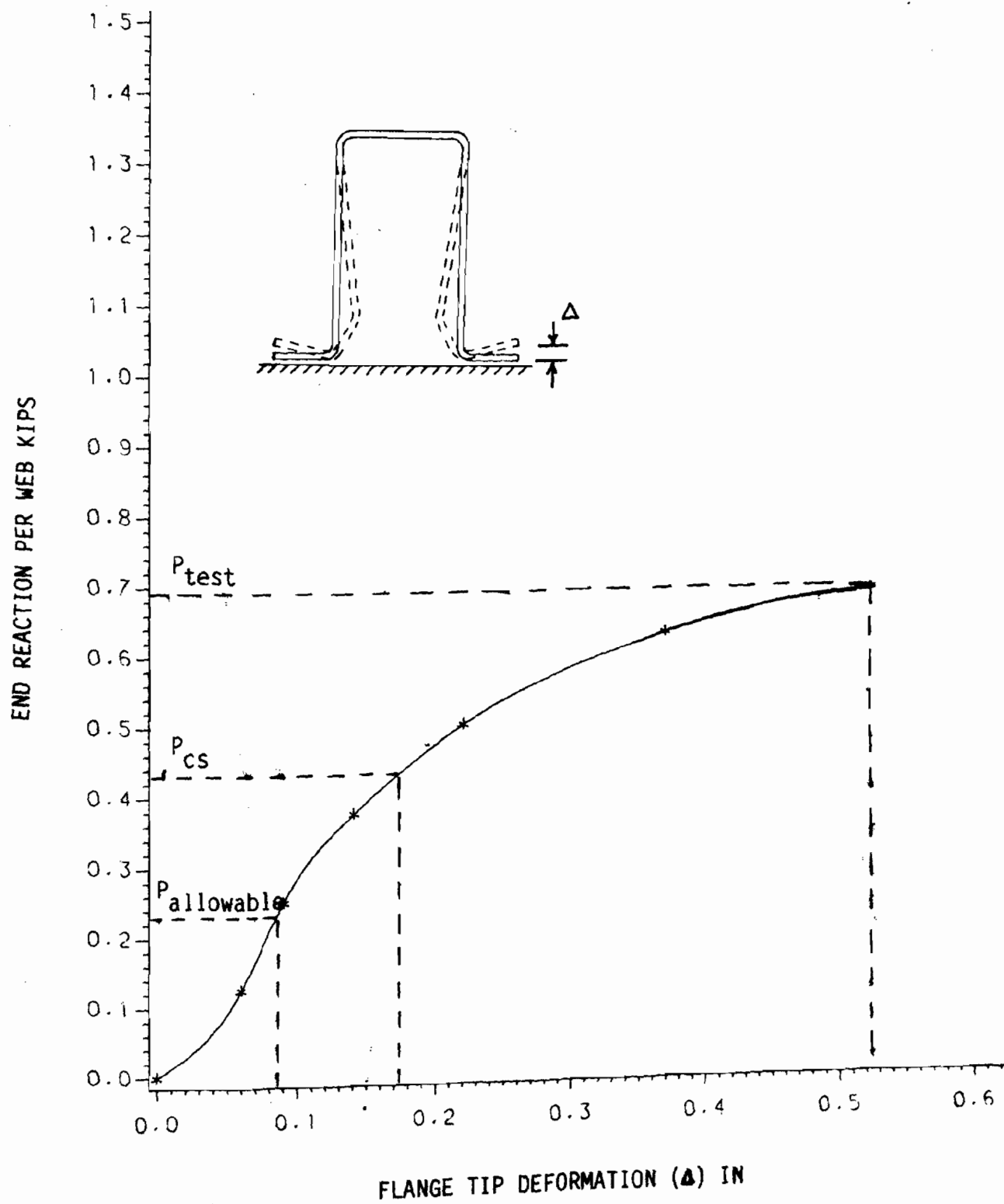


Fig. 26. Applied Load vs. Flange Tip Deformation of Hat Section Under End One-Flange Loading (Specimen No. 1-HE-21)



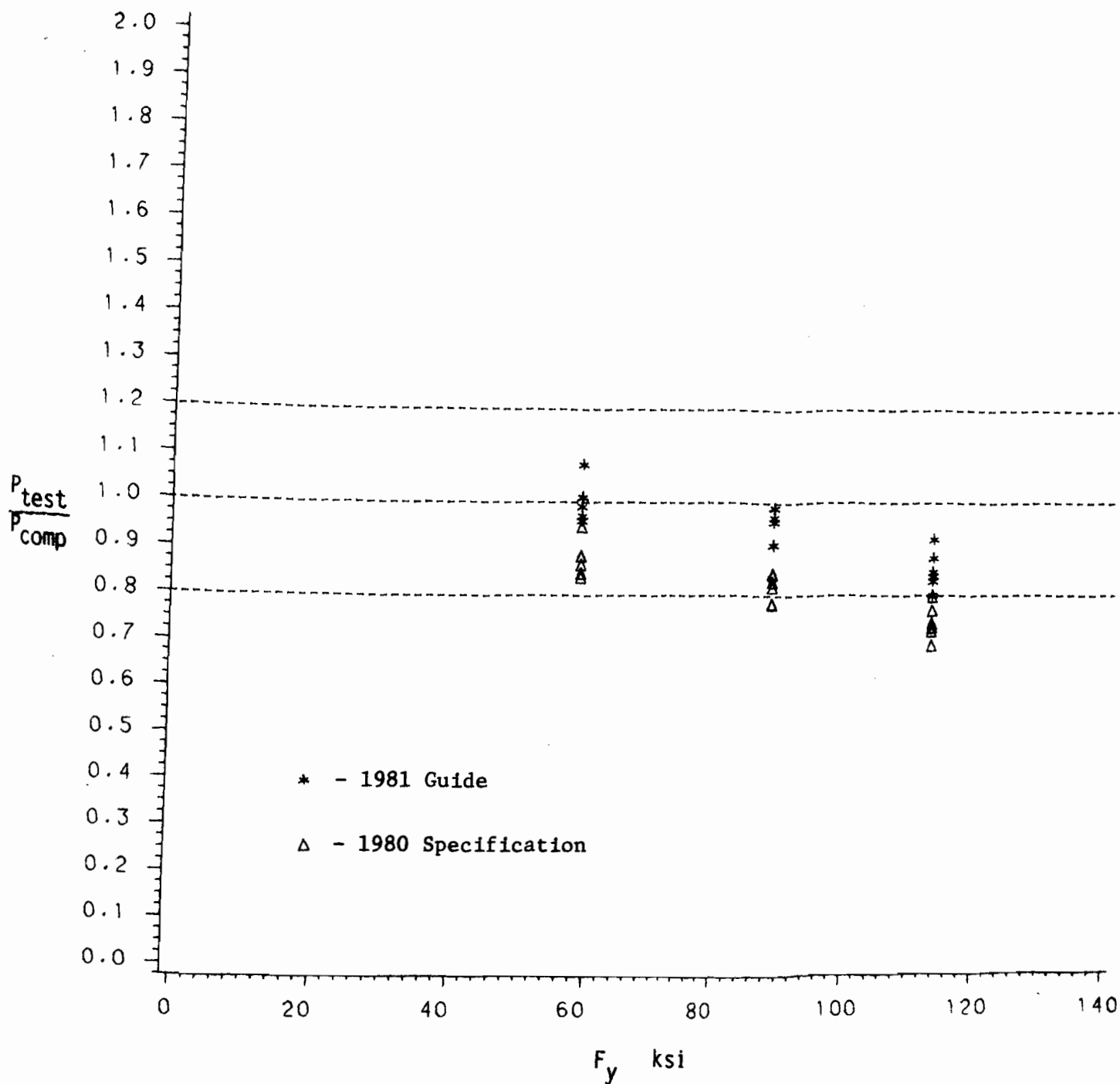


Fig. 27 Effect of  $F_y$  on the Ratio  $P_{test}/P_{comp}$  for Interior One-Flange Loading of I-Sections Based on the 1981 Guide and the 1980 Specification

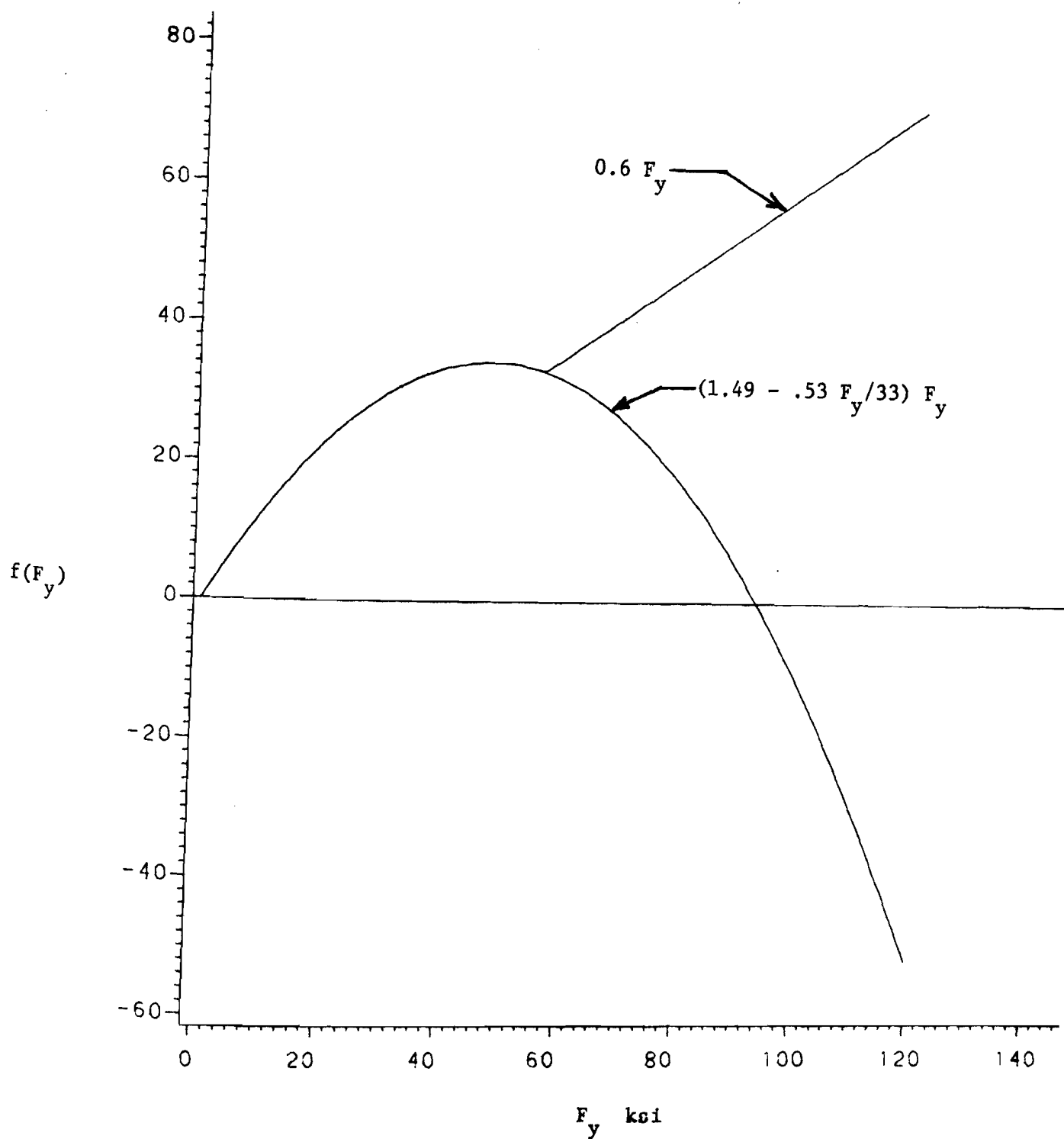
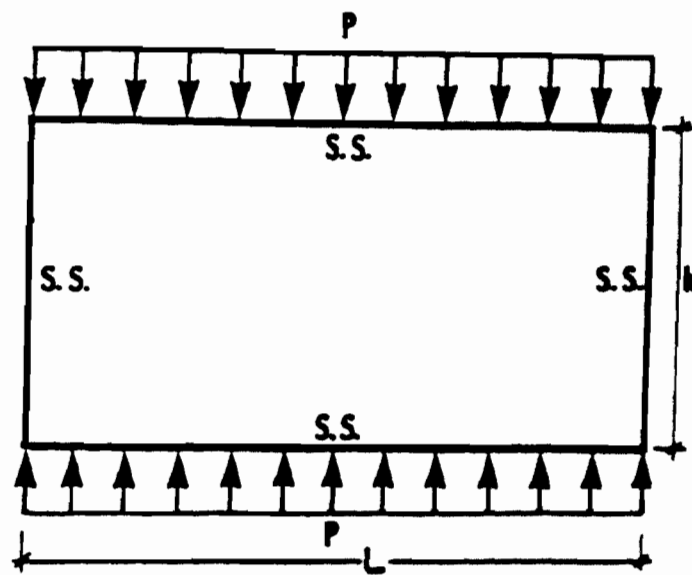


Fig. 28. Function of  $F_y$  for I-Sections Subjected to Interior One-Flange Loading.



(a) Plate Loading

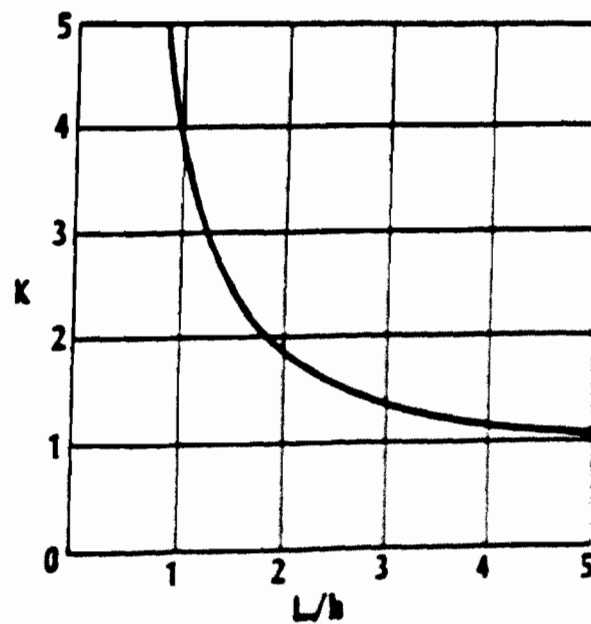
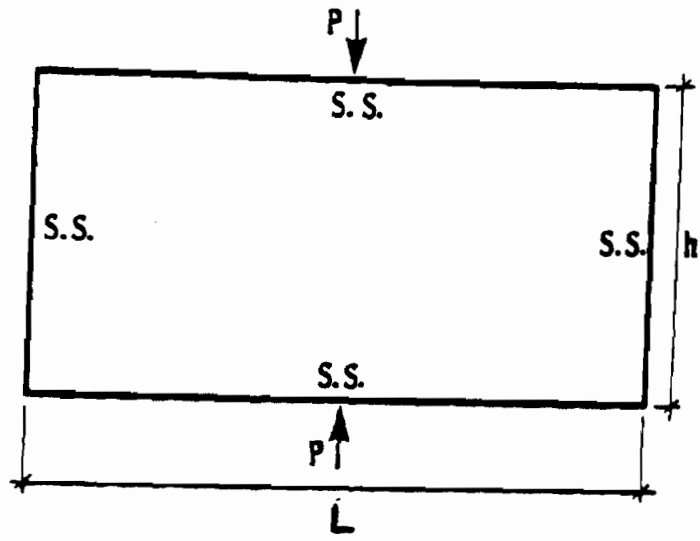
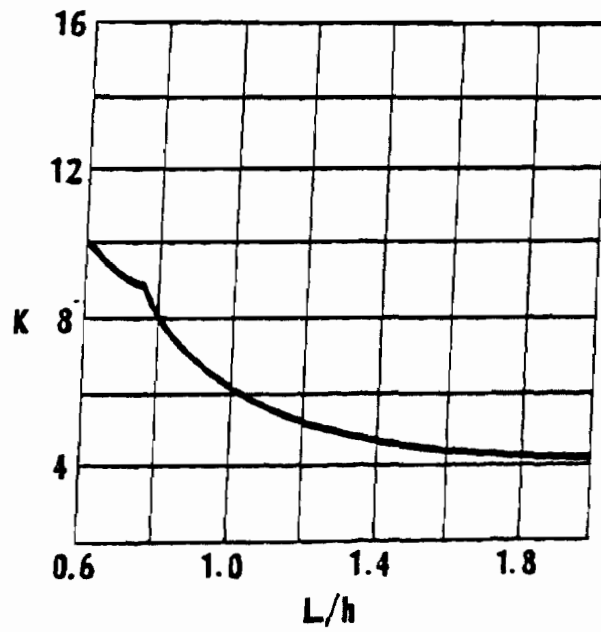
(b) Plate Buckling Coefficient,  $K$ 

Fig. 29. Simply Supported Plate Subjected to Uniformly Distributed Load<sup>13</sup>

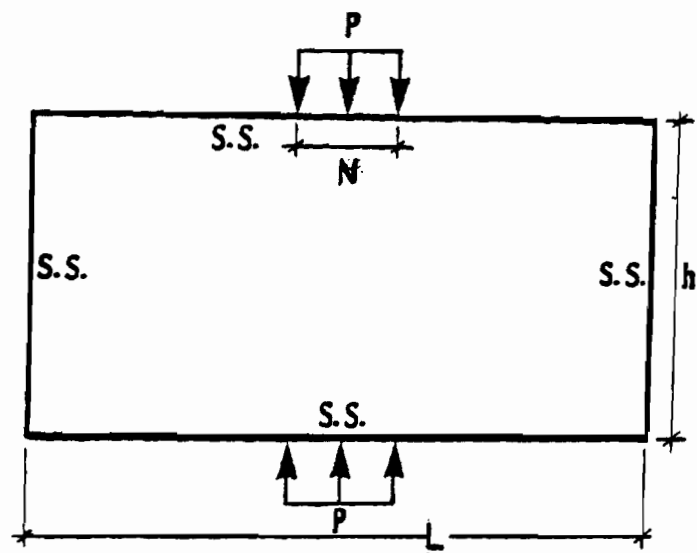


(a) Plate Loading

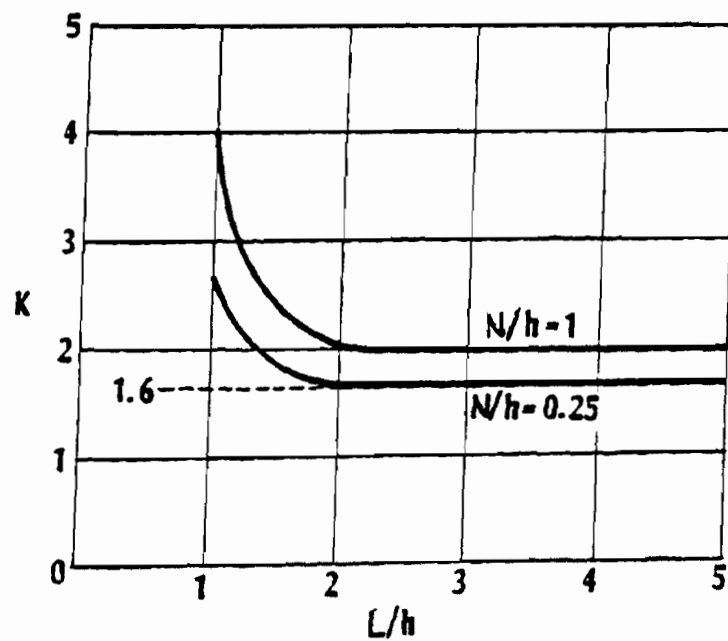


(b) Plate Buckling Coefficient, K

Fig. 30. Simply Supported Plate Subjected to Two Opposite Concentrated Load<sup>14,15</sup>

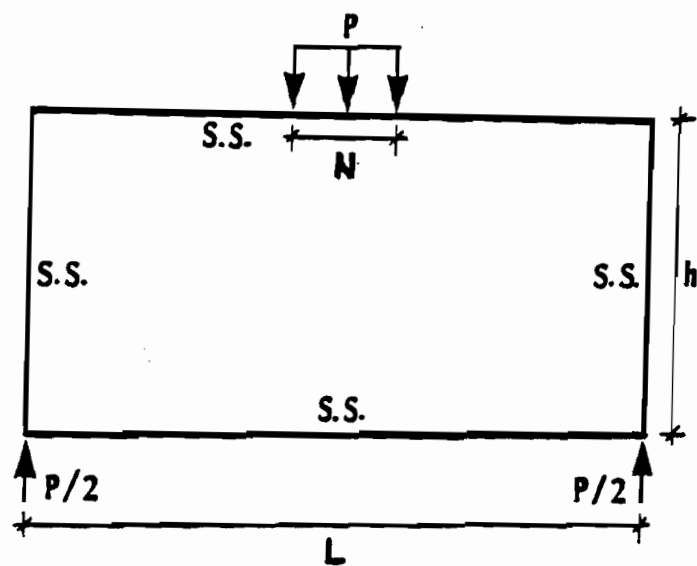


(a) Plate Loading



(b) Plate Buckling Coefficient, K

Fig. 31. Simply Supported Plate Subjected to Two Opposite Partially Distributed Load<sup>16,17</sup>



(a) Plate loading

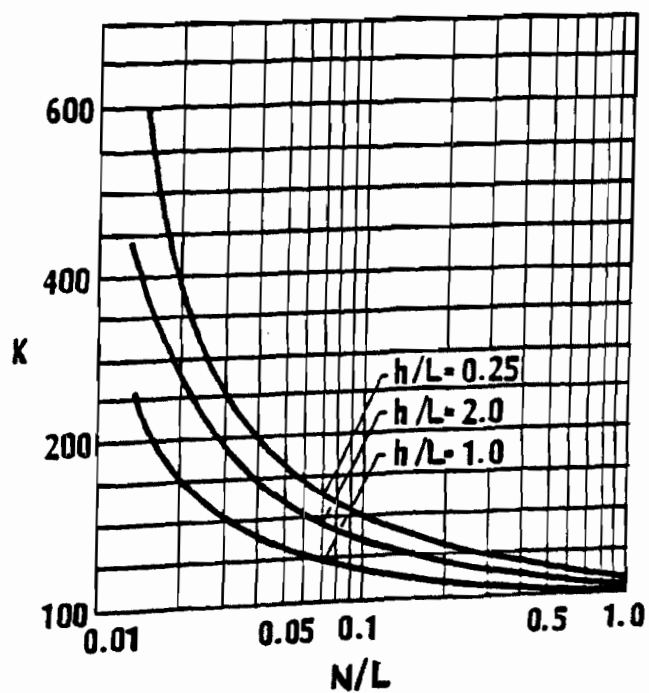
(b) Plate Buckling Coefficient,  $K$ 

Fig. 32. Simply Supported Plate Subjected to Partial Edge Loading<sup>18</sup>

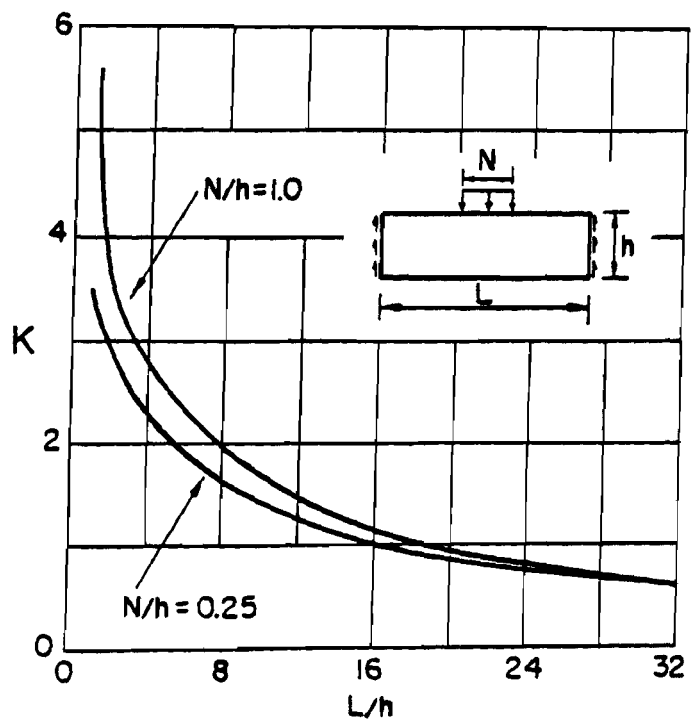


Fig. 33 Buckling Coefficient as the Function of  $N/h$  and  $L/h$  Ratios<sup>16,17</sup>

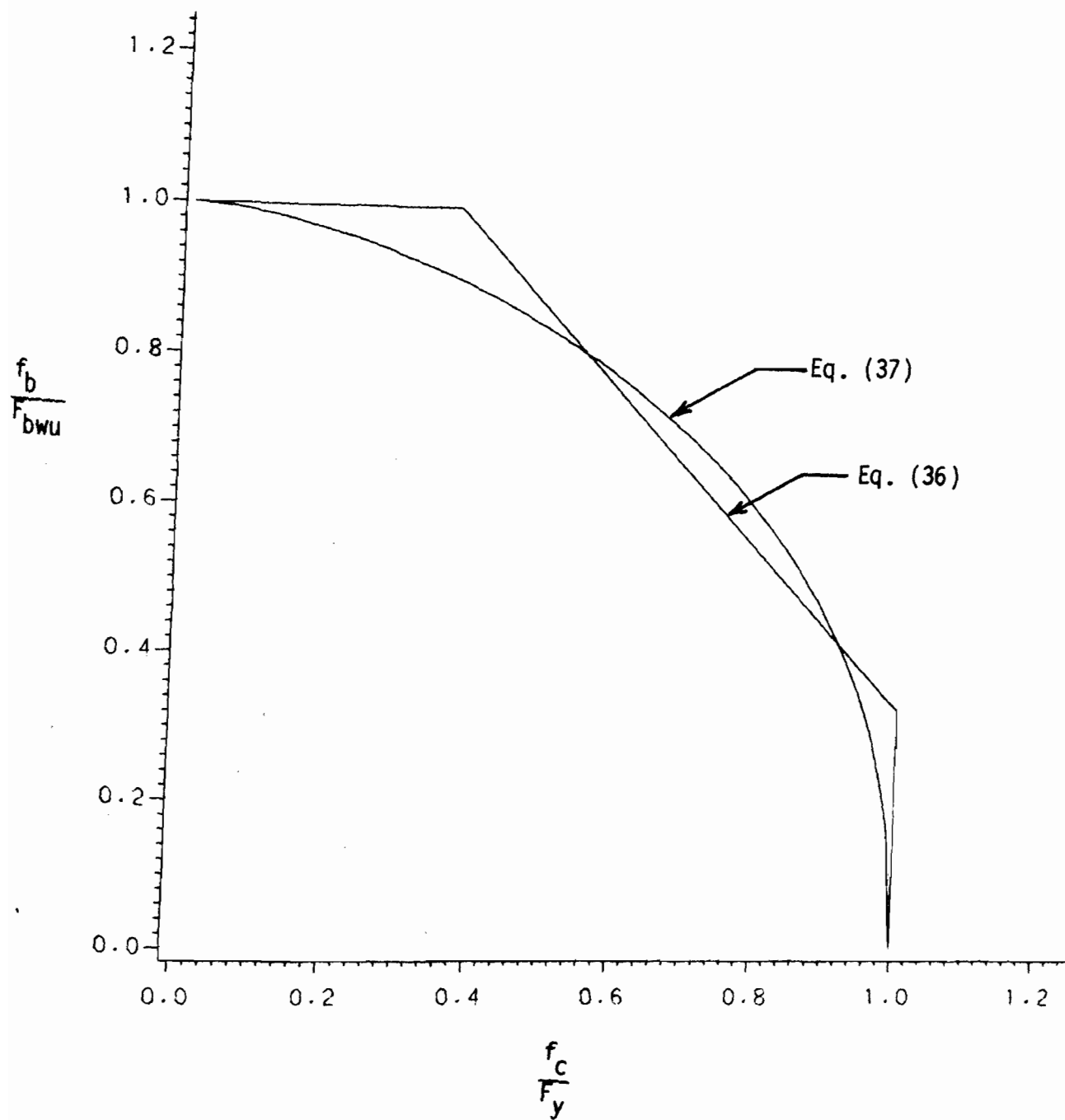


Fig. 34. Plot of Interaction Equations for Combined Bending and Web Crippling



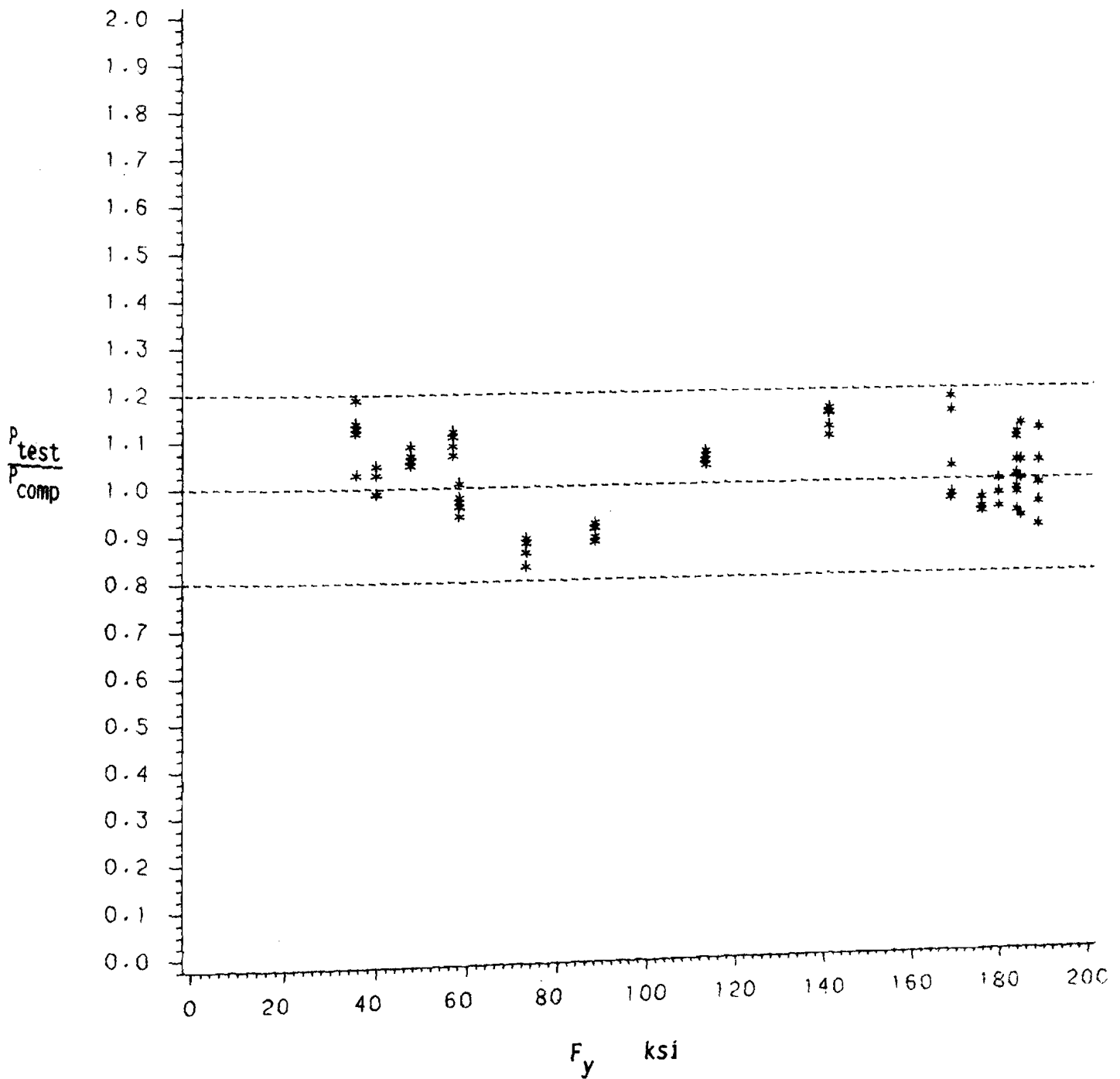


Fig. 35. Effect of  $F_y$  on the Ratio  $\frac{P_{test}}{P_{comp}}$  using Equations (29), (36) and (31)

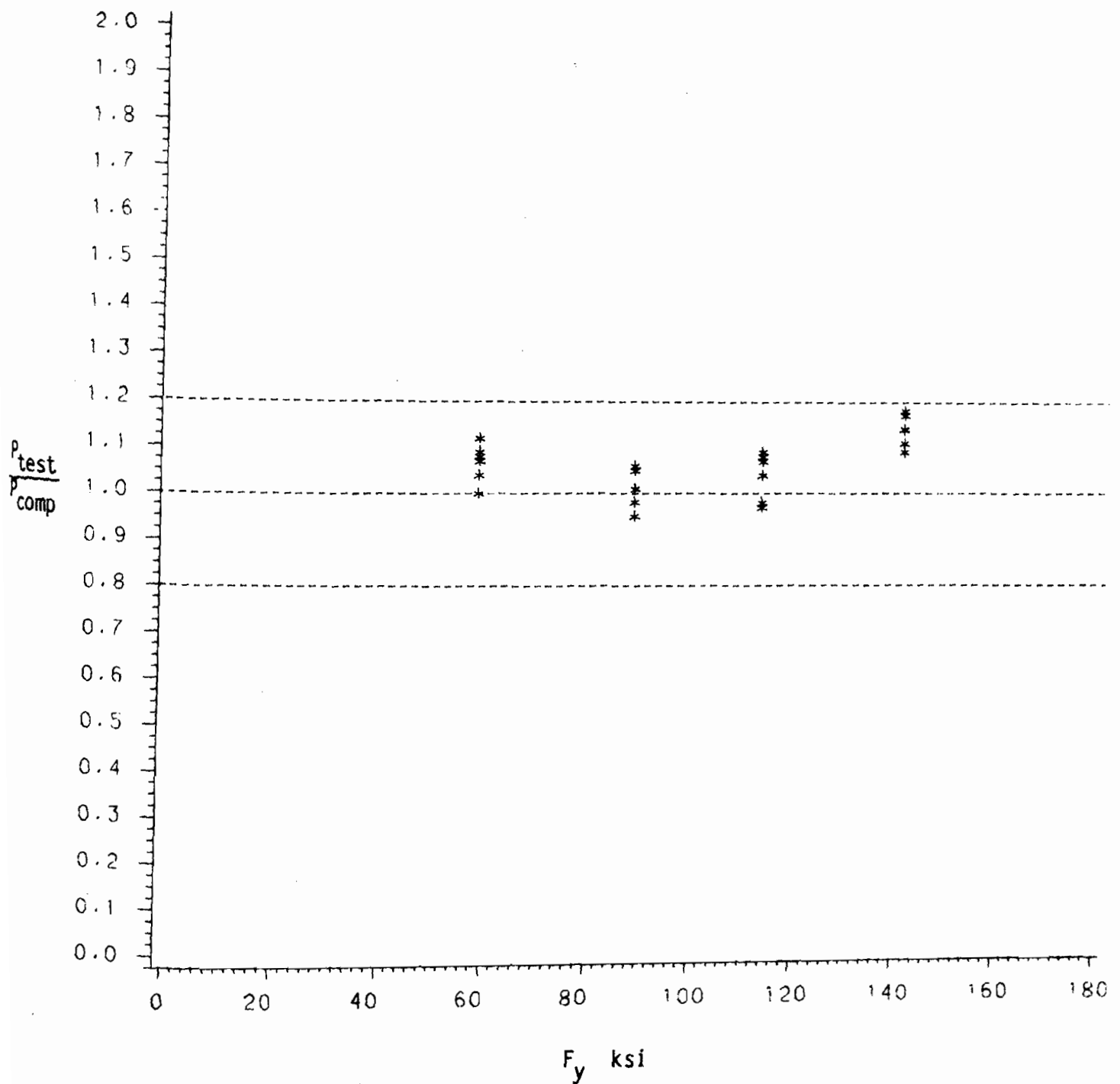


Fig. 36. Effect of  $F_y$  on the Ratio  $P_{test}/P_{comp}$  Using Equations (40) and (41)

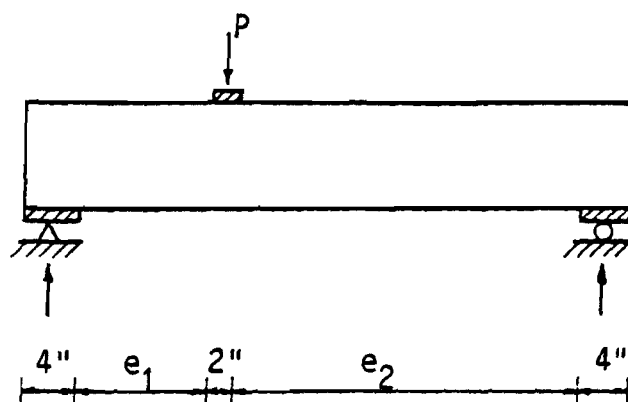


Fig. 37. Test Setup to Verify Equation (31)

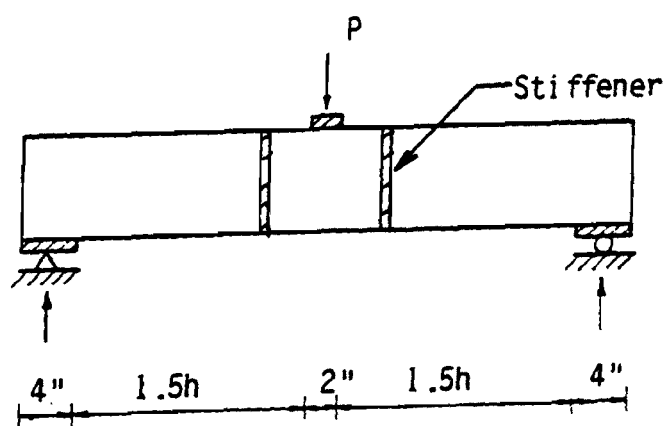


Fig. 38. Test Setup to Verify Equation (29)

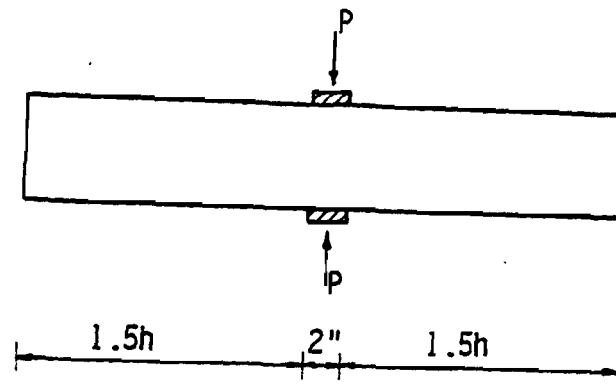


Fig. 39. Test Setup for Interior Two-Flange Loading

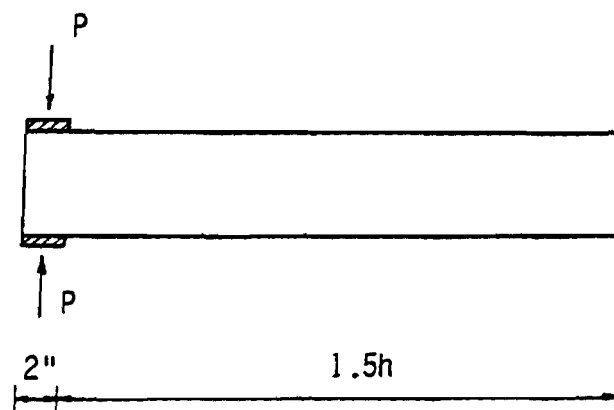


Fig. 40. Test Setup for End Two-Flange Loading

APPENDIX A  
LOADING CONDITIONS FOR WEB CRIPPLING

The classification of loading conditions as specified in the AISI 1980 Specification for the Design of Cold-Formed Steel Structural Members is based on the following dimensions:<sup>3</sup>

- 1)  $e_1$ , the distance between the edge of bearing of a reaction or a concentrated load to the free end of the beam.
- 2)  $e_2$ , the distance between the edges of bearing of the adjacent opposite concentrated loads or reactions.

Fig. A-1 gives the designations of the distances  $e_1$  and  $e_2$ .

The following four loading conditions are now classified in the AISI Specification:<sup>3</sup>

- 1) Interior one-flange loading:  $e_1 > 1.5h$  and  $e_2 > 1.5h$
- 2) End one-flange loading:  $e_1 < 1.5h$  and  $e_2 > 1.5h$
- 3) Interior two-flange loading:  $e_1 > 1.5h$  and  $e_2 < 1.5h$
- 4) End two-flange loading:  $e_1 < 1.5h$  and  $e_2 < 1.5h$

The application of these loading conditions, as illustrated in the AISI Commentary on the 1980 Specification, is presented in Fig. A-2

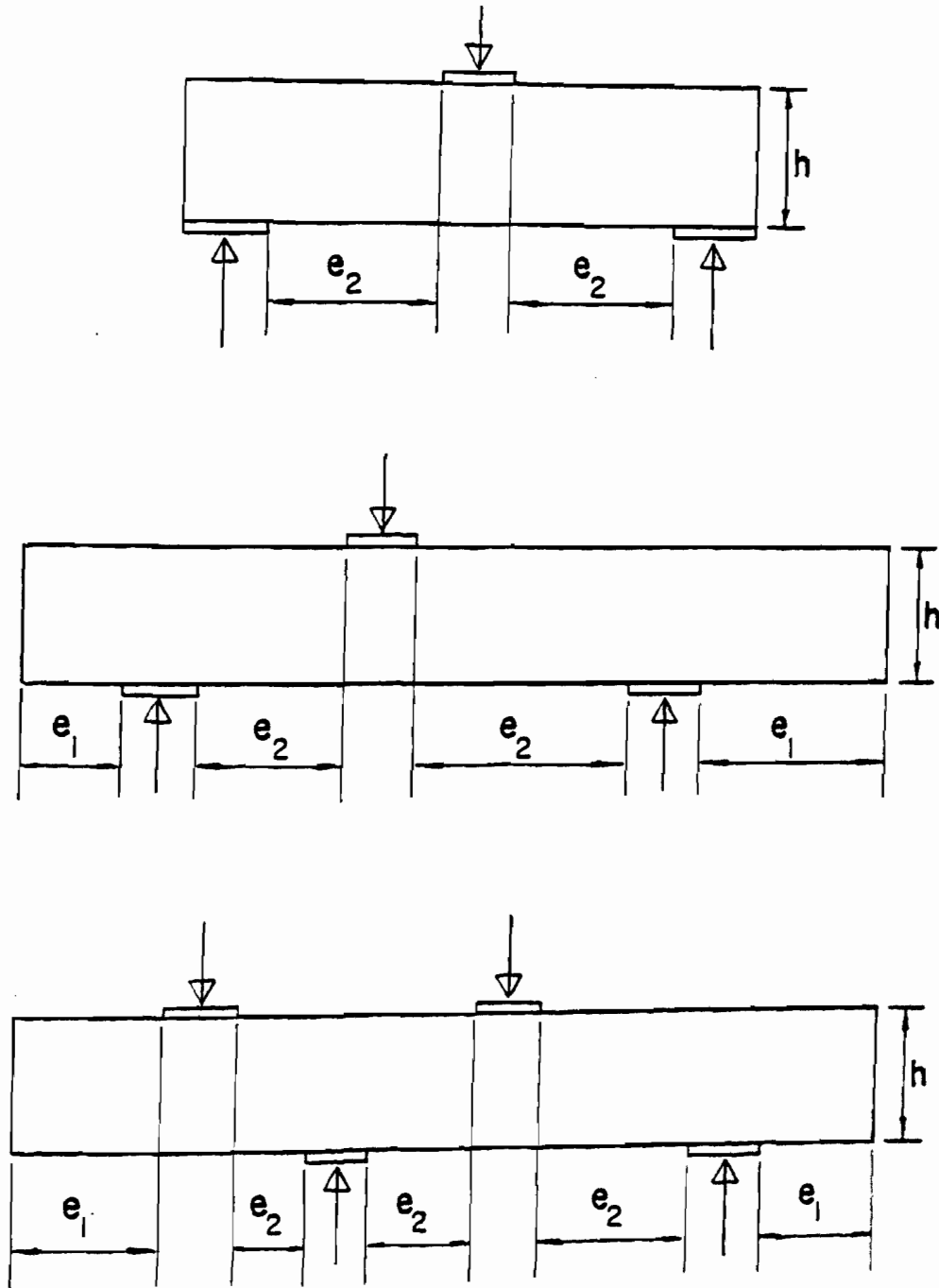


Fig. A-1 Designations of Distances  $e_1$  and  $e_2$

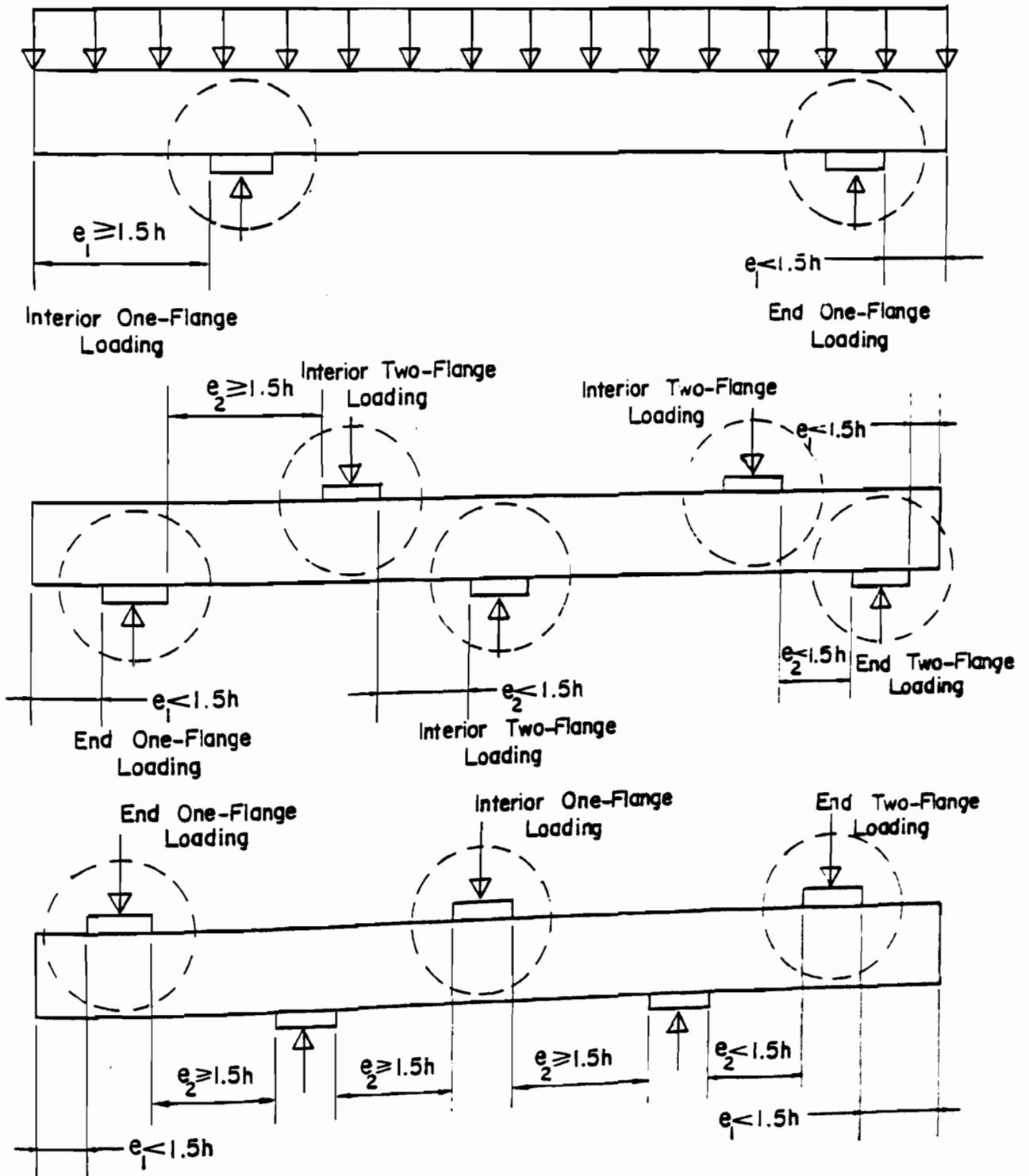


Fig. A-2 Application of Loading Conditions for Web Crippling

## APPENDIX B

## DATA OBTAINED FROM PREVIOUS UMR STUDY

TABLE B-1

Measured Dimension of Test Specimens from Reference 11  
Used for Interior One-Flange Loading

Specimen No.	t (in.)	B1 (in.)	B2 (in.)	D1 (in.)	D2 (in.)	D3 (in.)	R (in.)	N (in.)	L (in.)
SU-1-IOF-1	.048	1.524	1.482	9.924	0.617	0.690	.1330	1	42
SU-1-IOF-2	.047	1.486	1.497	9.504	0.597	0.671	.1250	1	42
SU-1-IOF-5	.049	1.466	1.503	9.951	0.686	0.602	.1250	3	42
SU-1-IOF-6	.048	1.503	1.495	9.944	0.661	0.679	.1250	3	42
SU-2-IOF-1	.049	1.512	1.454	12.345	0.632	0.688	.1250	1	48
SU-2-IOF-2	.050	1.457	1.498	12.310	0.683	0.682	.1250	1	48
SU-2-IOF-5	.048	1.514	1.464	12.305	0.647	0.706	.1250	3	48
SU-2-IOF-6	.049	1.483	1.487	12.345	0.662	0.668	.1250	3	48
SU-5-IOF-1	.049	2.648	2.660	6.193	0.611	0.606	.0938	1	30
SU-5-IOF-2	.050	2.651	2.662	6.177	0.606	0.600	.0938	1	30
SU-5-IOF-3	.050	2.641	2.651	6.194	0.606	0.619	.0977	2	30
SU-5-IOF-4	.051	2.650	2.655	6.180	0.622	0.607	.0938	2	30
SU-5-IOF-5	.050	2.655	2.661	6.186	0.613	0.615	.0898	3	30
SU-5-IOF-6	.050	2.647	2.648	6.192	0.609	0.616	.0938	3	30
SU-6-IOF-1	.050	3.134	3.139	7.371	0.615	0.618	.0938	1	30
SU-6-IOF-2	.050	3.134	3.113	7.410	0.616	0.597	.0859	1	30
SU-6-IOF-3	.049	3.137	3.131	7.380	0.616	0.598	.0898	2	30
SU-6-IOF-4	.050	3.104	3.118	7.438	0.597	0.610	.0938	2	30
SU-6-IOF-5	.049	3.135	3.136	7.396	0.620	0.596	.0938	3	30
SU-6-IOF-6	.050	3.133	3.137	7.379	0.612	0.604	.0898	3	30
M-SU-6-IOF-1	.050	3.124	3.134	7.397	0.615	0.607	.0938	1	30
M-SU-6-IOF-2	.050	3.128	3.120	7.389	0.625	0.609	.0938	1	30
M-SU-6-IOF-5	.051	3.148	3.121	7.386	0.616	0.613	.0938	3	30
M-SU-6-IOF-6	.050	3.136	3.139	7.363	0.619	0.614	.0938	3	30
U-SU-17-IOF-5	.049	1.396	1.417	4.908	0.0	0.0	.0470	3	26
U-SU-17-IOF-6	.049	1.390	1.385	4.901	0.0	0.0	.0470	3	26
U-SU-18-IOF-5	.049	2.175	2.188	9.540	0.0	0.0	.0470	3	40
U-SU-18-IOF-6	.049	2.184	2.163	9.609	0.0	0.0	.0470	3	40

Note: See Definitions of symbols in Fig. B-1



TABLE B-2

Measured Dimension of Test Specimens from Reference 19  
Used for Interior One-Flange Loading

Specimen No.	t (in.)	B1 (in.)	B2 (in.)	D1 (in.)	D2 (in.)	D3 (in.)	R (in.)	N (in.)	L (in.)
C3-1	.050	2.521	2.517	4.920	0.606	0.618	.0781	1	11.0
C3-2	.050	2.514	2.523	4.946	0.600	0.604	.0781	1	11.0
C3-3	.051	2.513	2.507	4.962	0.616	0.614	.0781	1	15.9
C3-4	.051	2.512	2.506	4.963	0.621	0.615	.0781	1	15.9
C3-5	.051	2.523	2.521	4.950	0.602	0.604	.0781	1	20.8
C3-6	.050	2.501	2.518	4.958	0.610	0.590	.0781	1	20.8
C3-7	.050	2.519	2.526	4.939	0.617	0.606	.0781	1	25.7
C3-8	.051	2.525	2.502	4.956	0.611	0.610	.0781	1	25.7
C3-9	.049	2.512	2.526	4.945	0.630	0.580	.0781	1	30.6
C3-10	.050	2.514	2.509	4.948	0.600	0.630	.0781	1	30.6
C3-11	.045	2.521	2.496	5.892	0.603	0.700	.0859	1	11.0
C3-12	.045	2.507	2.493	5.903	0.594	0.714	.0859	1	11.0
C3-13	.045	2.496	2.499	5.926	0.543	0.692	.0859	1	16.9
C3-14	.045	2.514	2.497	5.946	0.566	0.716	.0859	1	16.9
C3-15	.049	2.641	2.646	6.156	0.625	0.621	.0703	1	22.8
C3-16	.049	2.633	2.667	6.143	0.622	0.640	.0703	1	22.8
C3-17	.052	3.016	3.015	5.845	0.751	0.737	.0703	1	28.7
C3-18	.052	3.045	3.032	5.828	0.656	0.607	.0703	1	28.7
C3-19	.052	3.036	3.036	5.914	0.555	0.576	.0703	1	34.6
C3-20	.052	3.030	3.044	5.909	0.602	0.560	.0703	1	34.6

Note: See Definitions of symbols in Fig. B-1

TABLE B-3

Measured Dimension of Test Specimens from Reference 11  
Used for End One-Flange Loading

Specimen No.	t (in.)	B1 (in.)	B2 (in.)	D1 (in.)	D2 (in.)	D3 (in.)	R (in.)	N (in.)	L (in.)
SU-1-EOF-1	.047	1.510	1.488	9.977	0.617	0.677	.1250	1	42
SU-1-EOF-2	.048	1.472	1.507	9.961	0.696	0.610	.1250	1	42
SU-1-EOF-5	.049	1.514	1.494	9.958	0.649	0.619	.1250	3	42
SU-1-EOF-6	.050	1.533	1.490	9.961	0.604	0.667	.1406	3	42
SU-2-EOF-1	.049	1.462	1.450	12.225	0.698	0.719	.1250	1	48
SU-2-EOF-2	.048	1.461	1.459	12.220	0.714	0.729	.1250	1	48
SU-2-EOF-5	.048	1.453	1.441	12.290	0.693	0.750	.1250	3	48
SU-2-EOF-6	.047	1.465	1.484	12.245	0.727	0.691	.1250	3	48
SU-4-EOF-1	.050	2.164	2.161	4.925	0.610	0.620	.0870	1	30
SU-4-EOF-2	.050	2.157	2.148	4.931	0.613	0.625	.0781	1	30
SU-4-EOF-3	.050	2.157	2.163	4.921	0.619	0.615	.0859	2	30
SU-4-EOF-4	.049	2.157	2.163	4.945	0.620	0.600	.0876	2	30
SU-4-EOF-5	.050	2.165	2.167	4.938	0.610	0.595	.0846	3	30
SU-4-EOF-6	.049	2.152	2.152	4.952	0.618	0.603	.0859	3	30
SU-5-EOF-1	.050	2.695	2.655	6.189	0.603	0.599	.0938	1	30
SU-5-EOF-2	.051	2.667	2.677	6.157	0.613	0.614	.0898	1	30
SU-5-EOF-3	.051	2.651	2.651	6.206	0.614	0.596	.0938	2	30
SU-5-EOF-4	.051	2.648	2.643	6.204	0.619	0.609	.1016	2	30
SU-5-EOF-5	.051	2.658	2.651	6.190	0.616	0.604	.0938	3	30
SU-5-EOF-6	.050	2.653	2.656	6.188	0.615	0.602	.0938	3	30
SU-6-EOF-1	.050	3.135	3.142	7.384	0.607	0.611	.0859	1	30
SU-6-EOF-2	.049	3.134	3.131	7.392	0.617	0.607	.0938	1	30
SU-6-EOF-3	.049	3.126	3.142	7.387	0.619	0.597	.0859	2	30
SU-6-EOF-4	.049	3.126	3.142	7.394	0.605	0.609	.0977	2	30
SU-6-EOF-5	.050	3.142	3.139	7.394	0.610	0.603	.0938	3	30
SU-6-EOF-6	.050	3.139	3.136	7.400	0.604	0.606	.0938	3	30
M-SU-4-EOF-1	.050	2.161	2.184	4.899	0.603	0.619	.0898	1	30
M-SU-4-EOF-2	.051	2.169	2.164	4.939	0.606	0.611	.0938	1	30
M-SU-4-EOF-5	.050	2.159	2.174	4.895	0.607	0.607	.0859	3	30
M-SU-4-EOF-6	.050	2.165	2.174	4.919	0.605	0.601	.0938	3	30
M-SU-6-EOF-1	.050	3.124	3.131	7.371	0.620	0.613	.0938	1	30
M-SU-6-EOF-2	.051	3.128	3.146	7.375	0.616	0.604	.0938	1	30
M-SU-6-EOF-5	.050	3.148	3.132	7.365	0.617	0.609	.0938	3	30
M-SU-6-EOF-6	.051	3.136	3.136	7.380	0.616	0.610	.0938	3	30
U-SU-17-EOF-1	.049	1.397	1.387	4.959	0.0	0.0	.0470	1	26
U-SU-17-EOF-1	.049	1.429	1.386	4.915	0.0	0.0	.0470	1	26
U-SU-17-EOF-1	.049	1.433	1.424	4.891	0.0	0.0	.0470	3	26
U-SU-17-EOF-1	.049	1.388	1.446	4.919	0.0	0.0	.0470	3	26
U-SU-17-EOF-1	.049	1.388	1.446	4.919	0.0	0.0	.0470	1	40
U-SU-18-EOF-1	.049	2.182	2.177	9.555	0.0	0.0	.0470	1	40
U-SU-18-EOF-1	.049	2.124	2.133	9.636	0.0	0.0	.0470	1	40
U-SU-18-EOF-1	.050	2.130	2.131	9.330	0.0	0.0	.0470	3	40
U-SU-18-EOF-1	.050	2.130	2.131	9.330	0.0	0.0	.0470	3	40
U-SU-18-EOF-1	.049	2.133	2.136	9.332	0.0	0.0	.0470	3	40

Note: See Definitions of symbols in Fig. B-1

TABLE B-4

Measured Dimension of Test Specimens from Reference 19  
Used for End One-Flange Loading

Specimen No.	t (in.)	B1 (in.)	B2 (in.)	D1 (in.)	D2 (in.)	D3 (in.)	R (in.)	N (in.)	L (in.)
C2-3	.050	2.507	2.506	4.943	0.611	0.619	.0781	1	11.9
C2-4	.050	2.521	2.505	4.938	0.611	0.607	.0781	1	11.9
C2-5	.050	2.516	2.521	4.912	0.612	0.612	.0781	1	16.9
C2-6	.050	2.513	2.501	4.940	0.621	0.595	.0781	1	16.9
C2-7	.050	2.503	2.502	4.960	0.618	0.611	.0781	1	21.8
C2-8	.050	2.517	2.521	4.932	0.614	0.612	.0781	1	21.8
C2-9	.050	2.519	2.530	4.950	0.604	0.612	.0781	1	26.7
C2-10	.050	2.530	2.505	4.949	0.612	0.600	.0781	1	16.7
C2-13	.052	2.545	2.550	5.991	0.532	0.568	.0703	1	12.9
C2-14	.052	2.549	2.560	5.994	0.620	0.532	.0703	1	12.9
C2-15	.052	2.552	2.559	5.973	0.554	0.600	.0703	1	18.8
C2-16	.052	2.539	2.545	5.973	0.620	0.604	.0703	1	18.8
C2-17	.052	2.541	2.539	5.978	0.589	0.607	.0703	1	24.7
C2-18	.052	2.551	2.567	5.950	0.608	0.587	.0703	1	24.7
C2-19	.052	2.544	2.565	5.927	0.612	0.608	.0703	1	30.6
C2-20	.052	2.559	2.533	5.956	0.592	0.609	.0703	1	30.6

Note: See Definitions of symbols in Fig. B-1

TABLE B-5

Measured Dimension of Test Specimens from Reference 11  
Used for Combined Web Crippling and Bending Moment

Specimen No.	t (in.)	B1 (in.)	B2 (in.)	D1 (in.)	D2 (in.)	D3 (in.)	R (in.)	N (in.)	L (in.)
SU-BC-1-1	.046	1.959	1.908	4.774	0.607	0.585	.0625	3	40.0
SU-BC-1-2	.046	1.930	1.913	4.781	0.582	0.590	.0625	3	40.0
SU-BC-1-3	.046	1.935	1.936	4.727	0.613	0.601	.0625	3	74.0
SU-BC-1-4	.047	1.926	1.954	4.689	0.632	0.639	.0625	3	74.0
SU-BC-1-5	.047	1.930	1.932	4.723	0.633	0.637	.0625	3	138.0
SU-BC-1-6	.046	1.889	1.929	4.699	0.629	0.640	.0625	3	138.0
SU-BC-3-1	.049	1.642	1.649	9.808	0.639	0.617	.0470	3	66.0
SU-BC-3-2	.049	1.638	1.639	9.781	0.641	0.617	.0470	3	66.0
SU-BC-3-3	.049	1.644	1.643	9.778	0.635	0.620	.0470	3	94.0
SU-BC-3-4	.049	1.638	1.635	9.812	0.639	0.632	.0470	3	94.0
SU-BC-3-5	.048	1.636	1.633	9.780	0.625	0.638	.0470	3	128.0
SU-BC-3-6	.049	1.645	1.639	9.807	0.628	0.632	.0470	3	128.0
SU-BC-15-1	.050	3.141	3.160	7.428	0.620	0.584	.0781	3	46.0
SU-BC-15-2	.051	3.130	3.166	7.443	0.603	0.625	.0781	3	46.0
SU-BC-15-3	.051	3.154	3.145	7.423	0.605	0.615	.0781	3	86.0
SU-BC-15-4	.051	3.124	3.155	7.431	0.581	0.620	.0781	3	86.0
SU-BC-15-5	.051	3.155	3.156	7.406	0.615	0.612	.0781	3	138.0
SU-BC-15-6	.052	3.153	3.154	7.412	0.611	0.613	.0781	3	138.0
SU-4-IOF-1	.049	2.158	2.156	4.960	0.596	0.585	.0781	1	25.0
SU-4-IOF-2	.050	2.155	2.153	4.935	0.593	0.610	.0781	1	25.0
SU-4-IOF-3	.050	2.169	2.173	4.941	0.587	0.610	.0938	2	25.0
SU-4-IOF-4	.050	2.169	2.165	4.931	0.624	0.588	.0859	2	25.0
SU-4-IOF-5	.050	2.179	2.138	4.935	0.604	0.608	.0781	3	25.0
SU-4-IOF-6	.050	2.173	2.149	4.909	0.600	0.609	.0781	3	25.0
M-SU-4-IOF-1	.050	2.156	2.162	4.974	0.591	0.619	.0938	1	25.0
M-SU-4-IOF-2	.051	2.174	2.152	4.908	0.607	0.623	.0977	1	25.0
M-SU-4-IOF-5	.051	2.167	2.137	4.931	0.603	0.608	.0938	3	25.0
M-SU-4-IOF-6	.050	2.165	2.162	4.936	0.615	0.600	.0898	3	25.0

TABLE B-5 (Cont'd)

Measured Dimension of Test Specimens from Reference 11  
Used for Combined Web Crippling and Bending Moment

Specimen No.	t (in.)	B1 (in.)	B2 (in.)	D1 (in.)	D2 (in.)	D3 (in.)	R (in.)	N (in.)	L (in.)
SU-BC-6-1	.050	1.633	1.627	2.561	0.637	0.628	.0781	3	50.5
SU-BC-6-2	.050	1.638	1.631	2.571	0.643	0.611	.0781	3	50.5
SU-BC-6-3	.051	1.635	1.631	2.560	0.645	0.609	.0781	3	78.5
SU-BC-16-1	.051	1.502	1.501	4.016	0.603	0.616	.0625	3	64.5
SU-BC-16-2	.050	1.488	1.487	4.033	0.601	0.613	.0625	3	64.5
SU-BC-16-3	.051	1.483	1.491	4.056	0.598	0.619	.0625	3	104.5
SU-BC-13-4	.051	1.808	1.803	4.047	0.608	0.607	.0625	3	104.5
SU-BC-7-1	.047	2.498	2.486	4.786	0.598	0.581	.0625	3	76.5
SU-BC-7-2	.046	2.487	2.503	4.787	0.615	0.589	.0625	3	76.5
SU-BC-7-3	.046	2.497	2.510	4.733	0.614	0.598	.0625	3	108.5
SU-BC-7-4	.046	2.498	2.508	4.753	0.623	0.590	.0625	3	108.5
SU-BC-8-1	.050	3.042	3.000	6.150	0.606	0.607	.0781	3	86.5
SU-BC-8-2	.050	2.983	2.981	6.195	0.602	0.626	.0781	3	86.5
SU-BC-8-3	.050	2.995	3.005	6.190	0.616	0.602	.0781	3	118.5
SU-BC-8-4	.050	2.996	2.992	6.192	0.618	0.611	.0781	3	118.5
SU-BC-8'-1	.076	2.259	2.262	4.021	0.729	0.732	.0938	3	70.5
SU-BC-8'-2	.076	2.250	2.242	4.075	0.713	0.722	.0938	3	70.5
SU-BC-8'-3	.076	2.259	2.263	4.132	0.716	0.691	.0938	3	106.5
SU-BC-8'-4	.076	2.261	2.264	4.120	0.709	0.727	.0938	3	106.5

Note: See definitions of symbols in Fig. B-1

TABLE B-6

Parameters and Test Data for Specimens Used for  
Interior One-Flange Loading Condition  
Obtained from Reference 11

Specimen No.	t (in.)	h/t	R/t	N/t	N/h	F <sub>y</sub> (ksi)	P <sub>test</sub> (kips)
SU-1-IOF-1	0.048	204.7	2.77	20.83	0.10	43.82	1.260
SU-1-IOF-2	0.047	200.2	2.66	21.28	0.11	43.82	1.175
SU-1-IOF-5	0.049	201.1	2.55	61.22	0.30	43.82	1.450
SU-1-IOF-6	0.048	205.2	2.60	62.50	0.30	43.82	1.385
SU-2-IOF-1	0.049	249.9	2.55	20.41	0.08	43.82	1.145
SU-2-IOF-2	0.050	244.2	2.50	20.00	0.08	43.82	1.305
SU-2-IOF-5	0.048	254.4	2.60	62.50	0.25	43.82	1.385
SU-2-IOF-6	0.049	249.9	2.55	61.22	0.24	43.82	1.455
SU-5-IOF-1	0.049	124.4	1.91	20.41	0.16	47.12	1.403
SU-5-IOF-2	0.050	121.5	1.88	20.00	0.16	47.12	1.480
SU-5-IOF-3	0.050	121.9	1.95	40.00	0.33	47.12	1.750
SU-5-IOF-4	0.051	119.2	1.84	39.22	0.33	47.12	1.830
SU-5-IOF-5	0.050	121.7	1.80	60.00	0.49	47.12	2.080
SU-5-IOF-6	0.050	121.8	1.88	60.00	0.49	47.12	1.835
SU-6-IOF-1	0.050	145.4	1.88	20.00	0.14	47.12	1.480
SU-6-IOF-2	0.050	146.2	1.72	20.00	0.14	47.12	1.580
SU-6-IOF-3	0.049	148.6	1.83	40.82	0.27	47.12	1.890
SU-6-IOF-4	0.050	146.8	1.88	40.00	0.27	47.12	1.815
SU-6-IOF-5	0.049	148.9	1.91	61.22	0.41	47.12	2.085
SU-6-IOF-6	0.050	145.6	1.80	60.00	0.41	47.12	1.890
M-SU-6-IOF-1	0.050	145.9	1.88	20.00	0.14	47.12	1.650
M-SU-6-IOF-2	0.050	145.8	1.88	20.00	0.14	47.12	1.643
M-SU-6-IOF-5	0.051	142.8	1.84	58.82	0.41	47.12	2.045
M-SU-6-IOF-6	0.050	145.3	1.88	60.00	0.41	47.12	2.140
U-SU-17-IOF-5	0.049	98.2	0.96	61.22	0.62	36.26	1.500
U-SU-17-IOF-6	0.049	98.0	0.96	61.22	0.62	36.26	1.525
U-SU-18-IOF-5	0.049	192.7	0.96	61.22	0.32	36.26	1.690
U-SU-18-IOF-6	0.049	194.1	0.96	61.22	0.32	36.26	1.465

TABLE B-7

Parameters and Test Data for Specimens Used for  
Interior One-Flange Loading Condition  
Obtained from Reference 19

Specimen No.	t (in.)	h/t	R/t	N/t	N/h	F <sub>y</sub> (ksi)	P <sub>test</sub> (kips)
C3-1	0.050	96.4	1.56	20.00	0.21	48.55	1.640
C3-2	0.050	96.9	1.56	20.00	0.21	48.55	1.665
C3-3	0.051	95.3	1.53	19.61	0.21	48.55	1.690
C3-4	0.051	95.3	1.53	19.61	0.21	48.55	1.600
C3-5	0.051	95.1	1.53	19.61	0.21	48.55	1.685
C3-6	0.050	97.2	1.56	20.00	0.21	48.55	1.670
C3-7	0.050	96.8	1.56	20.00	0.21	48.55	1.600
C3-8	0.051	95.2	1.53	19.61	0.21	48.55	1.620
C3-9	0.049	98.9	1.59	20.41	0.21	48.55	1.535
C3-10	0.050	97.0	1.56	20.00	0.21	48.55	1.520
C3-11	0.045	128.9	1.91	22.22	0.17	38.94	0.970
C3-12	0.045	129.2	1.91	22.22	0.17	38.94	0.950
C3-13	0.045	129.7	1.91	22.22	0.17	38.94	1.200
C3-14	0.045	130.1	1.91	22.22	0.17	38.94	1.150
C3-15	0.049	123.6	1.43	20.41	0.17	47.42	1.565
C3-16	0.049	123.4	1.43	20.41	0.17	47.42	1.505
C3-17	0.052	110.4	1.35	19.23	0.17	54.00	1.835
C3-18	0.052	110.1	1.35	19.23	0.17	54.00	1.800
C3-19	0.052	111.7	1.35	19.23	0.17	54.00	1.825
C3-20	0.052	111.6	1.35	19.23	0.17	54.00	1.770

TABLE B-8

Parameters and Test Data for Specimens Used for  
End One-Flange Loading Condition  
Obtained from Reference 11

Specimen No.	t (in.)	h/t	R/t	N/t	N/h	F <sub>y</sub> (ksi)	P <sub>test</sub> (kips)
SU-1-EOF-1	0.047	210.3	2.66	21.28	0.10	43.82	0.575
SU-1-EOF-2	0.048	205.5	2.60	20.83	0.10	43.82	0.505
SU-1-EOF-5	0.049	201.2	2.55	61.22	0.30	43.82	0.650
SU-1-EOF-6	0.050	197.2	2.81	60.00	0.30	43.82	0.620
SU-2-EOF-1	0.049	247.5	2.55	20.41	0.08	43.82	0.495
SU-2-EOF-2	0.048	252.6	2.60	20.83	0.08	43.82	0.505
SU-2-EOF-5	0.048	254.0	2.60	62.50	0.25	43.82	0.560
SU-2-EOF-6	0.047	258.5	2.66	63.83	0.25	43.82	0.560
SU-4-EOF-1	0.050	96.5	1.74	20.00	0.21	47.12	0.898
SU-4-EOF-2	0.050	96.6	1.56	20.00	0.21	47.12	0.905
SU-4-EOF-3	0.050	96.4	1.72	40.00	0.41	47.12	1.038
SU-4-EOF-4	0.050	96.4	1.72	40.00	0.41	47.12	1.000
SU-4-EOF-5	0.049	98.9	1.79	40.82	0.41	47.12	1.125
SU-4-EOF-6	0.049	98.9	1.79	40.82	0.41	47.12	1.125
SU-4-EOF-5	0.050	96.8	1.69	60.00	0.62	47.12	1.105
SU-4-EOF-6	0.049	99.1	1.75	61.22	0.62	47.12	1.105
SU-5-EOF-1	0.050	121.8	1.88	20.00	0.16	47.12	0.880
SU-5-EOF-2	0.050	121.8	1.88	20.00	0.16	47.12	0.880
SU-5-EOF-3	0.051	118.7	1.76	19.61	0.17	47.12	0.838
SU-5-EOF-4	0.051	119.7	1.84	39.22	0.33	47.12	0.990
SU-5-EOF-5	0.051	119.7	1.84	39.22	0.33	47.12	0.970
SU-5-EOF-6	0.051	119.6	1.99	39.22	0.33	47.12	1.006
SU-5-EOF-5	0.051	119.4	1.84	58.82	0.49	47.12	1.068
SU-5-EOF-6	0.050	121.8	1.88	60.00	0.49	47.12	1.068
SU-6-EOF-1	0.050	145.7	1.72	20.00	0.14	47.12	0.888
SU-6-EOF-2	0.050	145.7	1.72	20.00	0.14	47.12	0.875
SU-6-EOF-3	0.049	148.9	1.91	20.41	0.14	47.12	0.875
SU-6-EOF-4	0.049	148.9	1.91	20.41	0.14	47.12	0.903
SU-6-EOF-5	0.049	148.8	1.75	40.82	0.27	47.12	0.935
SU-6-EOF-6	0.049	148.8	1.75	40.82	0.27	47.12	0.935
SU-6-EOF-4	0.049	148.9	1.99	40.82	0.27	47.12	1.045
SU-6-EOF-5	0.049	148.9	1.99	40.82	0.27	47.12	1.045
SU-6-EOF-6	0.050	145.9	1.88	60.00	0.41	47.12	1.119
SU-6-EOF-5	0.050	146.0	1.88	60.00	0.41	47.12	0.875
SU-6-EOF-6	0.050	146.0	1.88	60.00	0.41	47.12	0.875
M-SU-4-EOF-1	0.050	96.0	1.80	20.00	0.21	47.12	0.873
M-SU-4-EOF-2	0.050	96.0	1.80	20.00	0.21	47.12	0.873
M-SU-4-EOF-3	0.051	94.8	1.84	19.61	0.21	47.12	1.483
M-SU-4-EOF-4	0.051	94.8	1.84	19.61	0.21	47.12	1.483
M-SU-4-EOF-5	0.051	94.8	1.84	19.61	0.21	47.12	1.483
M-SU-4-EOF-6	0.050	95.9	1.72	60.00	0.63	47.12	1.406
M-SU-4-EOF-5	0.050	95.9	1.72	60.00	0.63	47.12	1.406
M-SU-4-EOF-6	0.050	96.4	1.88	60.00	0.62	47.12	0.850
M-SU-6-EOF-1	0.050	145.4	1.88	20.00	0.14	47.12	0.869
M-SU-6-EOF-2	0.050	145.4	1.88	20.00	0.14	47.12	0.869
M-SU-6-EOF-3	0.051	142.6	1.84	19.61	0.14	47.12	1.175
M-SU-6-EOF-4	0.051	142.6	1.84	19.61	0.14	47.12	1.175
M-SU-6-EOF-5	0.051	142.6	1.84	19.61	0.14	47.12	1.175
M-SU-6-EOF-6	0.050	145.3	1.88	60.00	0.41	47.12	1.180
M-SU-6-EOF-5	0.050	145.3	1.88	60.00	0.41	47.12	1.180
M-SU-6-EOF-6	0.051	142.7	1.84	58.82	0.41	47.12	0.628
U-SU-17-EOF-1	0.051	142.7	1.84	58.82	0.41	47.12	0.628
U-SU-17-EOF-1	0.049	99.2	0.96	20.41	0.21	36.26	0.598
U-SU-17-EOF-1	0.049	99.2	0.96	20.41	0.21	36.26	0.598
U-SU-17-EOF-1	0.049	98.3	0.96	20.41	0.21	36.26	0.898
U-SU-17-EOF-1	0.049	98.3	0.96	20.41	0.21	36.26	0.898
U-SU-17-EOF-1	0.049	97.8	0.96	61.22	0.63	36.26	0.835
U-SU-17-EOF-1	0.049	97.8	0.96	61.22	0.63	36.26	0.835
U-SU-17-EOF-1	0.049	98.4	0.96	61.22	0.62	36.26	0.472
U-SU-17-EOF-1	0.049	98.4	0.96	61.22	0.62	36.26	0.472
U-SU-17-EOF-1	0.049	98.4	0.96	61.22	0.62	36.26	0.472
U-SU-18-EOF-1	0.049	193.0	0.96	20.41	0.11	36.26	0.428
U-SU-18-EOF-1	0.049	193.0	0.96	20.41	0.11	36.26	0.428
U-SU-18-EOF-1	0.049	194.7	0.96	20.41	0.10	36.26	0.568
U-SU-18-EOF-1	0.049	194.7	0.96	20.41	0.10	36.26	0.568
U-SU-18-EOF-1	0.049	184.6	0.94	60.00	0.33	36.26	0.568
U-SU-18-EOF-1	0.050	184.6	0.94	60.00	0.33	36.26	0.568
U-SU-18-EOF-1	0.050	184.6	0.94	60.00	0.33	36.26	0.568
U-SU-18-EOF-1	0.049	188.4	0.96	61.22	0.32	36.26	0.545
U-SU-18-EOF-1	0.049	188.4	0.96	61.22	0.32	36.26	0.545



TABLE B-9

Parameters and Test Data for Specimens Used for  
End One-Flange Loading Condition  
Obtained from Reference 19

Specimen No.	t (in.)	h/t	R/t	N/t	N/h	F <sub>y</sub> (ksi)	P <sub>test</sub> (kips)
C2-3	0.050	96.9	1.56	20.00	0.21	48.55	0.845
C2-4	0.050	96.8	1.56	20.00	0.21	48.55	0.803
C2-5	0.050	96.2	1.56	20.00	0.21	48.55	0.945
C2-6	0.050	96.8	1.56	20.00	0.21	48.55	0.925
C2-7	0.050	97.2	1.56	20.00	0.21	48.55	0.983
C2-8	0.050	96.6	1.56	20.00	0.21	48.55	1.013
C2-9	0.050	97.0	1.56	20.00	0.21	48.55	0.940
C2-10	0.050	97.0	1.56	20.00	0.21	48.55	0.935
C2-13	0.052	113.2	1.35	19.23	0.17	51.05	0.833
C2-14	0.052	113.3	1.35	19.23	0.17	51.05	0.908
C2-15	0.052	112.9	1.35	19.23	0.17	51.05	1.085
C2-16	0.052	112.9	1.35	19.23	0.17	51.05	1.035
C2-17	0.052	113.0	1.35	19.23	0.17	51.05	1.143
C2-18	0.052	112.4	1.35	19.23	0.17	51.05	1.140
C2-19	0.052	112.0	1.35	19.23	0.17	51.05	1.063
C2-20	0.052	112.5	1.35	19.23	0.17	51.05	1.055

TABLE B-10

Parameters and Test Data for Specimens Used for  
Combined Web Crippling and Bending Moment  
Obtained from Reference 11

Specimen No.	t (in.)	h/t	R/t	N/t	N/h	F <sub>y</sub> (ksi)	P <sub>test</sub> (kips)
SU-BC-1-1	0.046	101.8	1.36	65.22	0.64	33.5	2.280
SU-BC-1-2	0.046	101.9	1.36	65.22	0.64	33.5	2.260
SU-BC-1-3	0.046	100.8	1.36	65.22	0.65	33.5	1.720
SU-BC-1-4	0.047	98.8	1.34	64.52	0.65	33.5	1.780
SU-BC-1-5	0.047	98.5	1.33	63.83	0.65	33.5	1.220
SU-BC-1-6	0.046	100.2	1.36	65.22	0.65	33.5	1.060
SU-BC-3-1	0.049	196.5	0.95	60.73	0.31	36.9	2.400
SU-BC-3-2	0.049	196.0	0.95	60.73	0.31	36.9	2.670
SU-BC-3-3	0.049	195.9	0.95	60.73	0.31	36.9	2.210
SU-BC-3-4	0.049	196.6	0.95	60.73	0.31	36.9	2.340
SU-BC-3-5	0.048	200.1	0.97	61.98	0.31	36.9	1.850
SU-BC-3-6	0.049	196.5	0.95	60.73	0.31	36.9	2.040
SU-BC-15-1	0.050	146.6	1.56	60.00	0.41	53.8	4.180
SU-BC-15-2	0.051	143.9	1.53	58.82	0.41	53.8	4.150
SU-BC-15-3	0.051	143.5	1.53	58.82	0.41	53.8	3.680
SU-BC-15-4	0.050	146.6	1.56	60.00	0.41	53.8	3.600
SU-BC-15-5	0.051	143.2	1.53	58.82	0.41	53.8	3.000
SU-BC-15-6	0.052	140.5	1.50	57.69	0.41	53.8	3.000
SU-4-IOF-1	0.049	98.4	1.58	20.24	0.21	47.1	3.052
SU-4-IOF-2	0.050	97.1	1.57	20.08	0.21	47.1	3.050
SU-4-IOF-3	0.050	96.4	1.87	39.84	0.41	47.1	3.540
SU-4-IOF-4	0.050	96.6	1.72	40.00	0.41	47.1	3.550
SU-4-IOF-5	0.050	96.7	1.56	60.00	0.62	47.1	4.170
SU-4-IOF-6	0.050	96.2	1.56	60.00	0.62	47.1	3.970
M-SU-4-IOF-1	0.050	97.5	1.88	20.00	0.21	47.1	3.210
M-SU-4-IOF-2	0.051	95.2	1.93	19.80	0.21	47.1	3.260
M-SU-4-IOF-5	0.051	94.7	1.84	58.82	0.62	47.1	4.400
M-SU-4-IOF-6	0.050	96.1	1.79	59.64	0.62	47.1	4.150

TABLE B-10 (Cont'd)

Parameters and Test Data for Specimens Used for  
Combined Web Crippling and Bending Moment  
Obtained from Reference 11

Specimen No.	t (in.)	h/t	R/t	N/t	N/h	F <sub>y</sub> (ksi)	P <sub>test</sub> (kips)
SU-BC-6-1	0.050	49.5	1.57	60.36	1.22	36.9	1.760
SU-BC-6-2	0.050	49.7	1.57	60.36	1.21	36.9	1.680
SU-BC-6-3	0.051	48.5	1.54	59.17	1.22	36.9	1.130
SU-BC-16-1	0.051	76.7	1.23	58.82	0.77	53.8	2.880
SU-BC-16-2	0.050	78.7	1.25	60.00	0.76	53.8	2.700
SU-BC-16-3	0.051	77.5	1.23	58.82	0.76	53.8	2.010
SU-BC-13-4	0.051	77.4	1.23	58.82	0.76	53.8	2.210
SU-BC-7-1	0.047	99.8	1.33	63.83	0.64	33.5	2.000
SU-BC-7-2	0.046	102.1	1.36	65.22	0.64	33.5	1.880
SU-BC-7-3	0.046	100.9	1.36	65.22	0.65	33.5	1.400
SU-BC-7-4	0.046	101.3	1.36	65.22	0.64	33.5	1.510
SU-BC-8-1	0.050	121.0	1.56	60.00	0.50	47.1	3.070
SU-BC-8-2	0.050	121.9	1.56	60.00	0.49	47.1	2.940
SU-BC-8-3	0.050	121.8	1.56	60.00	0.49	47.1	2.620
SU-BC-8-4	0.050	121.8	1.56	60.00	0.49	47.1	2.600
SU-BC-8'-1	0.076	50.9	1.23	39.47	0.78	43.6	4.410
SU-BC-8'-2	0.076	52.0	1.24	39.74	0.76	43.6	4.730
SU-BC-8'-3	0.076	52.4	1.23	39.47	0.75	43.6	3.180
SU-BC-8'-4	0.076	52.2	1.23	39.47	0.76	43.6	3.400

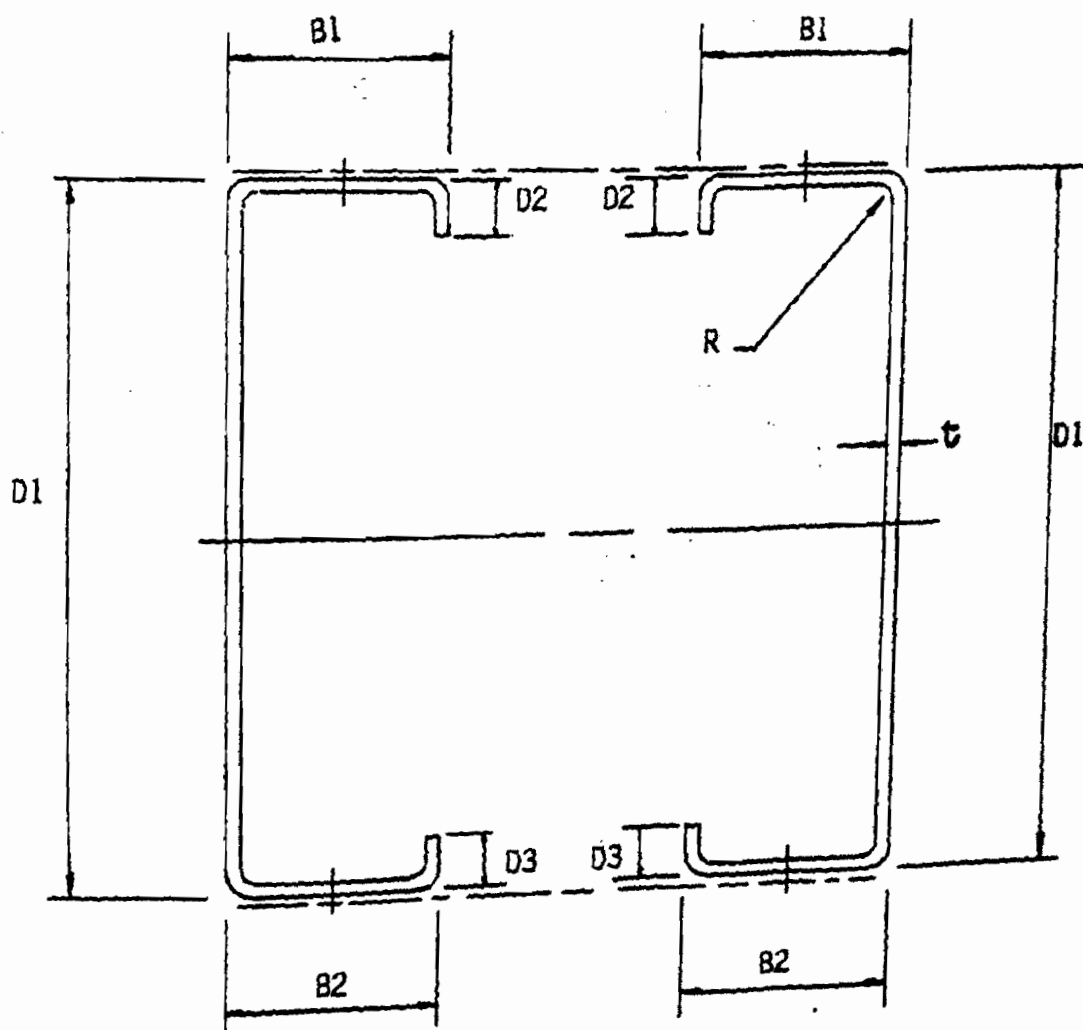


Fig. B-1 Cross Section of Specimens Used in References 11 and 19

## APPENDIX C

## NOTATION

Symbol	Definition
D	Flexural rigidity of plate, $Et^3/12(1-\mu^2)$
e	Clear distance between the closest opposite bearing plates measured along the length of beam, in.
E	Modulus of elasticity of steel = 29,500 ksi
$f_b$	Actual compression stress at junction of flange and web, ksi
$f_c$	Actual bearing stress in the web under the bearing plate, ksi
$F_{bwu}$	Maximum compression stress in the flat web of a beam due to bending, ksi
$F_y$	Yield strength, ksi
h	Clear distance between flanges measured along the plane of the web, in.
K	Buckling coefficient
L	Span length, in.
M	Applied bending moment, at or immediately adjacent to the point of application of the concentrated load or reaction, kip-in.
$M_u$	Ultimate bending moment if bending stress only exists, kip-in.
N	Actual length of bearing, in.
P	Concentrated load or reaction, kips
$P_c$	Computed ultimate web crippling load in the absence of bending moment, kips

Symbol	Definition
$P_{cb}$	Ultimate web crippling load due to web buckling, kips
$P_{comp}$	Predicted ultimate load, kips
$P_{cr}$	Elastic critical buckling load, kips
$P_{cy}$	Ultimate web crippling load due to overstressing under the bearing plate, kips
$P_m$	Computed ultimate load for moment only, kips
$P_{mc}$	Computed load for combined bending moment and web crippling, kips
$P_{ms}$	Computed load for combined bending moment and shear, kips
$P_s$	Computed ultimate load for shear in the web, kips
$P_{test}$	Tested failure load, kips
$P_{cg}$	Computed ultimate web crippling load based on the AISI 1981 Guide, kips
$P_{cs}$	Computed ultimate web crippling load based on the AISI 1980 Specification, kips
$R$	Inside bend radius, in.
$S_{eff}$	Effective section modulus computed on the basis of the effective design width of the compression flange, in. <sup>3</sup>
$t$	Base steel thickness, in.
$\mu$	Poisson's ratio